Target materials for ISOL

Stefano Corradetti

Contents

Outline:

- **Part 1:** Introduction

- **Part 2:** ISOL target materials

- **Part 3:** Production techniques

- **Part 4:** Characterization techniques

- **Part 5:** Simulations

- **Part 6:** A few examples of recent target developments

Istituto Nazionale di Fisica Nucleare
LABORATORI NAZIONALI DI LEGNARO

INFN (Istituto Nazionale di Fisica Nucleare)

Organization:

- 20 sections

- 6 groups

- 4 national laboratories

- 4 national centers

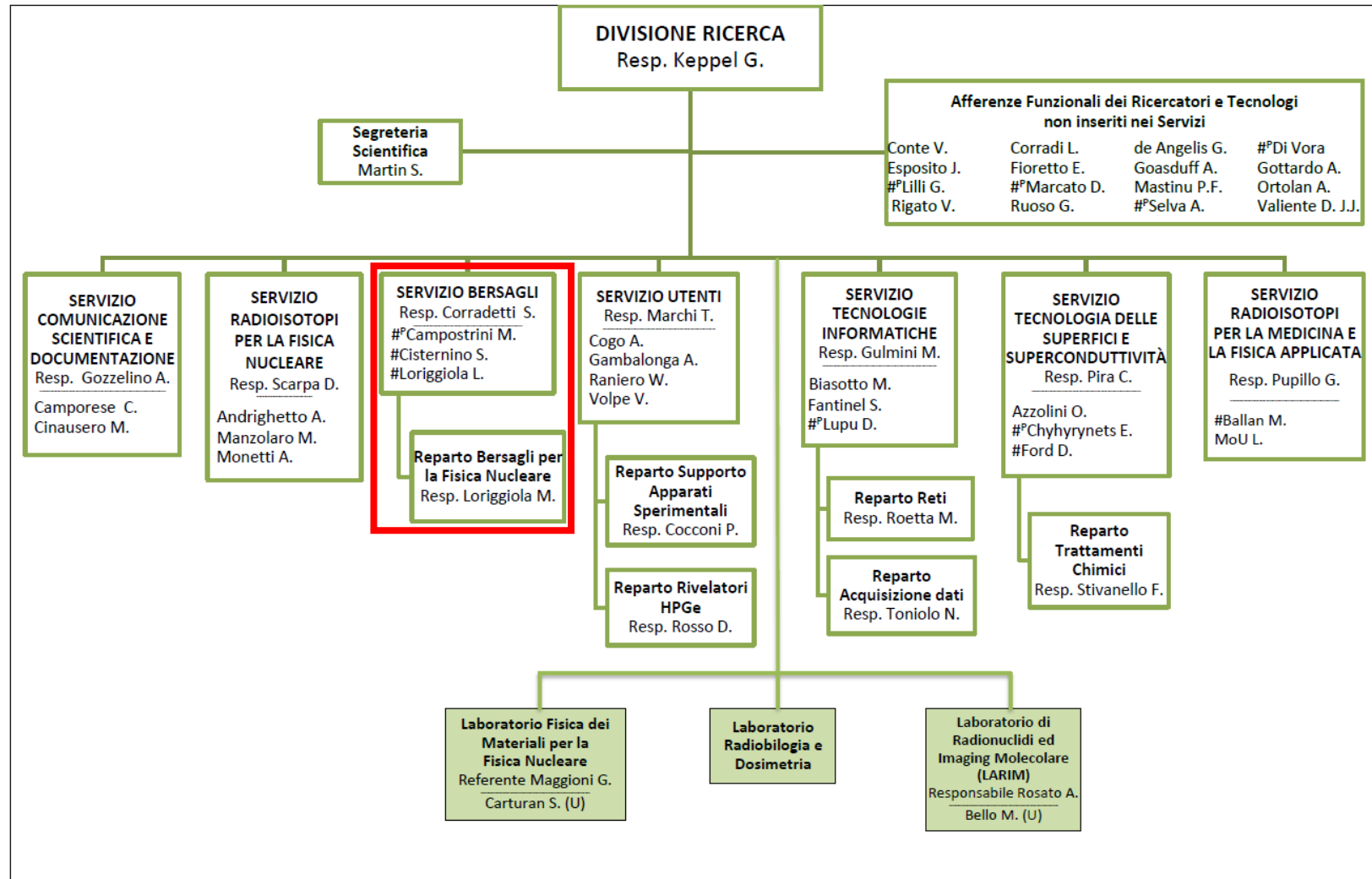- EGO consortium for gravitational waves

Legend:
- ○ National Laboratory
- ○ Section
- ○ Group
- ⬢ National Centers and Schools
- ⬢ Consortia
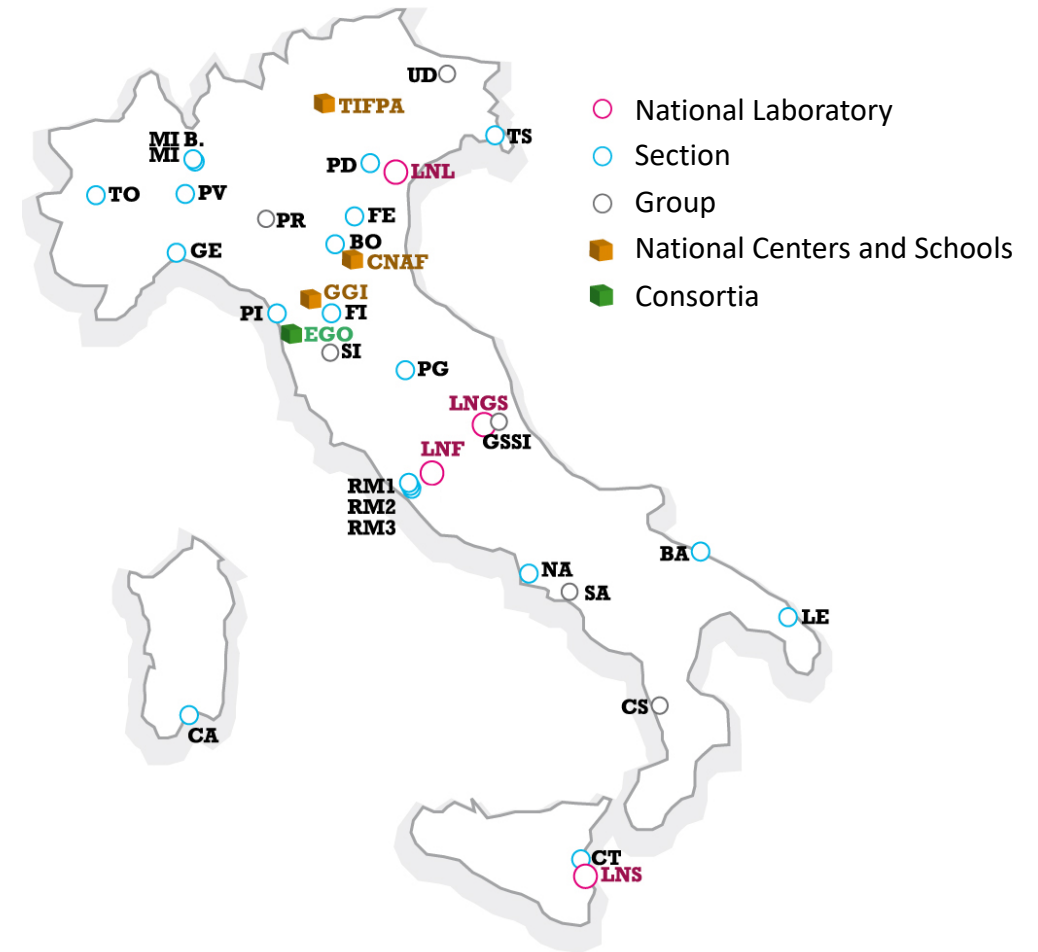
LNL (Legnaro National Laboratories)

LNL:

- **150 employees**
- **50 students, PhD, post-docs**
- **5 particle accelerators**
- **5 experimental halls**

The Target Service at INFN-LNL

LNL org. chart:

Targets Service

- Production of targets for the experiments at LNL accelerators and for the production of radioisotopes of interest for nuclear physics, medicine and other applications.

The Target Service at INFN-LNL

Activities of the service (Production)

- Targets for nuclear physics

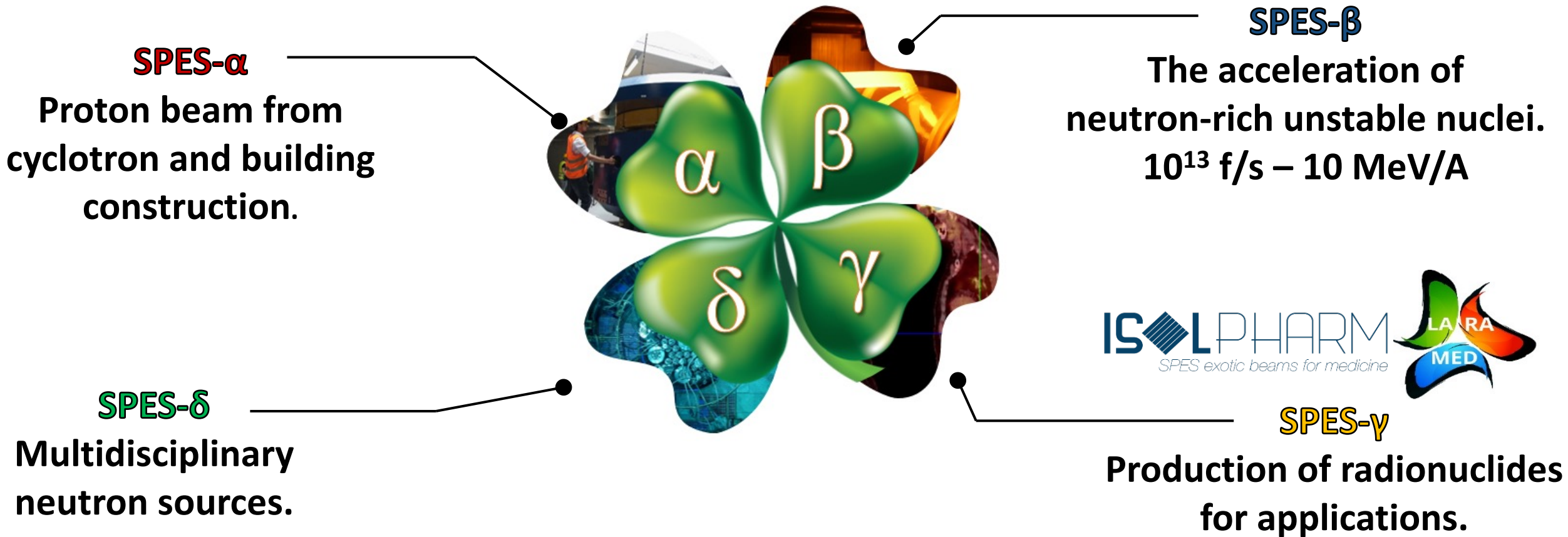- Targets for applications

- ISOL targets

High-power targets

Collaboration activities

- Characterization of innovative targets
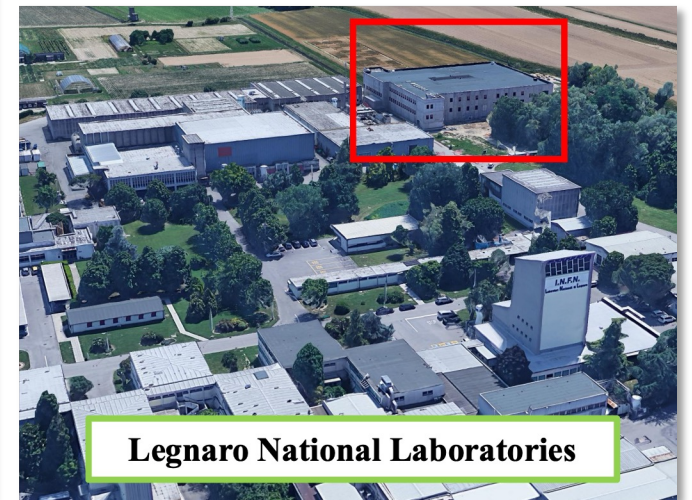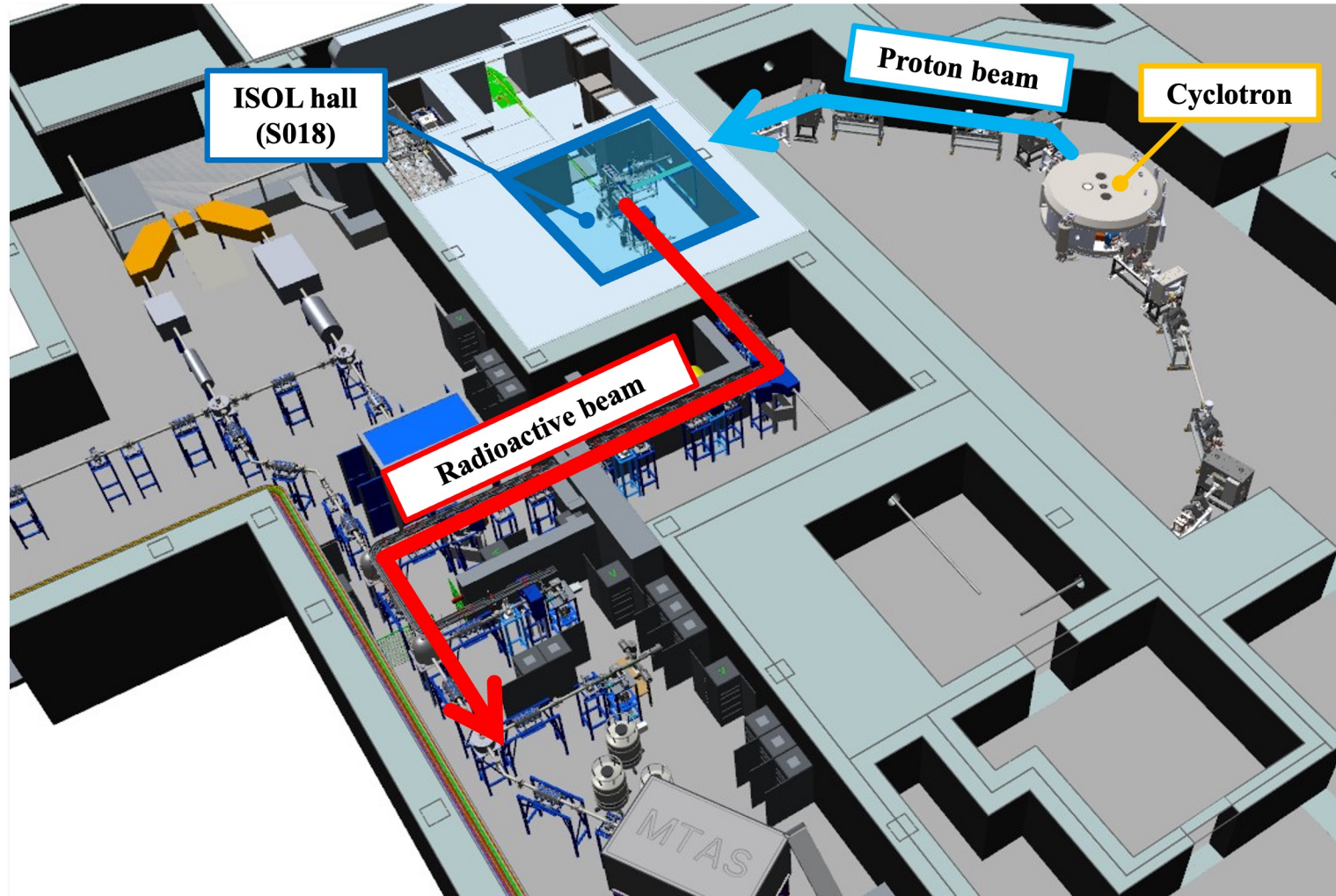
The SPES facility at INFN-LNL

SPES is: 1) A second generation ISOL facility (for neutron-rich radioactive ion beams)
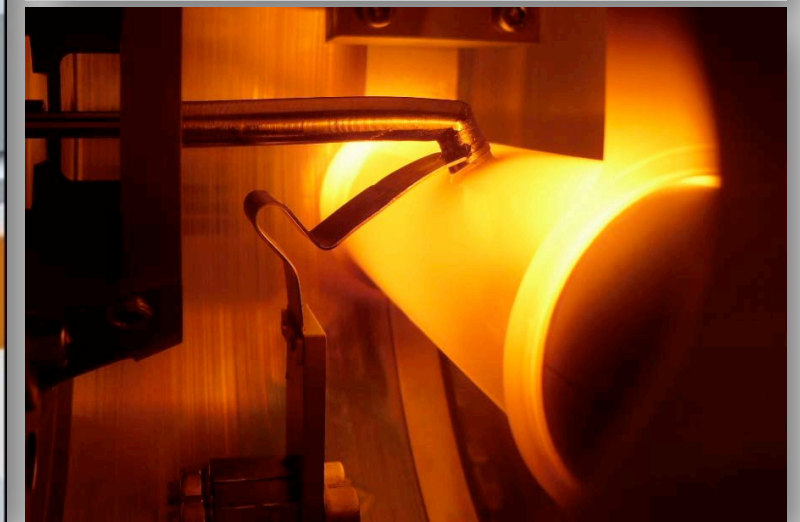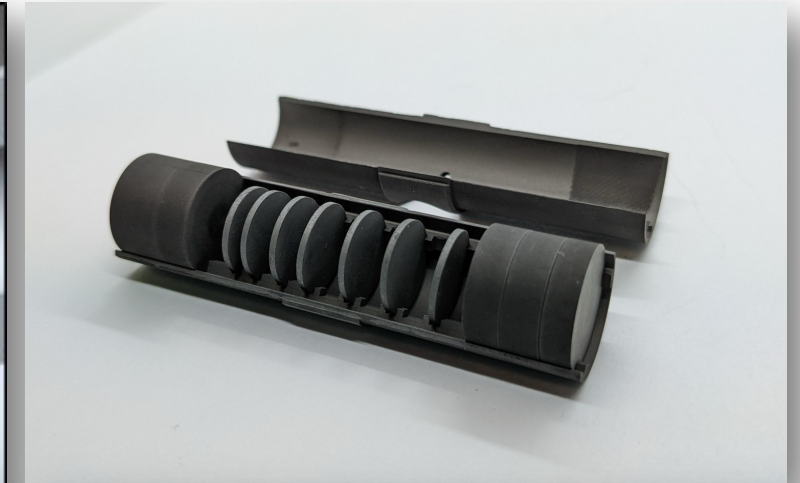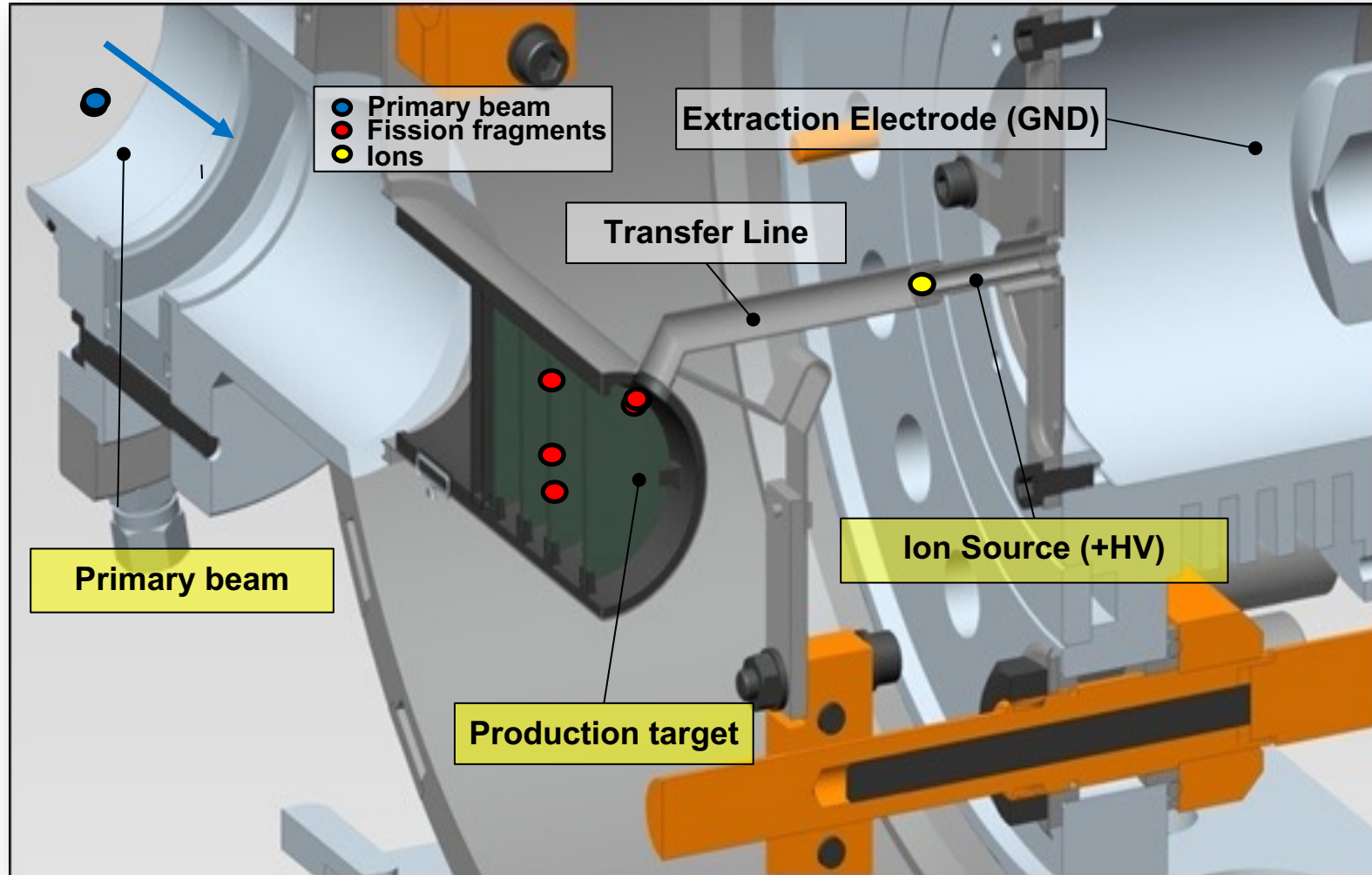2) An interdisciplinary research center (for p,n applications)

SPES-β
The acceleration of neutron-rich unstable nuclei. 10^{13} f/s – 10 MeV/A

SPES-α
Proton beam from cyclotron and building construction.

SPES-δ
Multidisciplinary neutron sources.

SPES-γ
Production of radionuclides for applications.

The SPES facility at INFN-LNL

ISOL hall (S018)

Proton beam

Cyclotron

Radioactive beam

MTAS

SPES building

Legnaro National Laboratories

ISOL target

Primary beam
Fission fragments
Ions

Extraction Electrode (GND)

Transfer Line

Ion Source (+HV)

Primary beam

Production target

ISOL target material research in Europe and worldwide

Nuclear Instruments and Methods in Physics Research B 288 (2012) 34–41

Contents lists available at SciVerse ScienceDirect

Nuclear Instruments and Methods in Physics Research B

journal homepage: www.elsevier.com/locate/nimb

An off-line method to characterize the fission product release from uranium carbide-target prototypes developed for SPIRAL2 project

B. Hy [a], N. Barré-Boscher [a], A. Özgümüs [a,b,*], B. Roussière [a], S. Tusseau-Nenez [a], C. Lau [a], M. Cheikh Mhamed [a], M. Raynaud [a], A. Said [a], K. Kolos [a], E. Cottereau [a], S. Essabaa [a], O. Tougait [c], M. Pasturel [c]

Nuclear Instruments and Methods in Physics Research B 317 (2013) 385–388

Contents lists available at ScienceDirect

Nuclear Instruments and Methods in Physics Research B

journal homepage: www.elsevier.com/locate/nimb

Porous silicon carbide and aluminum oxide with unidirectional open porosity as model target materials for radioisotope beam production

M. Czapski [a], T. Stora [a], C. Tardivat [b], S. Deville [b], R. Santos Augusto [a], J. Leloup [b], F. Bouville [b], R. Fernandes Luis [c]

Journal of Nuclear Materials 440 (2013) 110–116

Contents lists available at SciVerse ScienceDirect

Journal of Nuclear Materials

journal homepage: www.elsevier.com/locate/jnucmat

Composite uranium carbide targets at TRIUMF: Development and characterization with SEM, XRD, XRF and L-edge densitometry

Peter Kunz [a,*], Pierre Bricault [a], Marik Dombsky [a], Nicole Erdmann [b], Vicky Hanemaayer [a], John Wong [a], Klaus Lützenkirchen [b]

Nuclear Instruments and Methods in Physics Research B 317 (2013) 402–410

Contents lists available at ScienceDirect

Nuclear Instruments and Methods in Physics Research B

journal homepage: www.elsevier.com/locate/nimb

Recent developments of target and ion sources to produce ISOL beams

T. Stora [*]

Nuclear Instruments and Methods in Physics Research B 320 (2014) 83–88

Contents lists available at ScienceDirect

Nuclear Instruments and Methods in Physics Research B

journal homepage: www.elsevier.com/locate/nimb

Intense $^{31-35}$Ar beams produced with a nanostructured CaO target at ISOLDE

J.P. Ramos [a,b], A. Gottberg [a,c], T.M. Mendonça [a,c], C. Seiffert [a,f], A.M.R. Senos [b], H.O.U. Fynbo [d], O. Tengblad [c], J.A. Briz [c], M.V. Lund [d], G.T. Koldste [d], M. Carmona-Gallardo [c], V. Pesudo [c], T. Stora [a,e]

Nuclear Instruments and Methods in Physics Research B 376 (2016) 8–15

Contents lists available at ScienceDirect

Nuclear Instruments and Methods in Physics Research B

journal homepage: www.elsevier.com/locate/nimb

Target materials for exotic ISOL beams

A. Gottberg

Nuclear Instruments and Methods in Physics Research B 376 (2016) 81–85

Contents lists available at ScienceDirect

Nuclear Instruments and Methods in Physics Research B

journal homepage: www.elsevier.com/locate/nimb

Target nanomaterials at CERN-ISOLDE: synthesis and release data

J.P. Ramos [a,b,*], A. Gottberg [a,1], R.S. Augusto [a,c], T.M. Mendonca [a], K. Riisager [d], C. Seiffert [a,e], P. Bowen [b], A.M.R. Senos [f], T. Stora [a,e]

Available online at www.sciencedirect.com

ScienceDirect

Ceramics International 41 (2015) 8093–8099

www.elsevier.com/locate/ceramint

CERAMICS INTERNATIONAL

Sintering kinetics of nanometric calcium oxide in vacuum atmosphere

J.P. Ramos [a,b], C.M. Fernandes [a], T. Stora [b], A.M.R. Senos [a,*]

Nuclear Inst. and Methods in Physics Research B 433 (2018) 60–68

Contents lists available at ScienceDirect

Nuclear Inst. and Methods in Physics Research B

journal homepage: www.elsevier.com/locate/nimb

Development of radioactive beams at ALTO: Part 1. Physicochemical comparison of different types of UC$_x$ targets using a multivariate statistical approach

Julien Guillot [a,*], Sandrine Tusseau-Nenez [a], Brigitte Roussière [a], Nicole Barré-Boscher [a], François Brisset [c], Sylvain Denis [d]

Nuclear Inst. and Methods in Physics Research B 440 (2019) 1–10

Contents lists available at ScienceDirect

Nuclear Inst. and Methods in Physics Research B

journal homepage: www.elsevier.com/locate/nimb

Development of radioactive beams at ALTO: Part 2. Influence of the UC$_x$ target microstructure on the release properties of fission products

Julien Guillot [a,*], Brigitte Roussière [a], Sandrine Tusseau-Nenez [b], Denis Grebenkov [b], Nicole Barré-Boscher [a], Elie Borg [a], Julien Martin [a]

[a] Institut de Physique Nucléaire d'Orsay CNRS/IN2P3 UMR 8608 - Université Paris Sud - Université Paris Saclay, F-91406 ORSAY Cedex, France
[b] Laboratoire de Physique de la Matière Condensée, CNRS, Ecole Polytechnique - Université Paris Saclay, Route de Saclay, F-91128 Palaiseau, France

---

Journal of the European Ceramic Society 37 (2017) 3899–3908

Contents lists available at www.sciencedirect.com

Journal of the European Ceramic Society

journal homepage: www.elsevier.com/locate/jeurceramsoc

Development of a processing route for carbon allotrope-based TiC porous nanocomposites

J.P. Ramos [a,b,*], A.M.R. Senos [c], T. Stora [b], C.M. Fernandes [c], P. Bowen [a,**]

Journal of the European Ceramic Society 38 (2018) 4882–4891

Contents lists available at ScienceDirect

Journal of the European Ceramic Society

journal homepage: www.elsevier.com/locate/jeurceramsoc

Original Article

Thermal stability of nanometric TiC-carbon composites: effects of carbon allotropes and Zr milling impurities

J.P. Ramos [a,b,*], T. Stora [b], A.M.R. Senos [c], P. Bowen [b,*]

Nuclear Inst. and Methods in Physics Research B 463 (2020) 201–210

Contents lists available at ScienceDirect

Nuclear Inst. and Methods in Physics Research B

journal homepage: www.elsevier.com/locate/nimb

Thick solid targets for the production and online release of radioisotopes: The importance of the material characteristics – A review

J.P. Ramos

Nuclear Instruments and Methods in Physics Research B 394 (2017) 153–155

Contents lists available at ScienceDirect

Nuclear Instruments and Methods in Physics Research B

journal homepage: www.elsevier.com/locate/nimb

Influence of target thickness on the release of radioactive atoms

Julien Guillot [a,*], Brigitte Roussière [a], Sandrine Tusseau-Nenez [b], Nicole Barré-Boscher [a], Elie Borg [a], Julien Martin [a]

Nuclear Inst. and Methods in Physics Research B 463 (2020) 367–370

Contents lists available at ScienceDirect

Nuclear Inst. and Methods in Physics Research B

journal homepage: www.elsevier.com/locate/nimb

UC$_x$ target production at TRIUMF in the ARIEL era

Marla Cervantes [a,b], Pauline Fouquet-Métivier [c], Peter Kunz [b,d], Laura Lambert [a,1], Anders Mjos [a], Thomas Day Goodacre [a], John Wong [a], Alexander Gottberg [a,b,d]
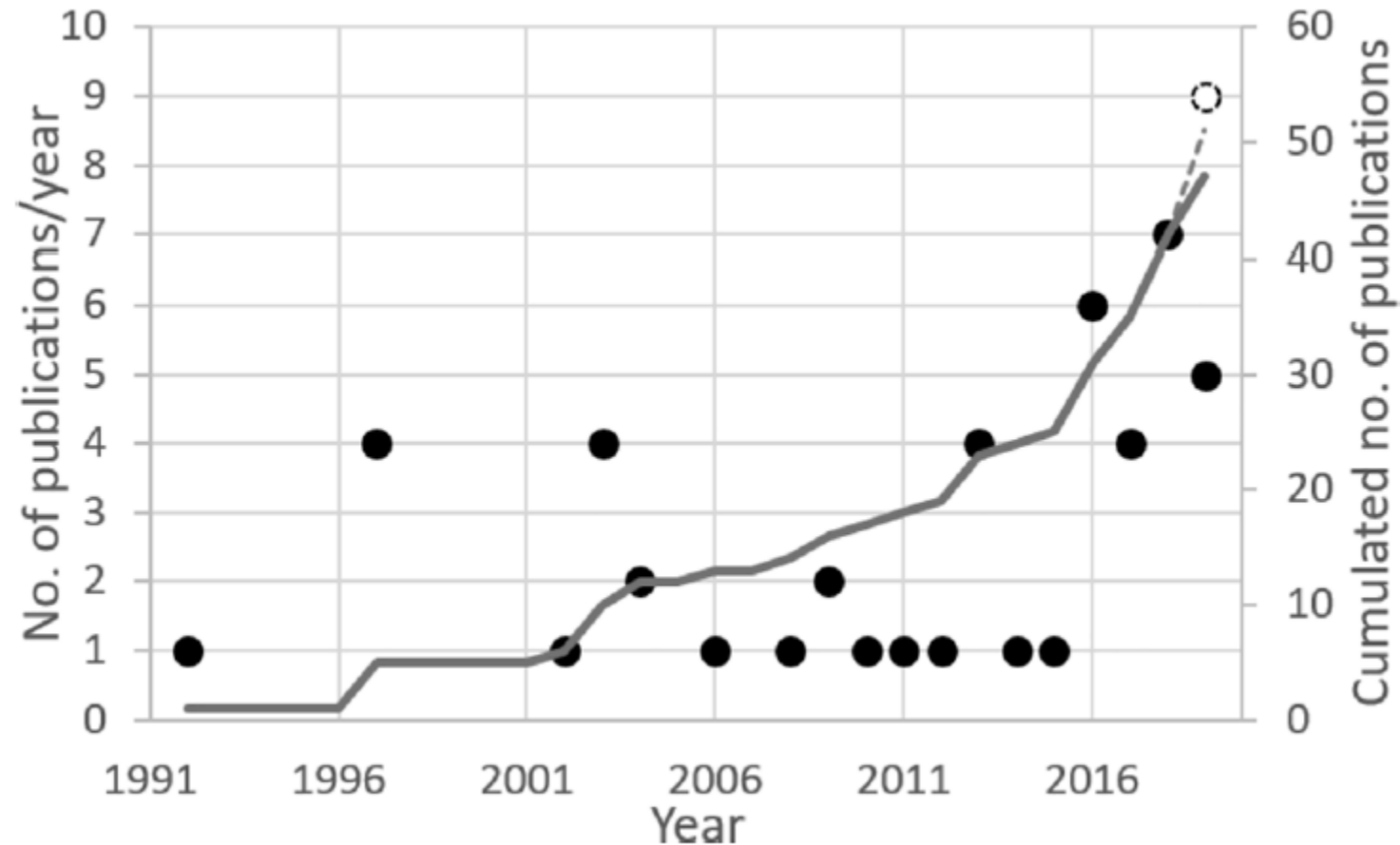

Nuclear Inst. and Methods in Physics Research B 463 (2020) 262–268

Contents lists available at ScienceDirect

Nuclear Inst. and Methods in Physics Research B

journal homepage: www.elsevier.com/locate/nimb

High-power target development for the next-generation ISOL facilities

Lucia Popescu [*], Donald Houngbo, Marc Dierckx

Istituto Nazionale di Fisica Nucleare
LABORATORI NAZIONALI DI LEGNARO

ISOL target material papers – focus on materials

J.P. Ramos, Nuclear Inst. and Methods in Physics Research B 463 (2020) 201–210.

ISOL target material research in Europe and worldwide

# A few notable articles/reviews

- J.P. Ramos, Thick solid targets for the production and online release of radioisotopes: The importance of the material characteristics – A review, Nuclear Instruments and Methods in Physics Research B 463 (2020) 201–210.

- J. Guillot et al., Development of radioactive beams at ALTO: Part 2. Influence of the UCx target microstructure on the release properties of fission products, Nuclear Instruments and Methods in Physics Research B 440 (2019) 1–10.

- J. Guillot et al., Development of radioactive beams at ALTO: Part 1. Physicochemical comparison of different types of UCx targets using a multivariate statistical approach, Nuclear Instruments and Methods in Physics Research B 433 (2018) 60-68.

- A. Gottberg, Target materials for exotic ISOL beams, Nuclear Instruments and Methods in Physics Research B 376 (2016) 8–15.

- J.P. Ramos et al., Target nanomaterials at CERN-ISOLDE: synthesis and release data, Nuclear Instruments and Methods in Physics Research B 376 (2016) 81–85.

- R. Kirchner, On the release and ionization efficiency of catcher-ion-source systems in isotope separation on-line, Nuclear Instruments and Methods in Physics Research B 70 (1992) 186-199.

ISOL target materials: production and release

grain   • isotope   pores
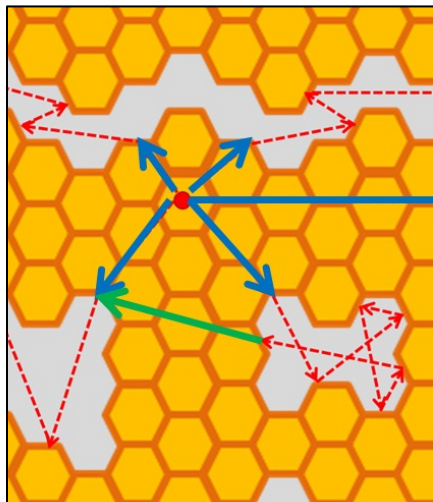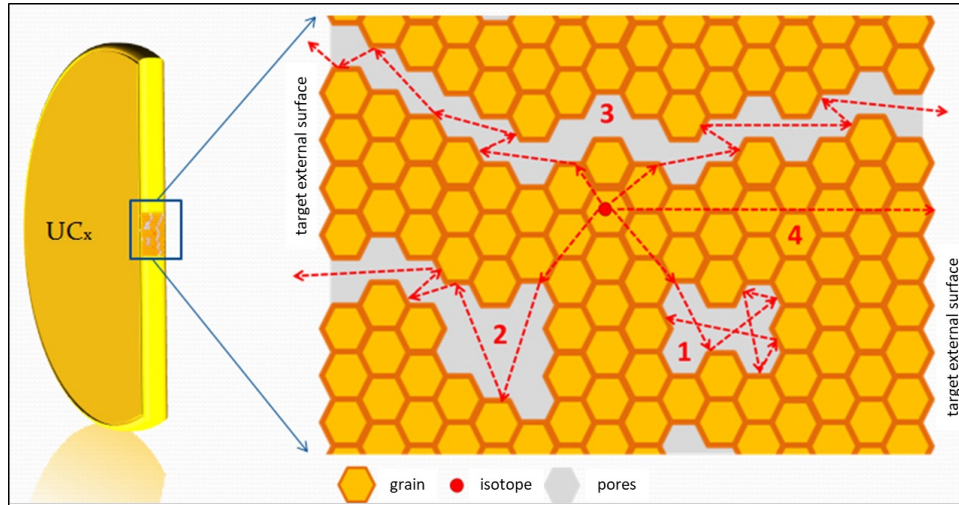
Total isotope yield deeply affected by **open porosity** (diffusion/effusion processes)

• Isotope generation

→ Diffusion paths

--→ Effusion paths

→ Re-diffusion paths
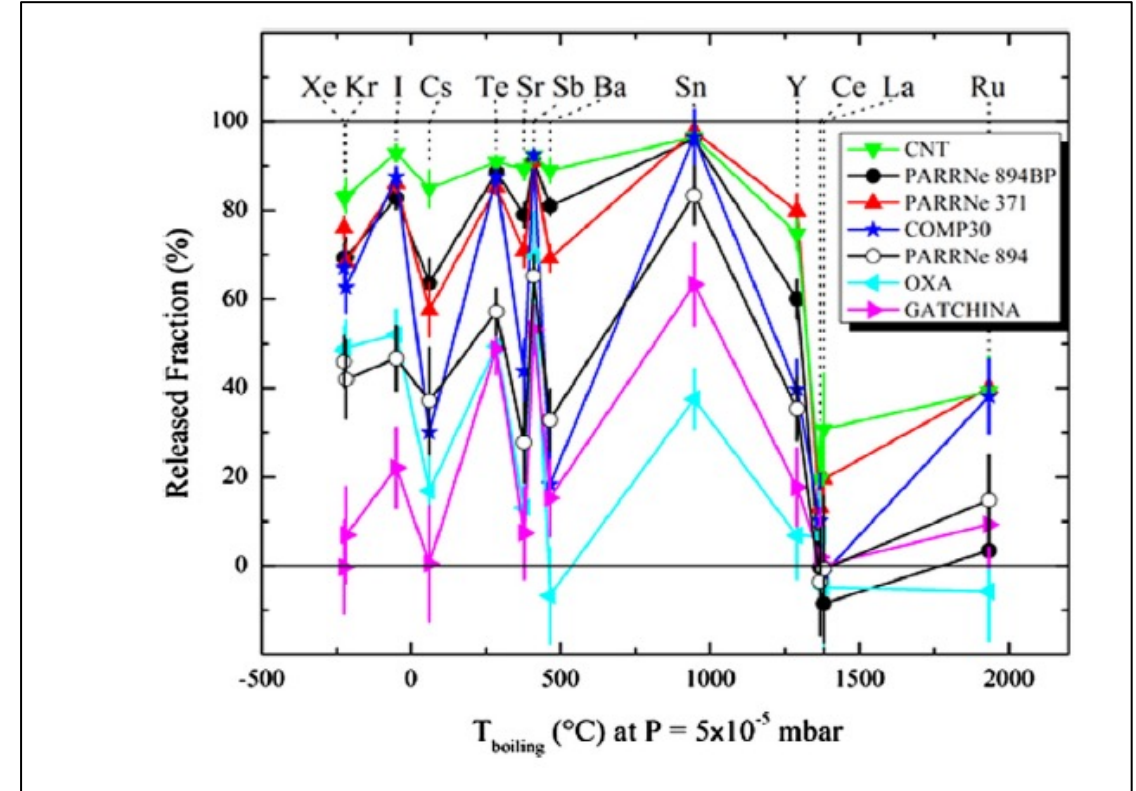
Production process should optimize:

- Presence of nanostructures
- Open porosity

ISOL target yield

ISOL target yield [s⁻¹]:

$$Y = Y_0(E)I_{prim}\varepsilon_{rel}(\lambda)\ \varepsilon_{form}\ \varepsilon_{irr}\ \varepsilon_{ion}$$

$$\varepsilon_{rel}(\lambda) = \int_0^\infty e^{-\lambda t}p(t)dt$$

$$t = t_{diff} + t_{ads} + t_{eff}$$

Where:

$Y_0(E)$: normalized production rate of the isotope [μC^{-1}] → depends on incident particle, production cross section (function of the beam energy, E) or in some cases secondary production channels

I_{prim}: primary beam intensity [μA]

ε_{form} : molecular sideband formation efficiency

ε_{irr} : chemical losses and irreversible adsorption on surfaces

ε_{ion} : ionization efficiency

ε_{rel} : **release efficiency → depends on losses due to the release time (t), isotope decay (λ) and probability density function (p(t)).**

$p(t)$: **probability density function (release curve) → depends on chemical element, target matrix, microstructure and geometry of the target-ion source assembly**

t_{diff}: **diffusion time**

t_{ads}: **delay due to surface sticking**

t_{eff}: **effusion time**

J.P. Ramos, Nuclear Inst. and Methods in Physics Research B 463 (2020) 201–210.

INFN Istituto Nazionale di Fisica Nucleare LABORATORI NAZIONALI DI LEGNARO

27 EU P Prismap

ISOL target release

Release curve:

$$\varepsilon_{rel}(\lambda) = \int_0^\infty e^{-\lambda t} p(t) dt$$

$$p(t) = \int_0^t p_D(\tau) p_E(t - \tau) d\tau$$

Where:

p_D(t): release curve relative to the diffusion process

p_E(t): release curve relative to the effusion process

[0,τ]: time interval for diffusion

[τ,t]: time interval for effusion

R. Kirchner, Nuclear Inst. and Methods in Physics Research B 70 (1992) 186-199.

Diffusion (in spherical particles)

Diffusion release curve and efficiency:

$$\frac{dc}{dt} = D\nabla^2 c$$

$$D = D_0 e^{-\frac{E_D}{RT}}$$

$$p_D(t) = \frac{6\mu}{\pi^2} \sum_{n=1}^{\infty} e^{-n^2 \mu t}$$

$$\mu = \pi^2 \frac{D}{r}$$

$$\varepsilon_D(t) = \frac{6\mu}{\pi^2} \sum_{n=1}^{\infty} \frac{e^{-(\lambda + n^2 \mu)t}}{\lambda + n^2 \mu}$$

Where:

c: concentration

D: diffusion coefficient [m²/s]

E_D: activation energy for diffusion [J/mol]

r: spherical particle radius [m]
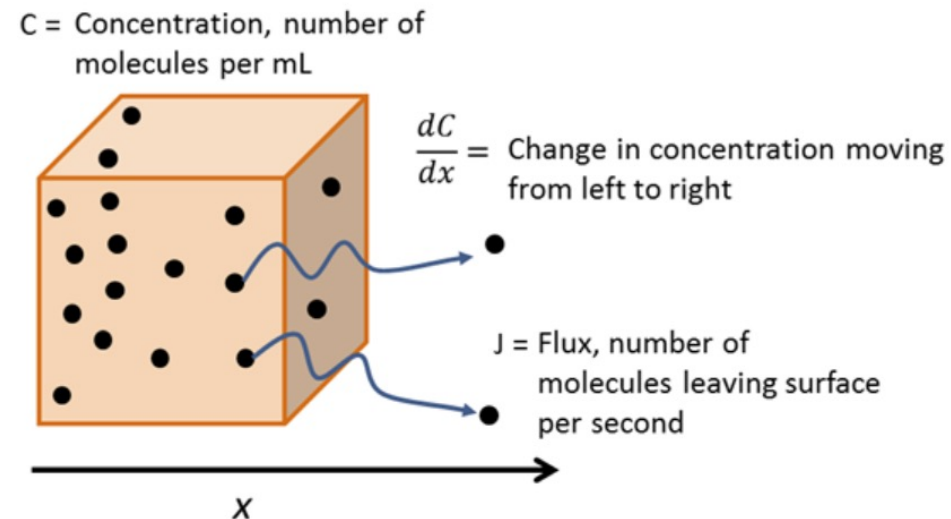
R. Kirchner, Nuclear Inst. and Methods in Physics Research B 70 (1992) 186-199.

Effusion

Release curve:

$$p_E(t) = v e^{-vt}$$

$$\varepsilon_E(\lambda) = \frac{v}{v + \lambda}$$

$$\tau_E = \frac{1}{v} = \omega(\tau_s + \tau_f)$$

Where:

v: time constant

ω: mean number of collisions

τ_s: sticking time per collision

τ_f: flight time between collisions
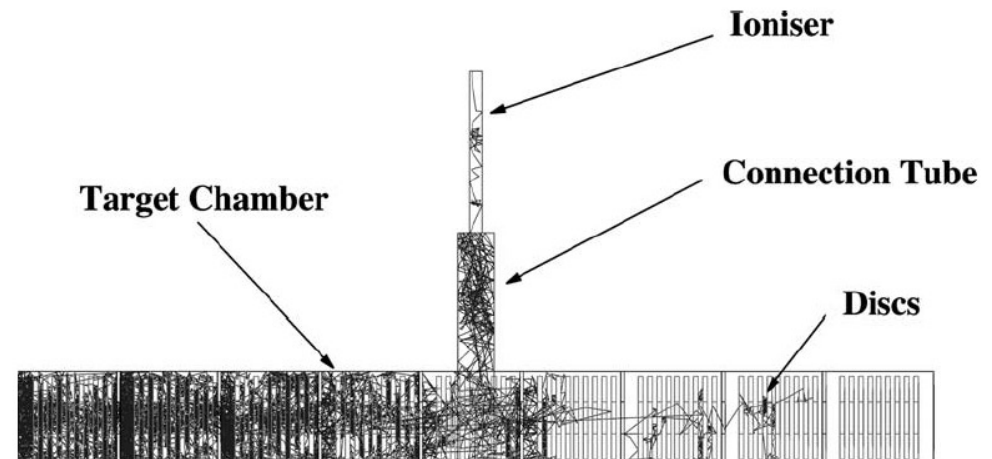
R. Kirchner, Nuclear Inst. and Methods in Physics Research B 70 (1992) 186-199.

ISOL target release: diffusion + effusion

Release curve:

$$\varepsilon_{rel}(\lambda) = \frac{3\upsilon}{\upsilon + \lambda}\left(\frac{W coth(W) - 1}{W^2}\right)$$

$$W = \pi \left(\frac{\lambda}{\mu}\right)^{\frac{1}{2}}$$

$$p(t) = \frac{6\mu\upsilon}{\pi^2}\sum_{n=1}^{\infty}\frac{e^{-\upsilon t} - e^{n^2\mu t}}{\upsilon + n^2\mu}$$

For short lived isotopes and fast effusion (v>>λ>μ), $\varepsilon(\lambda) = \frac{3}{r}\left(\frac{D}{\lambda}\right)^{\frac{1}{2}}$

- Work at the highest possible temperature

- Keep grain size as small as possible

R. Kirchner, Nuclear Inst. and Methods in Physics Research B 70 (1992) 186-199.

ISOL target materials: thermomechanical stability

average stress level during operation with primary beam
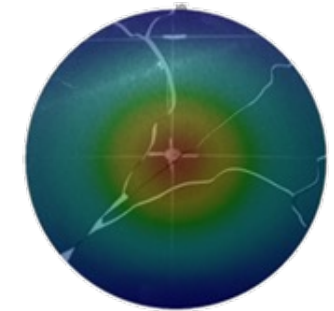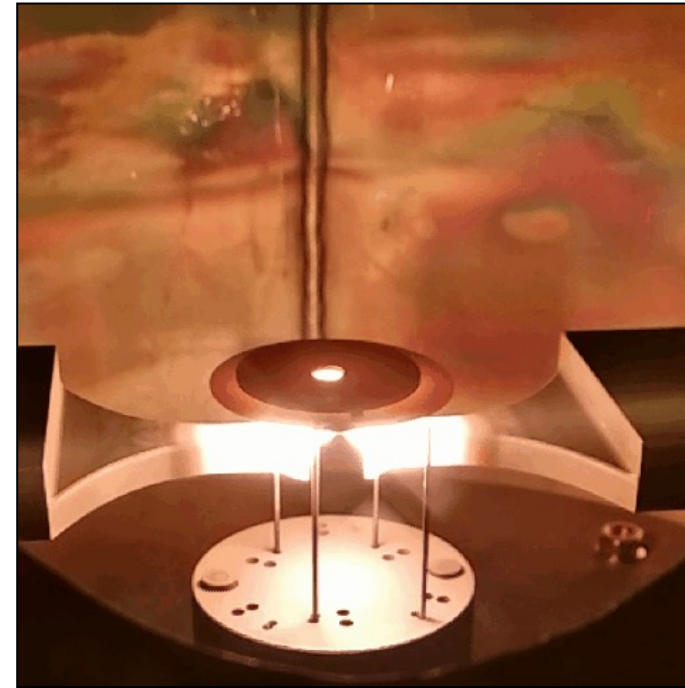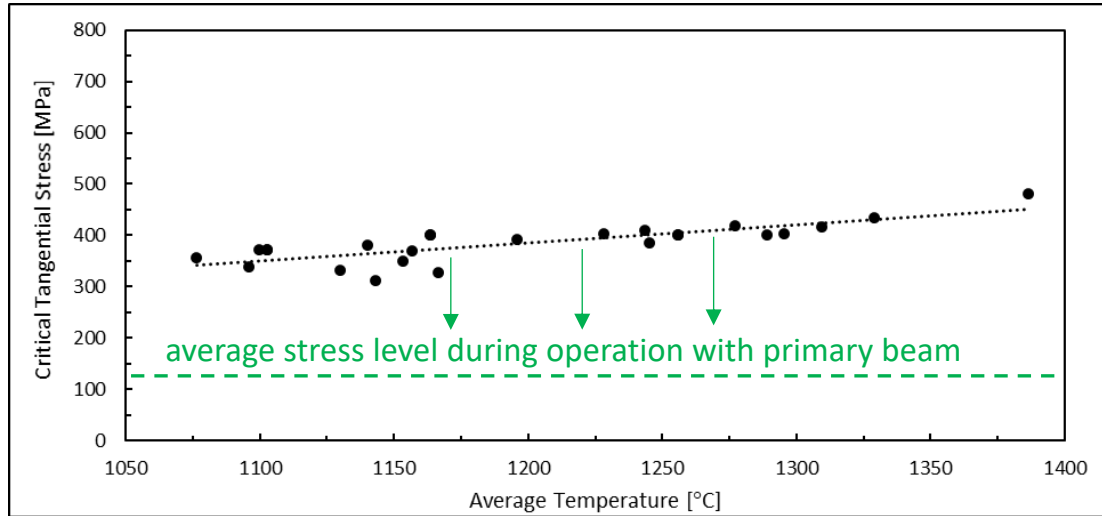
Temperature
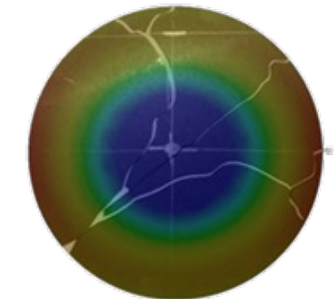
1st principal stress
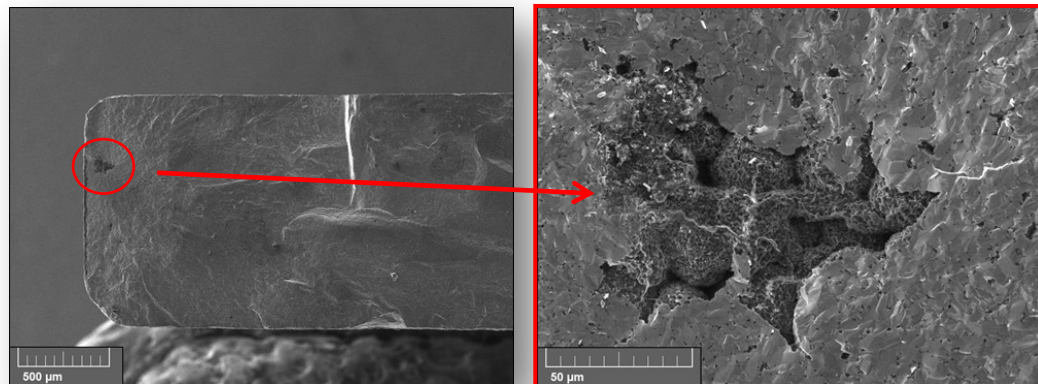
Production process should optimize:

- Thermal conductivity

- Emissivity

- Strengthening mechanisms

ISOL target materials: performance consistency
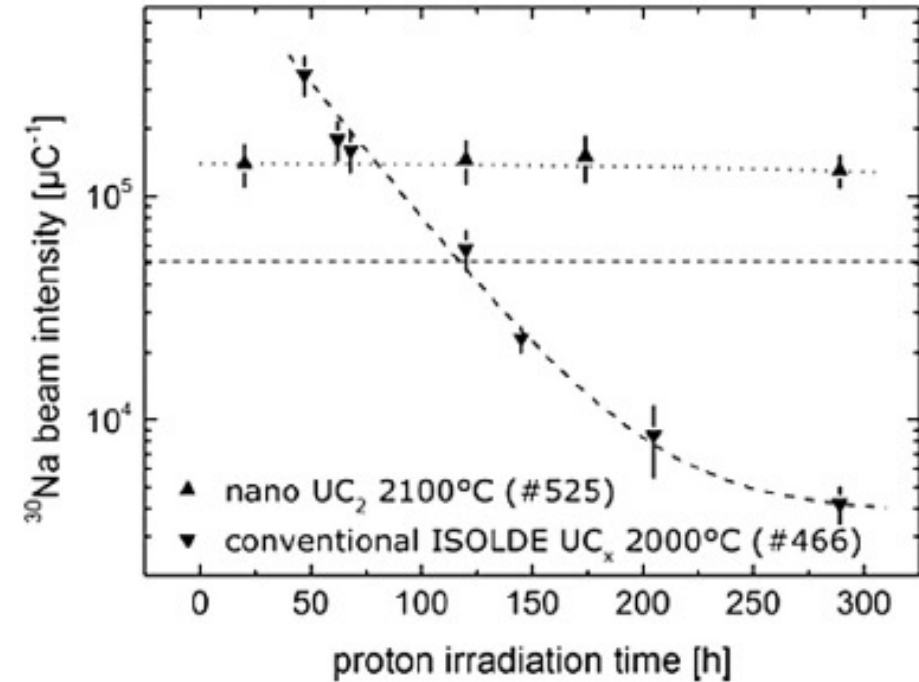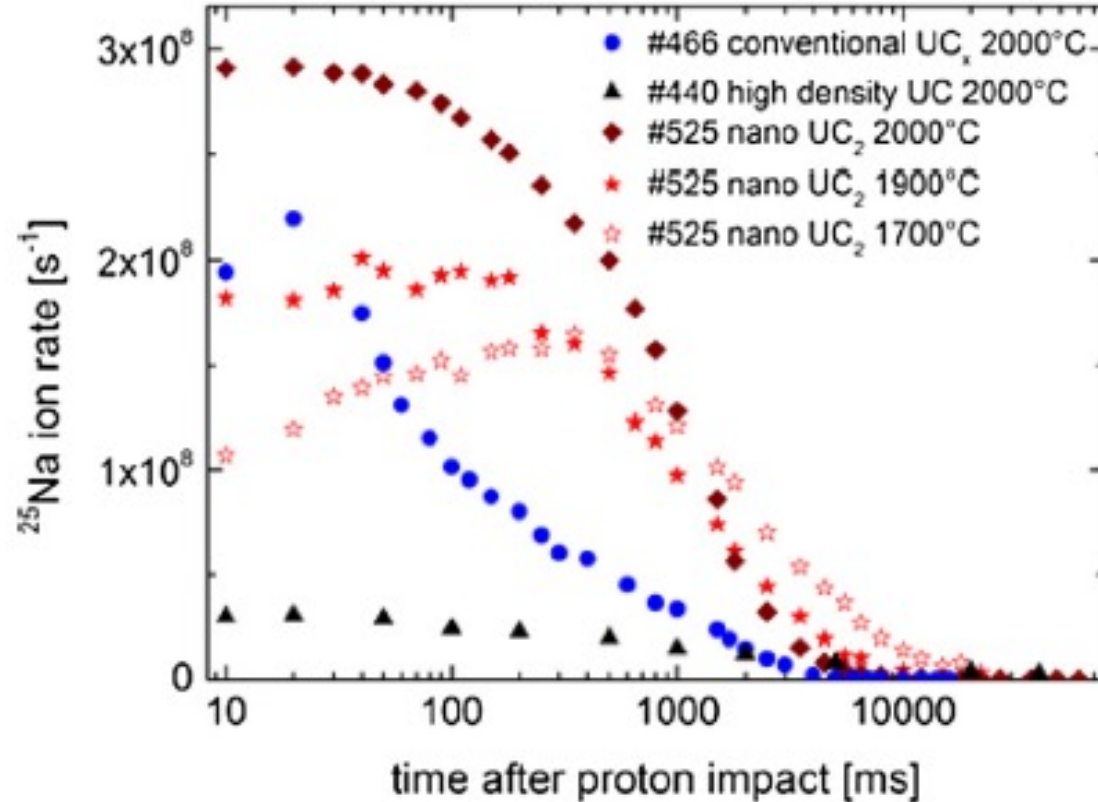
Production process should optimize:

- Presence of nanostructures

A. Gottberg, Nuclear Inst. and Methods in Physics Research B 376 (2016) 8-15.

ISOL target materials requirements

Target working conditions:

- Many days of continuous operation (10 ÷ 15)

- T = 1600 ÷ 2000 °C, even more in some cases

- Tens of kW power to dissipate (irradiation)

- High vacuum

- Radiation (p, n, γ, α, β, …)

Carbide/carbon composites
(UC_2+2C, TiC+2C, ThC_2+2C, …)

Two sets of properties to optimize: nanostructure-porosity and thermo-mechanical
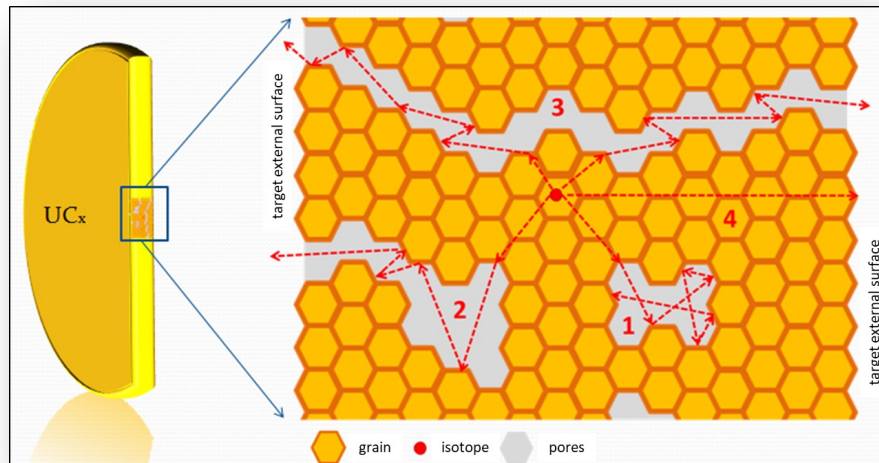
Easy to balance?

(No)

Open porosity and nanostructure to obtain faster and more stable release of isotopes

High thermal properties to efficiently dissipate heat

INFN Istituto Nazionale di Fisica Nucleare
LABORATORI NAZIONALI DI LEGNARO

ISOL target materials

- <u>Oxides</u>: usually constituted by sintered powders, fibers or films deposited onto highly permeable substrates. HfO_2, ZrO_2, Al_2O_3, CaO. Production of Ar and F. Reactivity issues (es. Al_2O_3 in contact with graphite), sintering a big problem for long-term operation. Low thermal conductivity!

- <u>Borides</u>: the more refractory ones have shown a too slow release. In some cases, as for CaB_6, the release was fast, but the amount of impurities contained in the material was too high, thus causing malfunctions in the ion source functioning.

- <u>Sulfides</u>: only a few sulfides are sufficiently refractory to be used as ISOL targets. In particular, CeS has been used for the production of p-rich Cl and P isotopes. Limiting temperature issues in contact with graphite. Not so many refractory ones available.

- <u>Pure metals</u>: metals, either in the form of sintered powders or thin foils have been extensively used as ISOL targets, especially for spallation-based production. The most used metals belong to groups 4 and 5 of the periodic table, since they possess very high limiting temperatures and guarantee fast release of isotopes. Less useful with low energy primary beams. Liquid metals promising but corrosive!

- <u>Carbides</u>: most used materials for ISOL targets, many off-line and on-line tests have been done to demonstrate their capability of fast releasing of short-lived isotopes. To obtain a faster release of isotopes, often the material used as a target consists in a dispersion of the desired carbide in a matrix of excess carbon.

ISOL target materials

Table 2

Overview (not exhaustive) of studied ISOL target materials. Underlined are materials that are currently, or have been recently, used for operations. (*) Engineered micro- or nano-structures have been developed for this material.

ISOL target materials				
Molten	Solid metals	Oxides	Carbides	Others
Au [24,25]	Cm [26]	Al_2O_3* [27,28]	AlC_2 [29]	AlN [28]
Ag [25]	Hf [30]	B_2O_3 [29]	B_4C [29]	BaB_6 [31]
Bi [24]	Ir [32,29]	BaO [33]	C (gr) [29,28]	$BaZrO_3$ [31]
Cd [34]	Ir/C [35]	BeO [36,29,28]	C (MWCNT)* [37–39]	BN [28]
Ce [25]	Ir/Ta [37]	CaO* [33,42,45]	CaC_2 [43]	Ca-zeolite [40]
Ce_3S_4 [31]	Mo [41]	CeO_2 [48]	CmC_x [26]	CaB_6 [33]
Er:Cu [24,25]	Nb [35,44]	Cr_2O_3 [32]	GdC_x [49]	$Ce(OH)_4$ [46]
Ge [47,34]	Os [32]	HfO_2* [50]	LaC_2* [33]	CaF_2 [43]
Gd:Cu [25]	Pu	La_2O_3 [48]	ScC_2 [35,33]	CeB_6 [31]
Hg [34]	Pt/C [44]	MgO [33,45,28]	SiC* [32,44,27,28]	CeS [31,28]
La [34,51]	Re [35,32]	NiO [54]	TaC_x [32,33]	LuF_3 [52]
La:Th [34]	Re/C [30]	SrO [55]	ThC_2 [44,33,26,56]	Na-zeolite [40]
La:X [34]	Ru [32]	Ta_2O_3 [30,32]	TiC* [32,38]	Ta_5Si_3 [32]
NaF:LiF [53]	Ru/C [30]	ThO_2* [48,32,50]	UC_x* [58,31,26,56]	Hf_5Ge_3 [32]
$NaF:ZrF_4$ [53]	Si layers [41]	TiO_2* [50]	VC [31,32]	Hf_5Si_3 [29]
Nd [25]	Sn/C [44]	UO_2 [59]	ZrC [32,59,49]	Hf_5Sn_3 [32]
Ni [25]	Ta* [35,57,29]	Y_2O_3* [61]		Ta_5Si_3 [32]
Pr [25]	Ti [35,44]	ZrO_2 [34,32,50]		Tl-zeolite [40]
Pt:B [24]	Th [41,26]			$Th(OH)_4$ [46]
Sc:La [34]	Th/Nb [35]			Zr_5Ge_3 [32,28]
Sn [34,60]	U [26]			Zr_5Si_3 [32,28]
Tb [34]	U/C [32]			
TeO_2:KCl:LiCl [32]	V [35,31]			
ThF_4:LiF [24]	W [31]			
Pb [34,51]	Zr [35,59]			
Pb:Bi [62]				
Y:La [34]				
U [63]				
U:Cr [34]				
Zn [34]				

A. Gottberg, Nuclear Inst. and Methods in Physics Research B 376 (2016) 8-15.

ISOL target materials
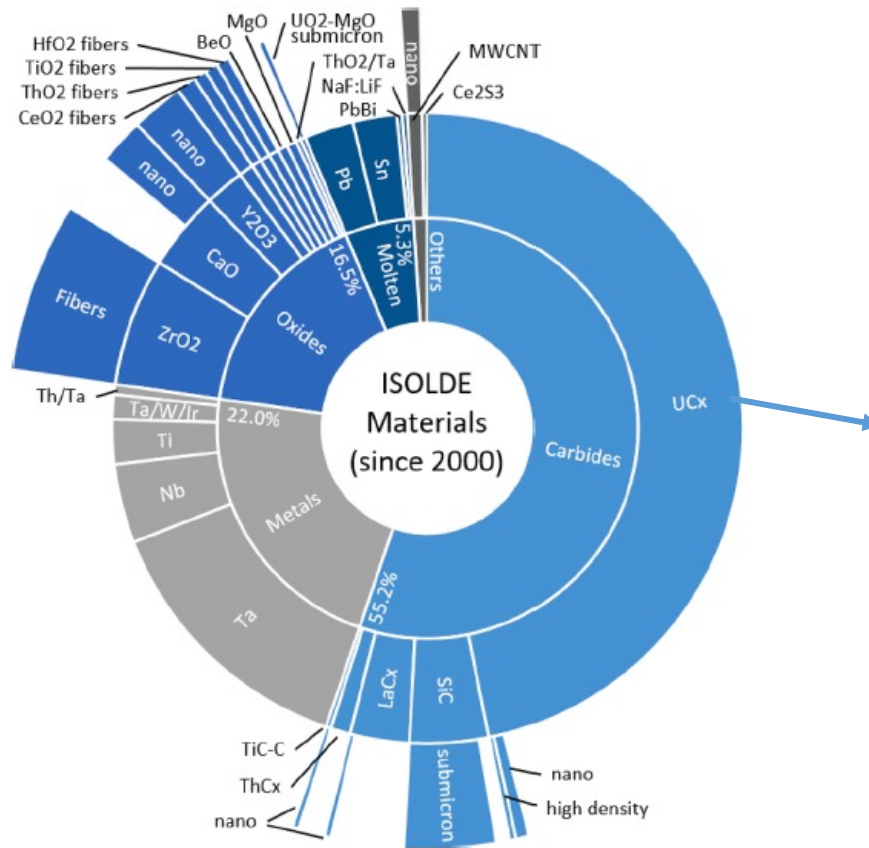
Targets used at ISOLDE 2000-2019
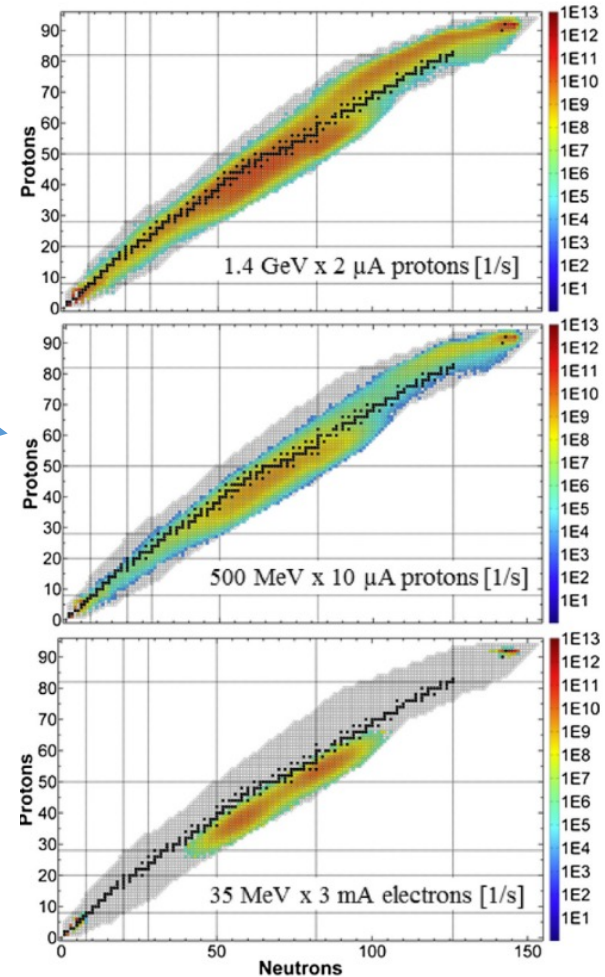
J.P. Ramos, Nuclear Inst. and Methods in Physics Research B 463 (2020) 201–210.   *A. Gottberg, Nuclear Inst. and Methods in Physics Research B 376 (2016) 8-15.*

Carbides

SiC

B$_4$C

TiC
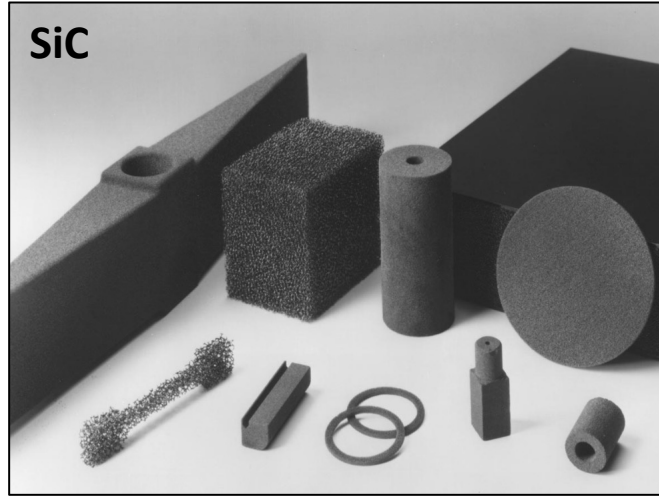
Generally speaking, a carbide is a compound formed by carbon with other elements with lower or about equal electronegativity. Most of these compounds are ceramics, and some of them are actually refractory, since they have high thermal and chemical stability and can therefore be used in extreme environments.

Synthesis:
- Direct reaction of metal with carbon: xM + yC → MxCy
- Reaction of metal with gas (hydrocarbons): thin films
- Carbothermal reduction: oxide + carbon → carbide + CO (high vacuum)
- Sol-gel process: lower temperature for the synthesis, followed by carbothermal reduction

Production techniques: traditional

Carbothermal reduction

Oxide + carbon → Carbide + (carbon) + CO

Weighing raw materials → Mixing → Grinding → Pressing → Heat treatment
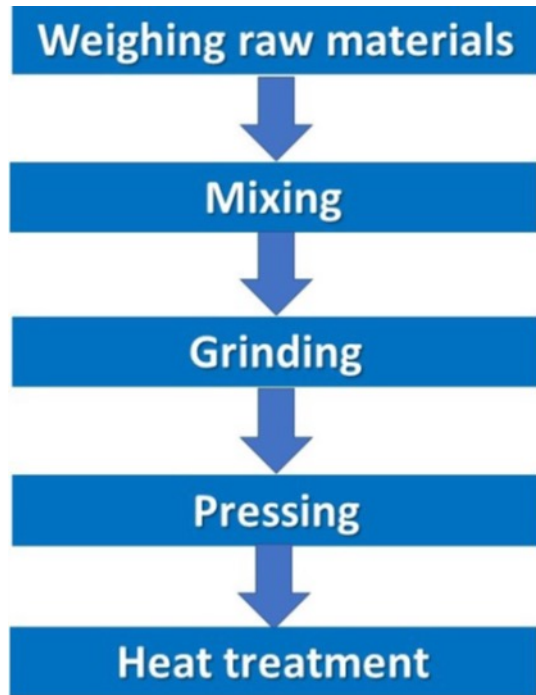
La_2O_3 + C after pressing
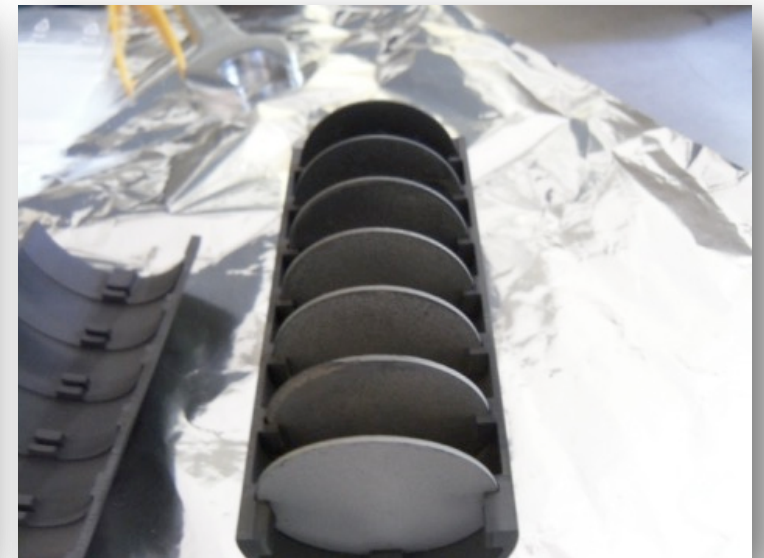
LaC_2 + 2C after heat treatment

Optimization of properties by:

- Choice of carbon precursors and residuals
- Heat treatment parameters

Production techniques: traditional

Raw materials → Sieving ⇄ Mixing/milling → Pressing → Carbothermal reduction → Sintering
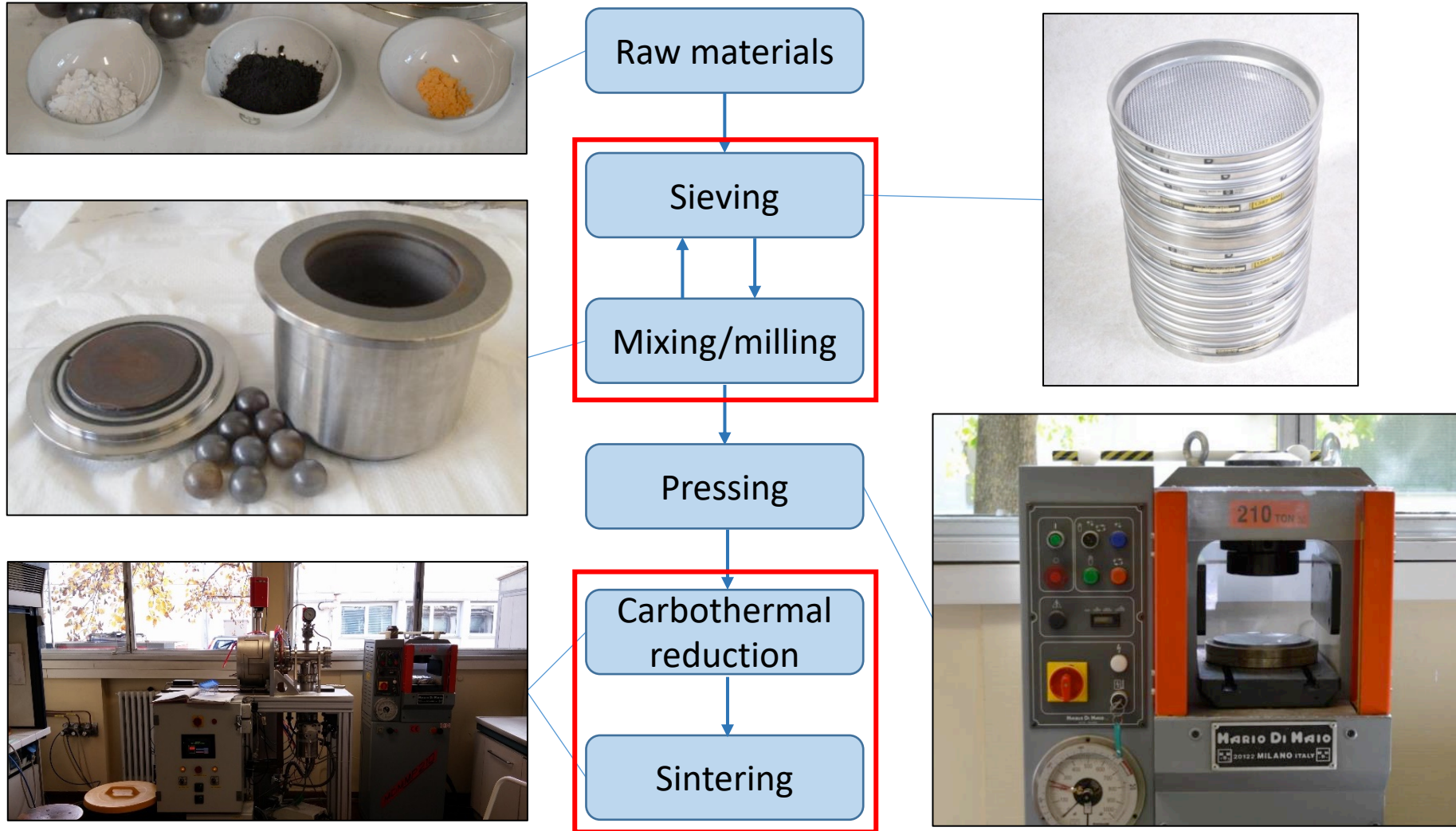
Production techniques: sol-gel
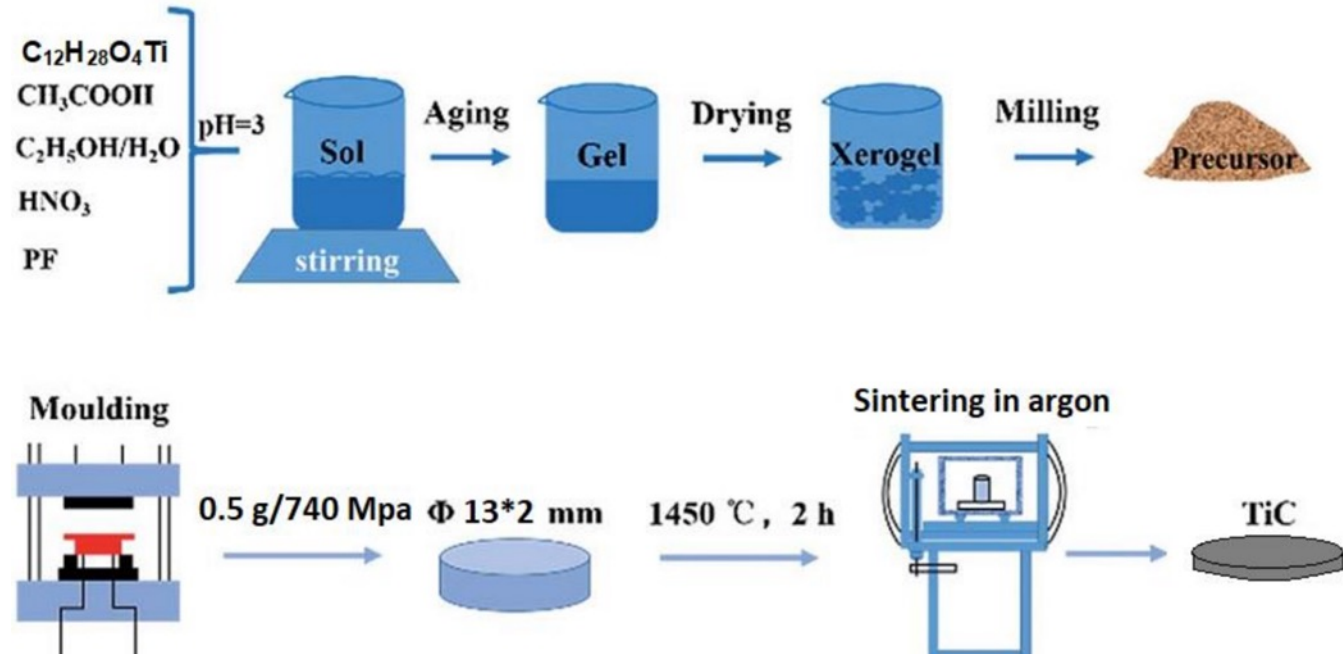
Sol to gel
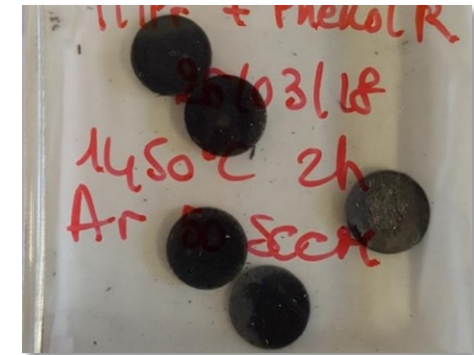
TiC targets after thermal treatment (sintering)

Optimization of properties by:

- Choice of organic/inorganic precursors
- Sol-gel conditions
- Heat treatments parameters

Production techniques: casting

Optimization of properties by:

- Choice of carbon precursors and residuals (and backing)
- Heat treatment parameters

M. Cervantes, P. Fouquet-Métivier, P. Kunz, et al., Nuclear Instruments and Methods in Physics Research B 463 (2020) 367–370.

Production techniques: electrospinning
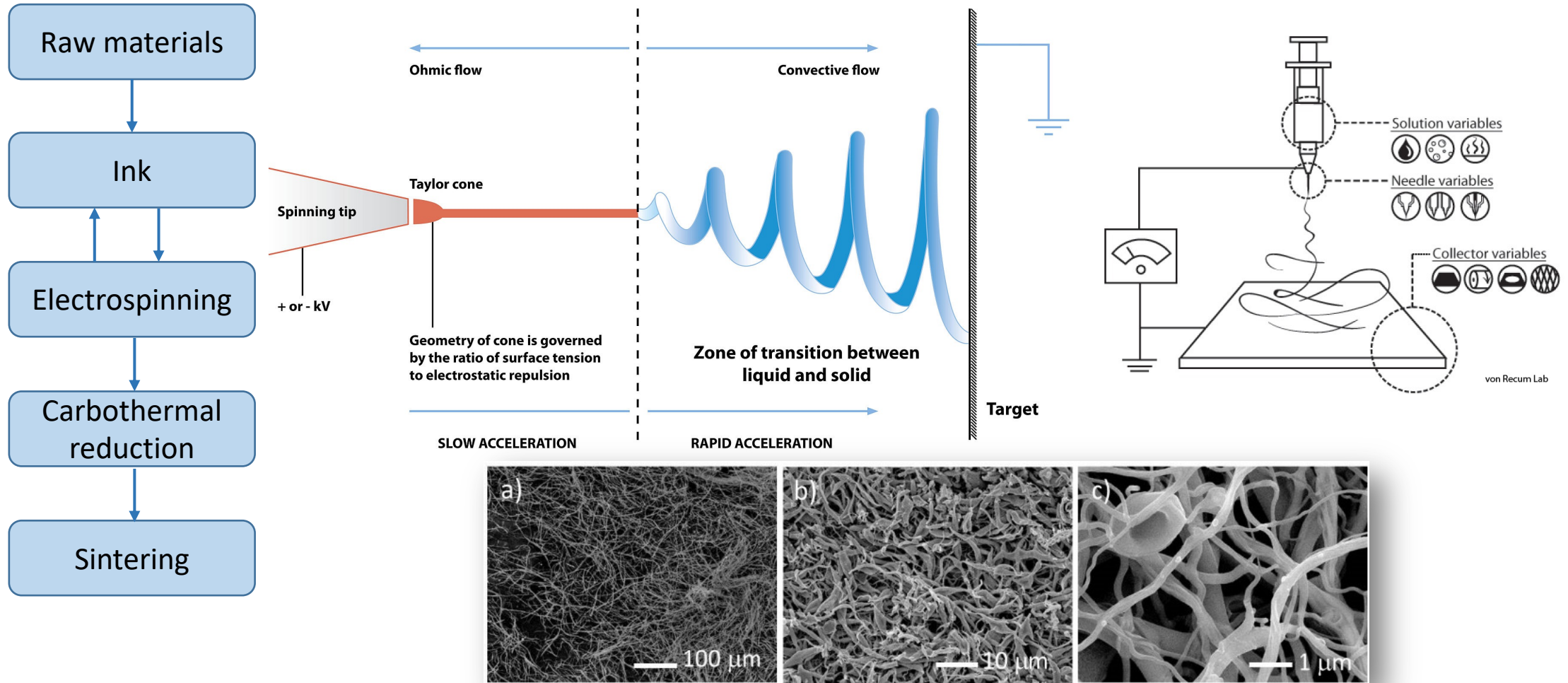
S. Chowdhury, L. Maria, A. Cruz, et al., Nanomaterials 10 (2020) 2458.

Production techniques: additive manufacturing

Ceramic ink formulation

AM Techniques

Porous Microstructure after thermal treatment

DIW ink

PµSL ink

3YZ NPs + PEGDA + thermal or photo-initiator

Initial parameters affect material properties after thermal treatment
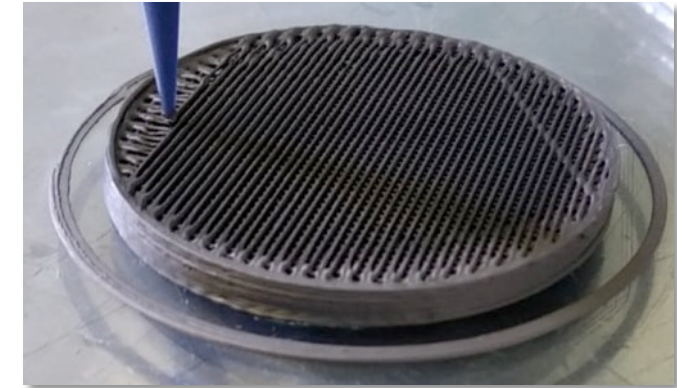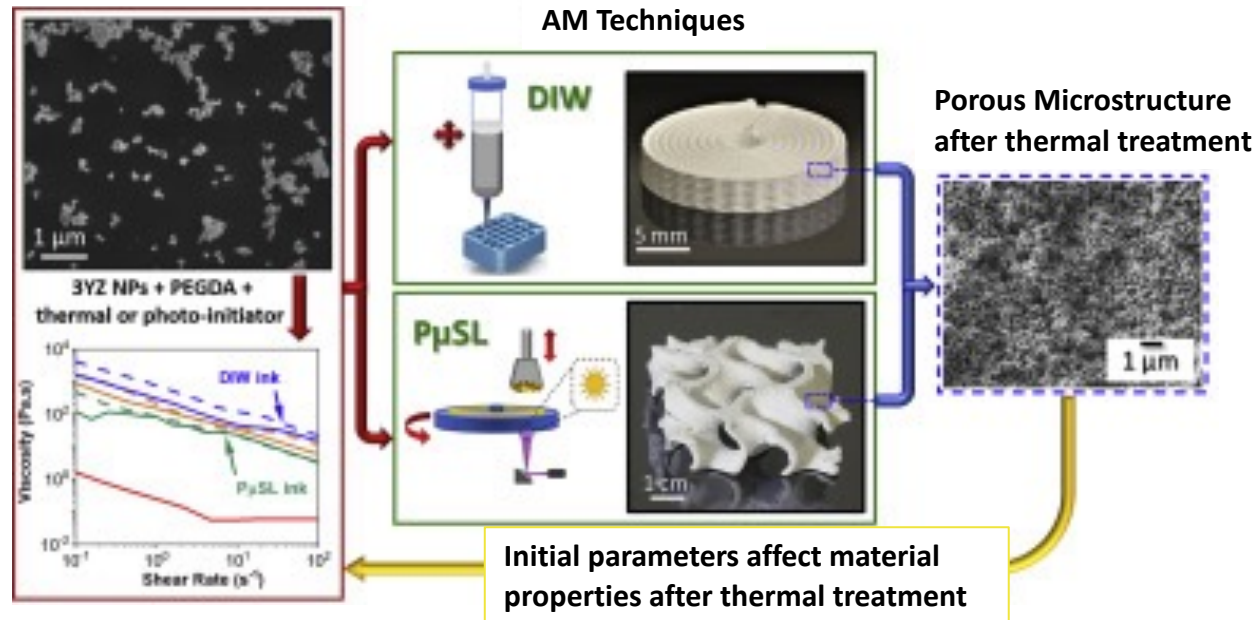
Printing process

After thermal treatment (sintering)

Optimization of properties by:

- Choice of organic/inorganic precursors
- Printing stage
- Heat treatments parameters

Additive Manufacturing of ceramics
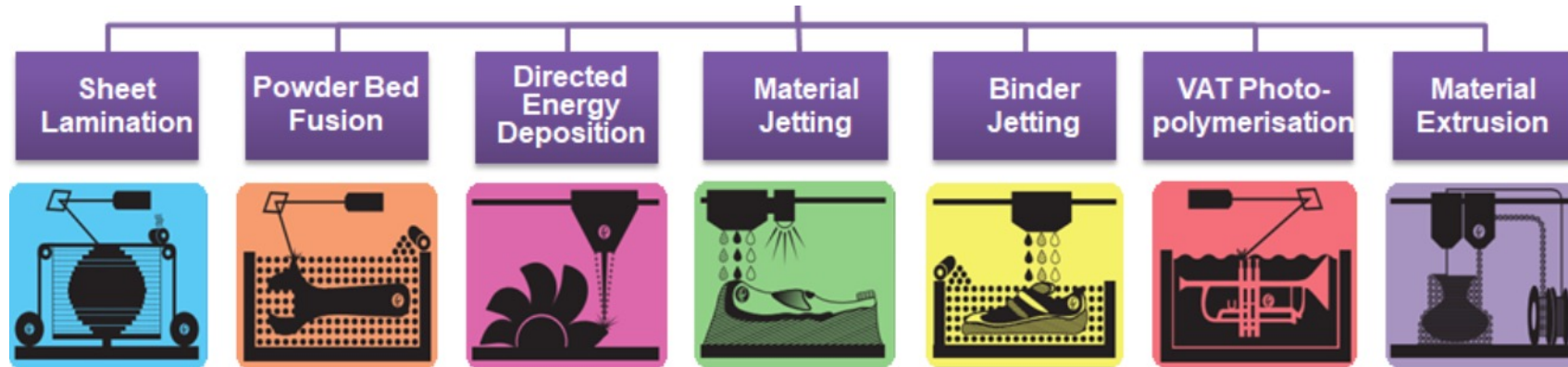
infographic courtesy of Hybrid Manufacturing Technologies

AM Technology	Feedstock (liquid, paste, powder, filament)	Part dimension$ (size that can be produced economically)	Surface (quality of parts, not of single struts)	Printing resolution
Binder jetting	Powder	M-XL	Medium	100 µm
Inkjet printing	Liquid	XS-M	High	10 µm
Laminated object manufacturing	Paste	M-L	Low	100 µm
Direct ink writing	Paste	S-XL	Low	60 µm
Fused deposition modeling	Filament	M-XL	Low	100 µm
Vat photopolymerization	Liquid	XS-M	High	25 µm
Two-photon polymerization	Liquid	XS-S	High	< 1 µm

$: XS = 100 µm; S = 1 mm; M = 10 mm; L = 0.1 m; XL = 1 m

P. Colombo, J. Schmidt, G. Franchin, A. Zocca, J. Günster, Bull. Am. Ceram. Soc., 96 (2017) 16.

Sintering
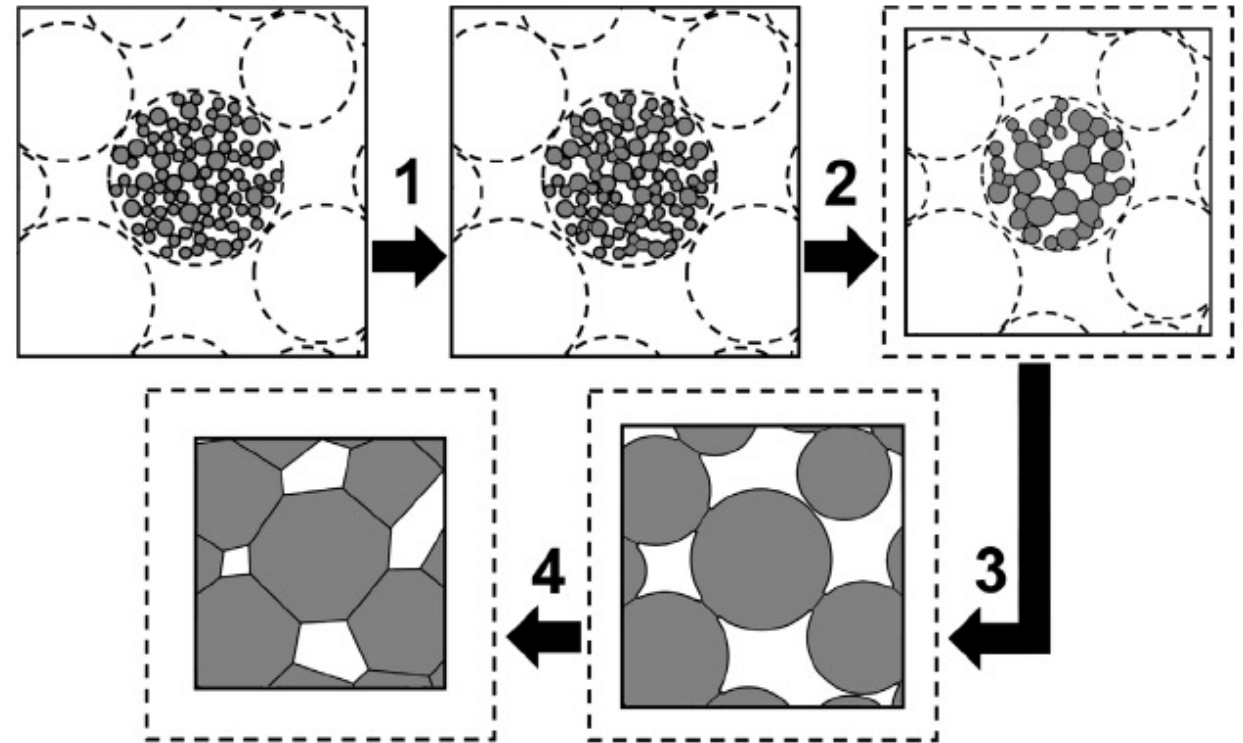
Careful with too much sintering!

C.B. Carter, M.G. Norton, Ceramic Materials, Science and Engineering, 2nd edition, Springer, New York, 2013

J.P. Ramos, A.M.R. Senos, T. Stora, et al., Journal of the European Ceramic Society 37 (2017) 3899-3908.

Characterization: micro and nanostructure

Electron microscopy
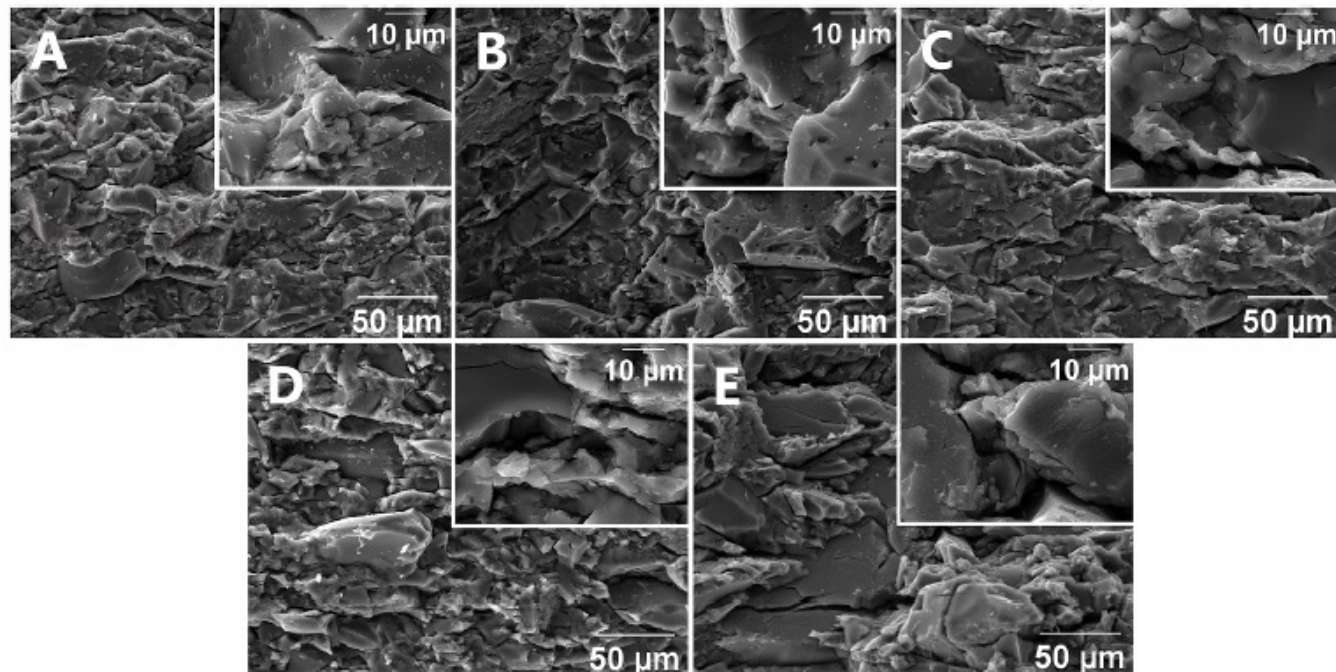
Scanning electron microscopy to study microstructure
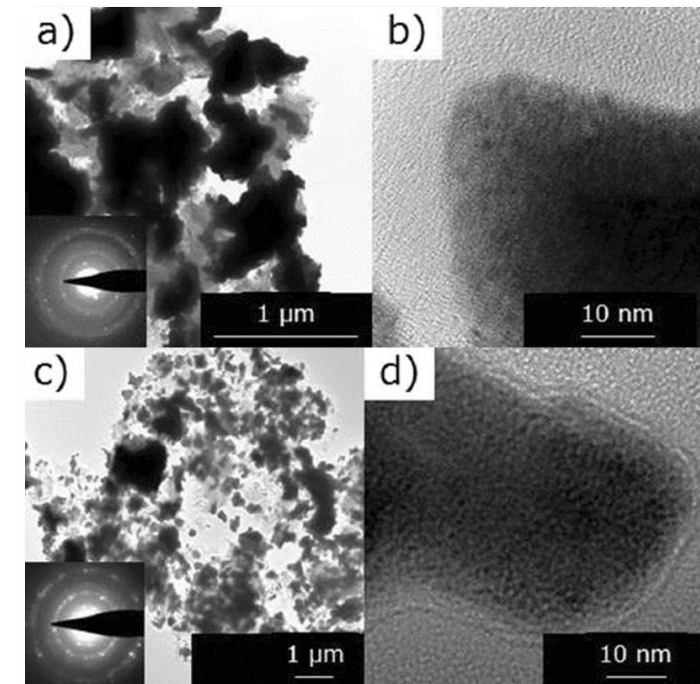
Transmission electron microscopy to study nanostructure

A. Zanini, S. Corradetti, S.M. Carturan, et al., Microporous and Mesoporous Materials 337 (2022) 111917.

L. Biasetto, S. Corradetti, S.M. Carturan, et al., Scientific Reports 8 (2018) 8272.

Characterization: porosity

Amount of pores
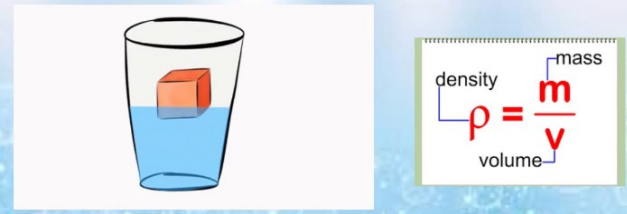
$$P_{tot} = 1 - \frac{\rho_{bulk}}{\rho_{th}}$$

Archimede's

Picnometry
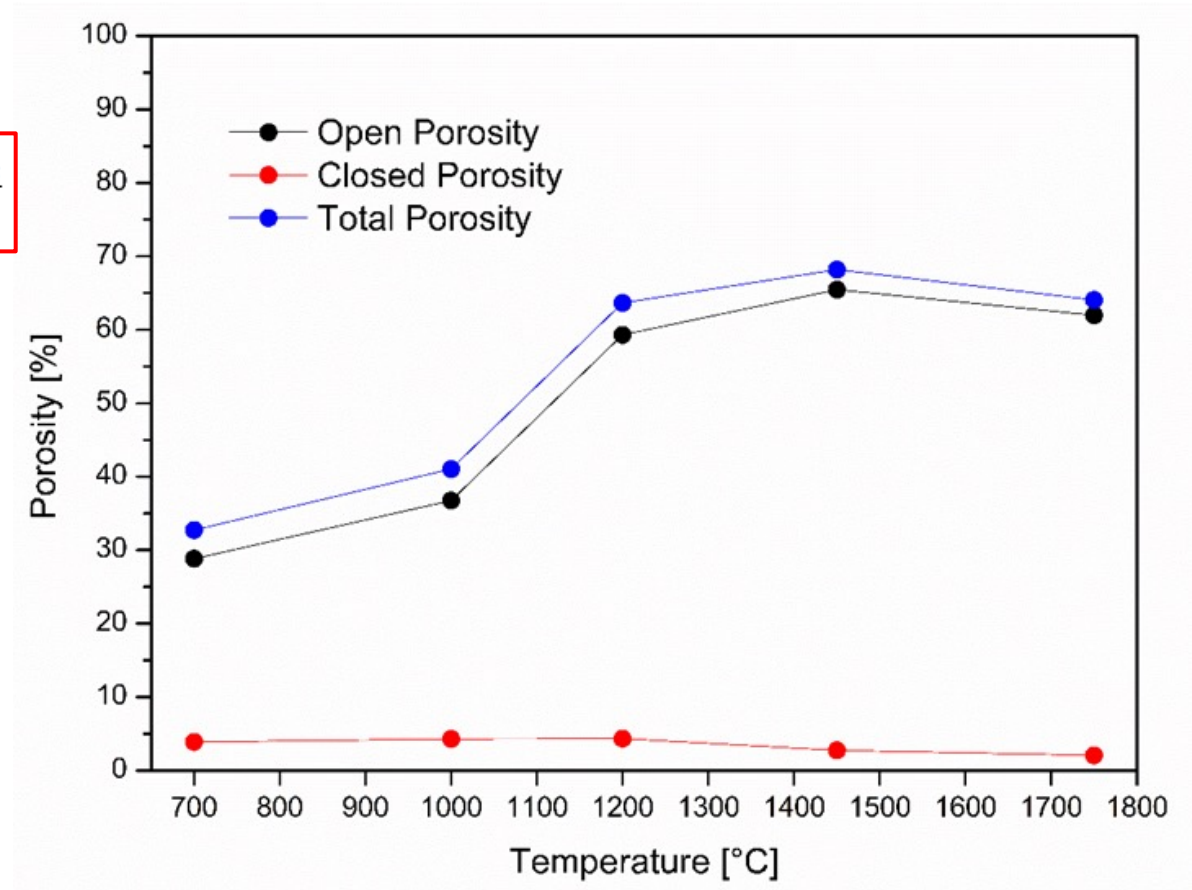
Characterization: porosity

Type and size of pores – micropores (<2 nm), mesopores (between 2 and 50 nm)

Gas physisorption
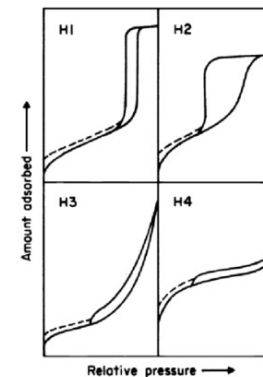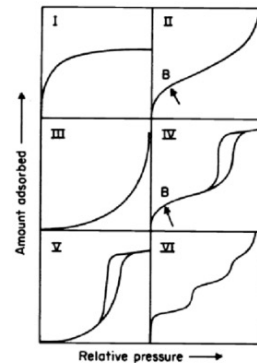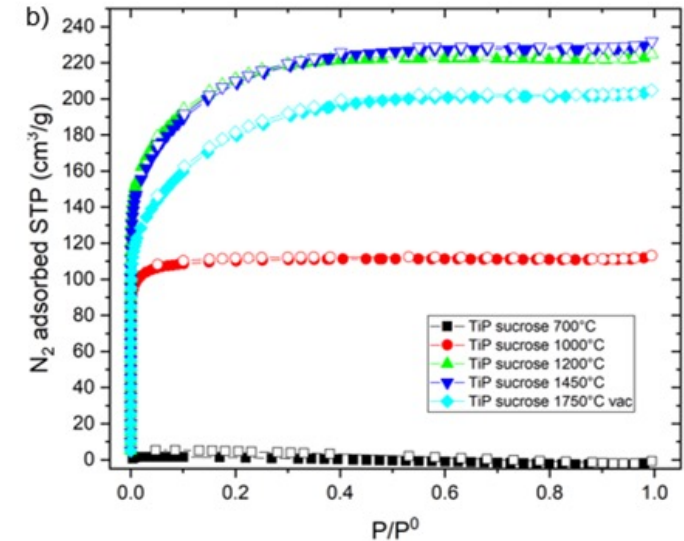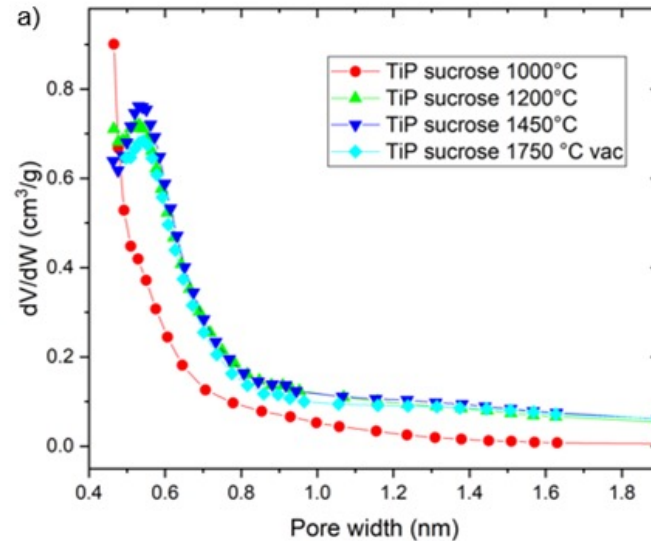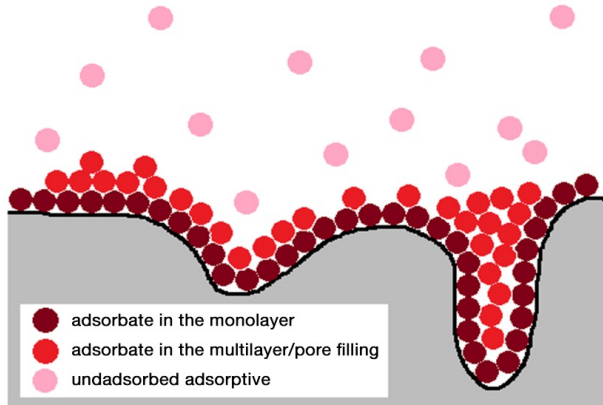
Allows calculation of surface area [m²/g] through different methods (BET for example)

Characterization: porosity
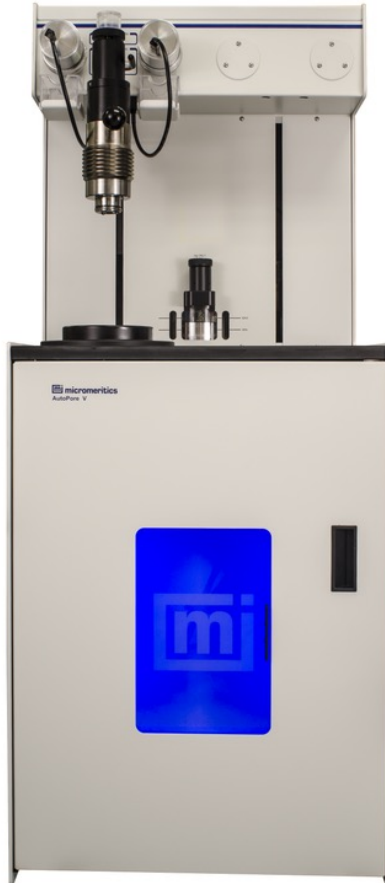
Type and size of pores – macropores (> 50 nm)

Hg porosimetry
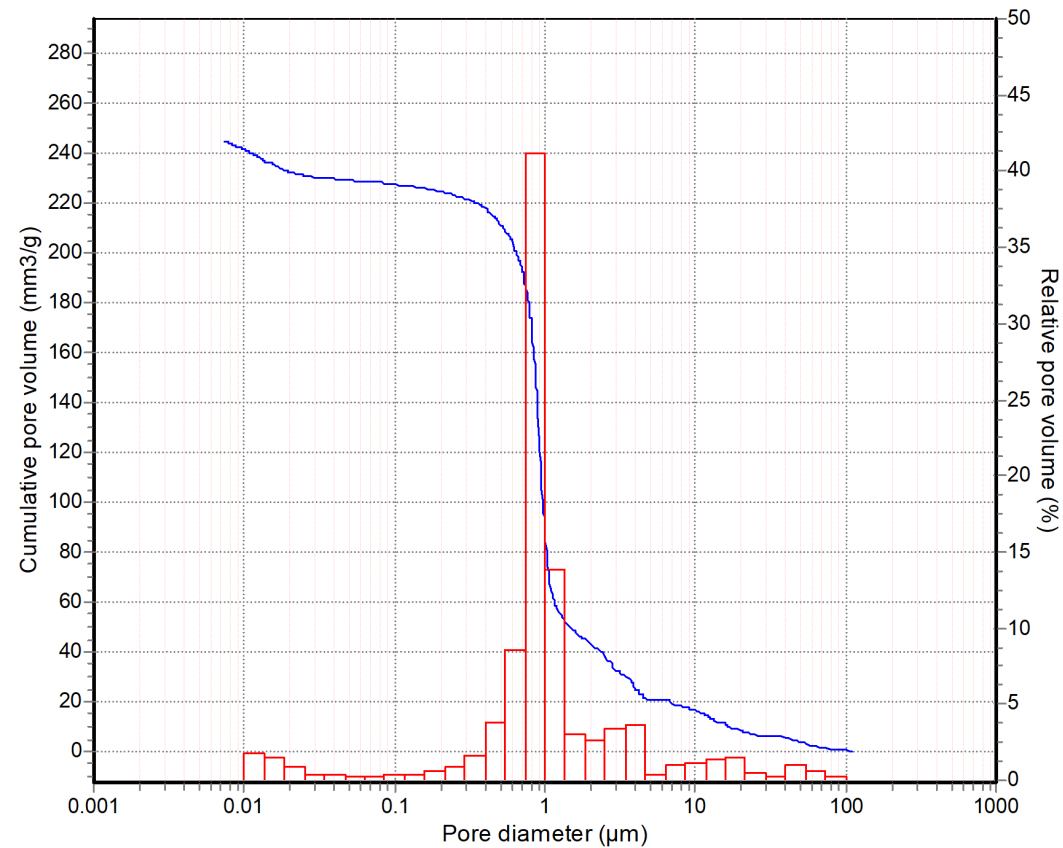
D. Sciti, S. Corradetti, et al. , Journal of the European Ceramic Society, in press, https://doi.org/10.1016/j.jeurceramsoc.2024.04.072

Characterization: porosity

https://www.micromeritics.com/autopore-v/
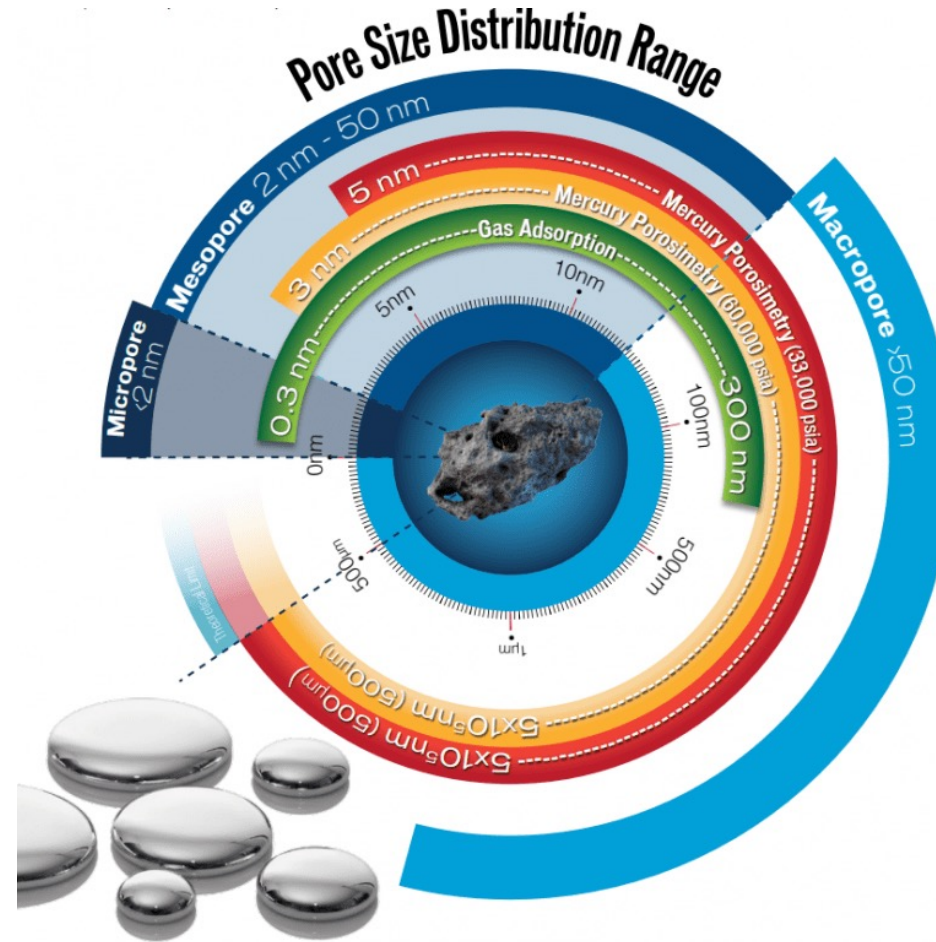
Characterization: thermal properties

Thermal conductivity and emissivity
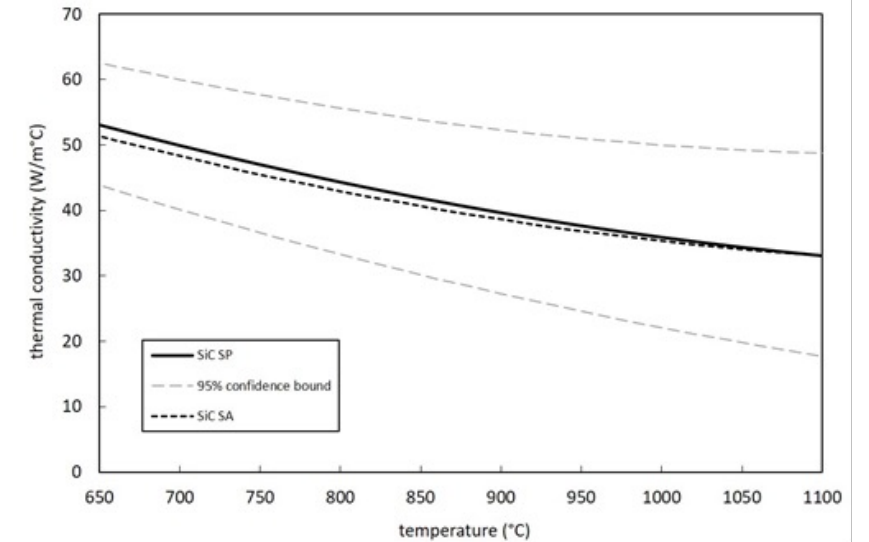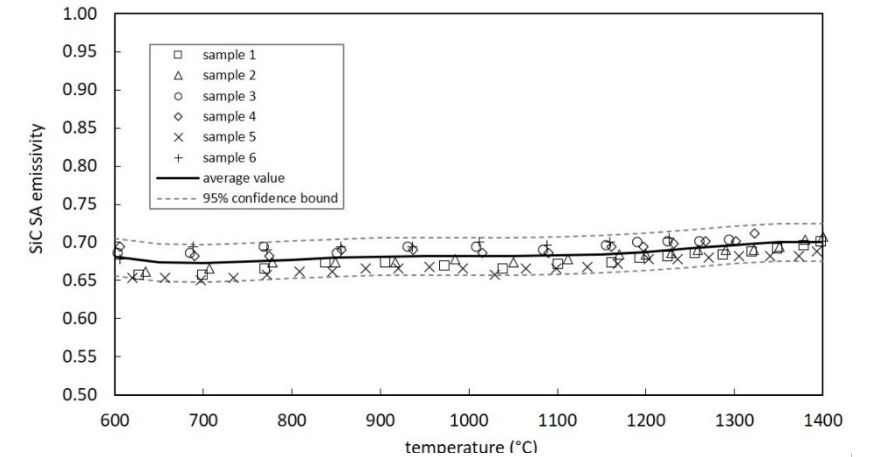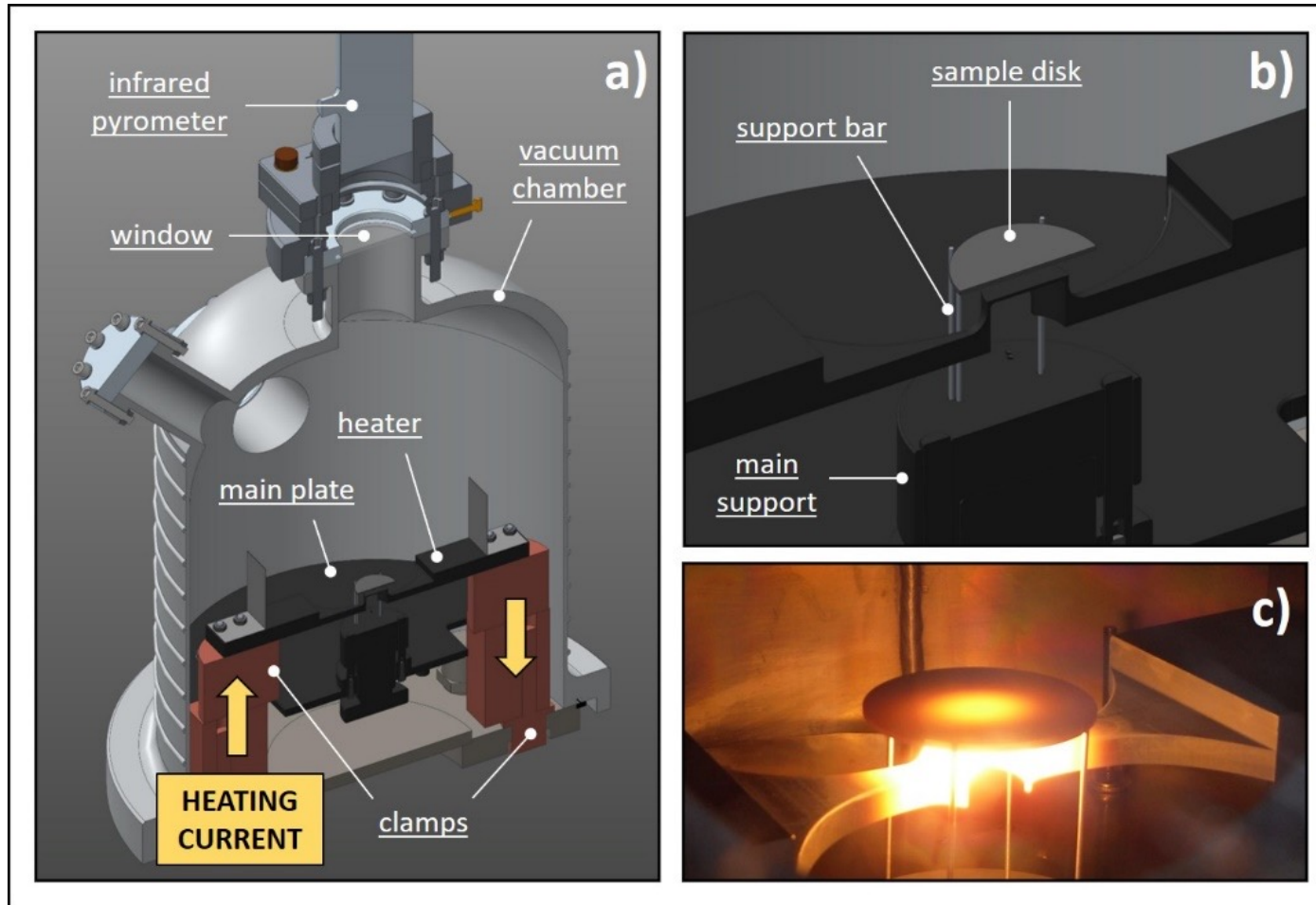
Characterization: thermal properties

Thermal conductivity – laser flash
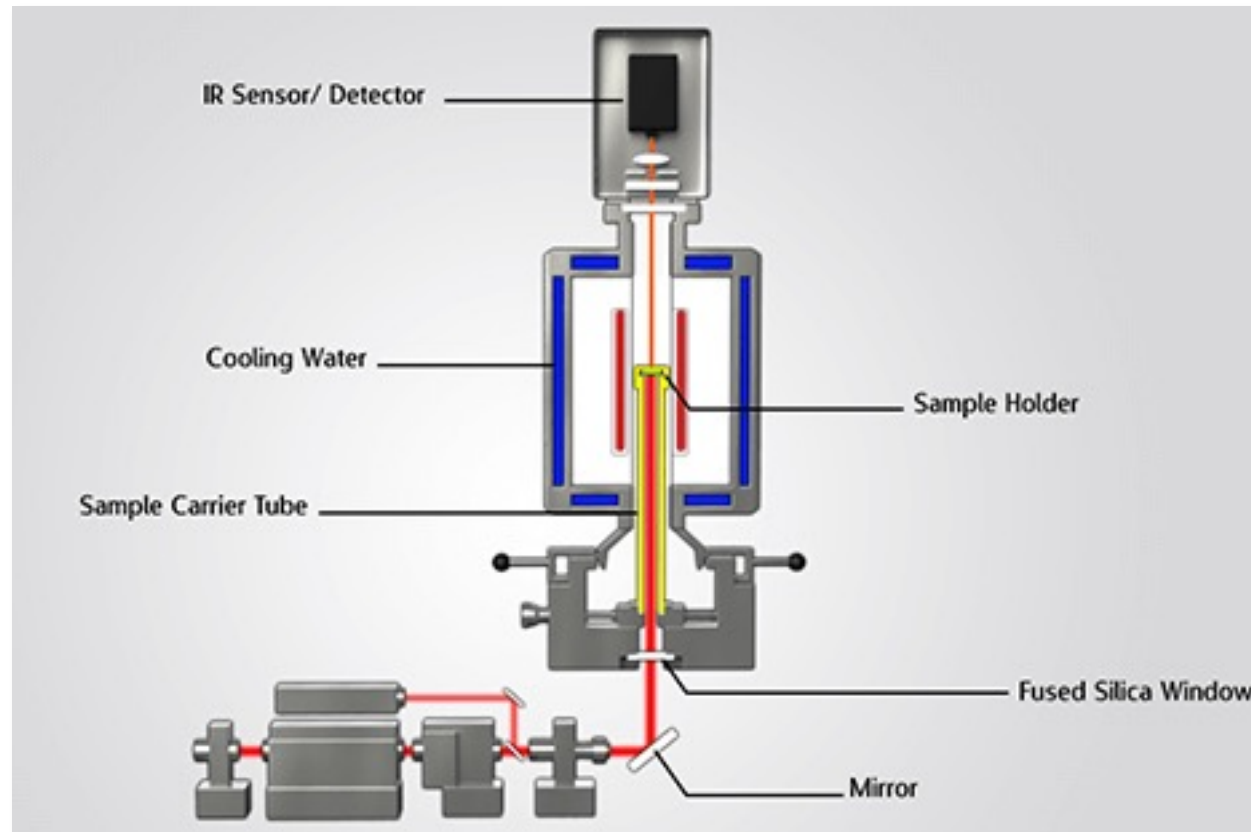
$k = \alpha \cdot \rho \cdot c_p$, where: k thermal conductivity [W/m*K], α thermal diffusivity [m²/s], ρ density [kg/m³], c_p specific heat [J/kg*K]

Characterization: thermal properties

Thermal conductivity – steady state and inverse analysis
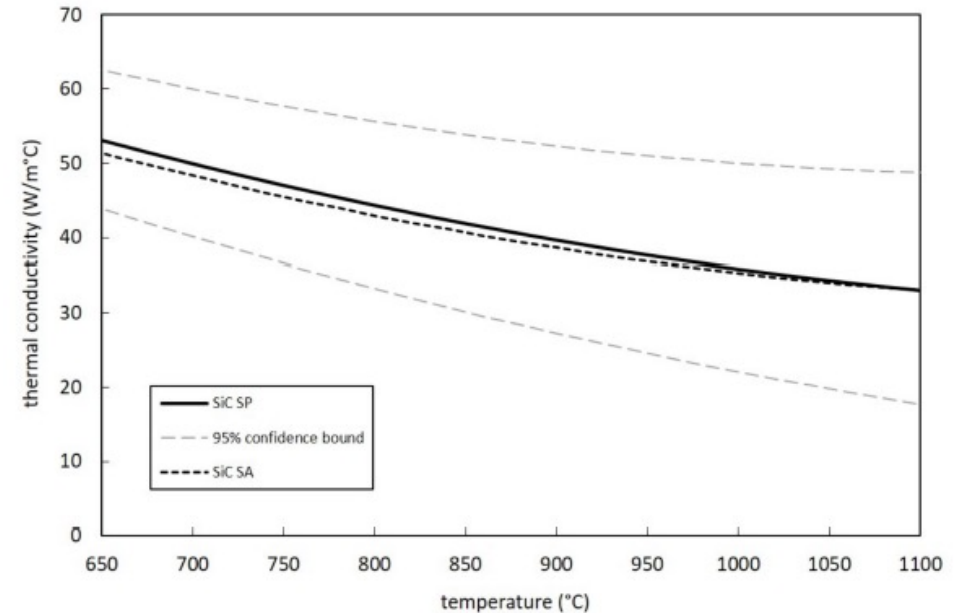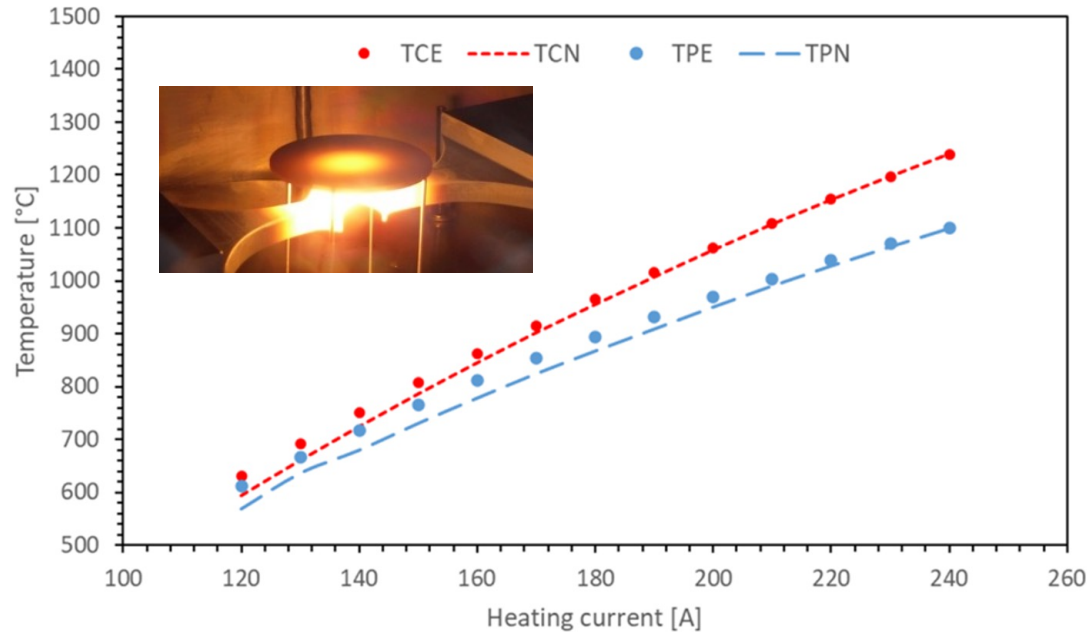
Minimizing a residual function $J(f) = \sum_{i=1}^{N_{CS}} \left[T_{C_{COMP_i}}(f) - T_{C\_MEAS\_i} \right]^2 + \left[T_{P_{COMP_i}}(f) - T_{P\_MEAS\_i} \right]^2$, where
$f = \{f_1, f_2, f_3\} = \{C_0, C_1, C_2\} \rightarrow k = C_0 + C_1 \cdot T + C_2 \cdot T^2$

M. Manzolaro, S. Corradetti, M. Ballan et al., Materials 14 (2021) 1689.

Characterization: thermal properties

Emissivity
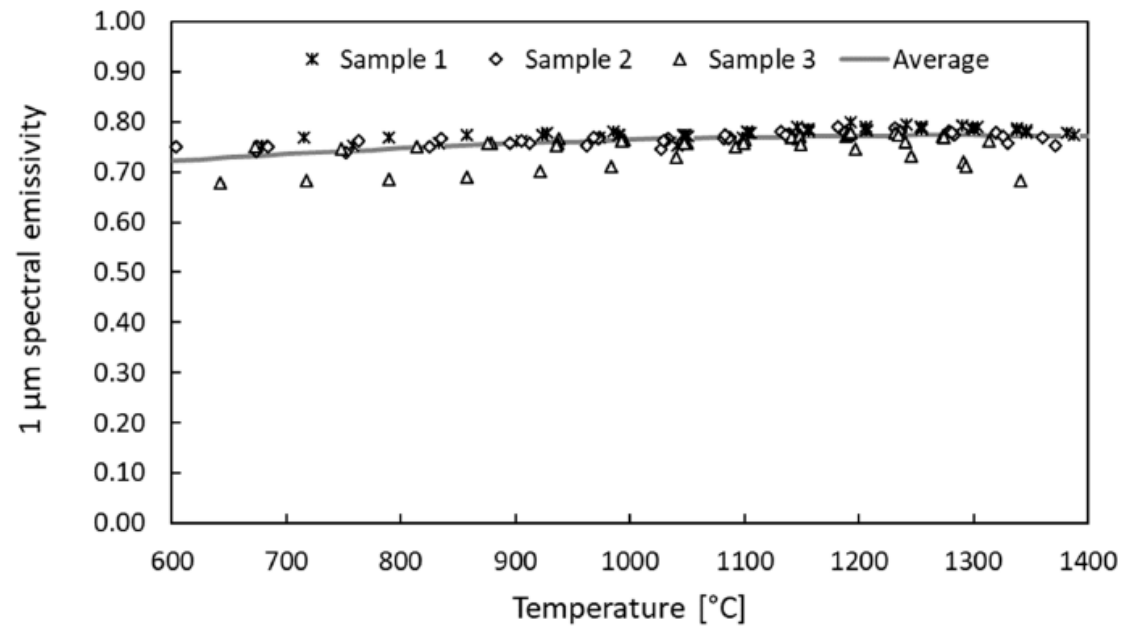
M. Ballan, S. Corradetti, M. Manzolaro, et al., Materials 15 (2022) 8358.
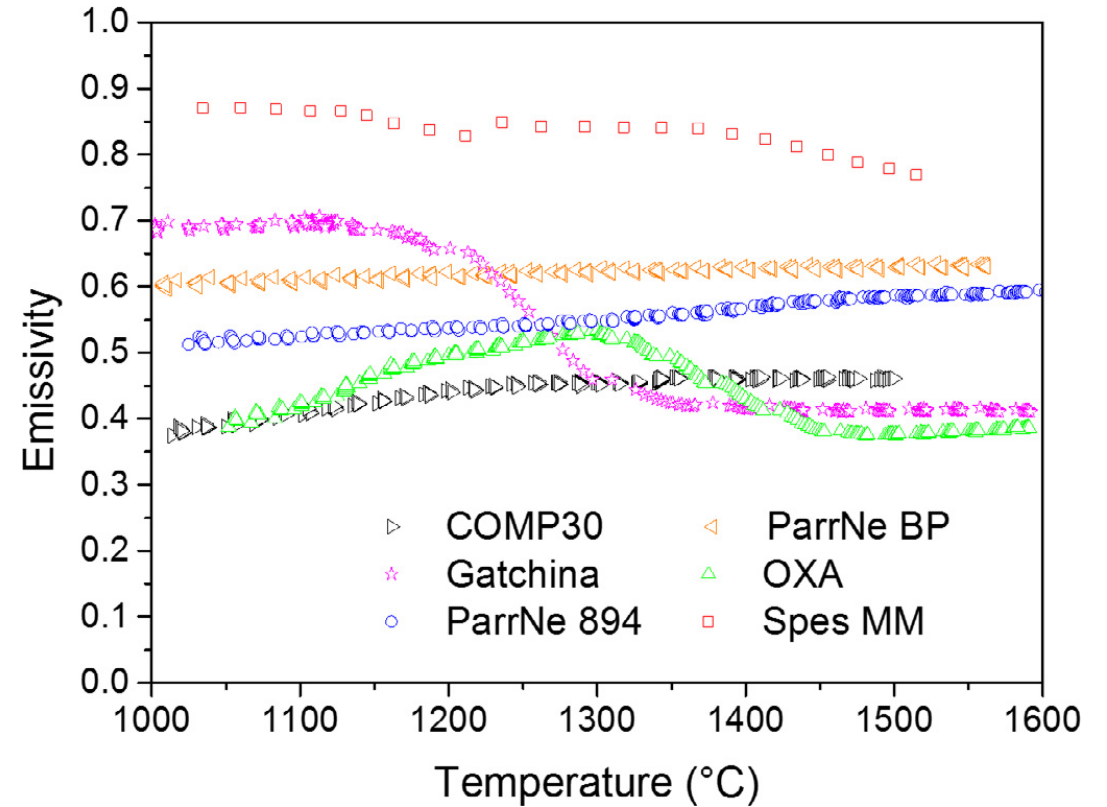
S. Corradetti, M. Manzolaro, A. Andrighetto, et al., Nuclear Instruments and Methods in Physics Research B 360 (2015) 46–53.
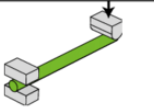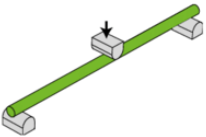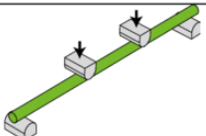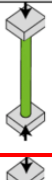
Characterization: structural properties
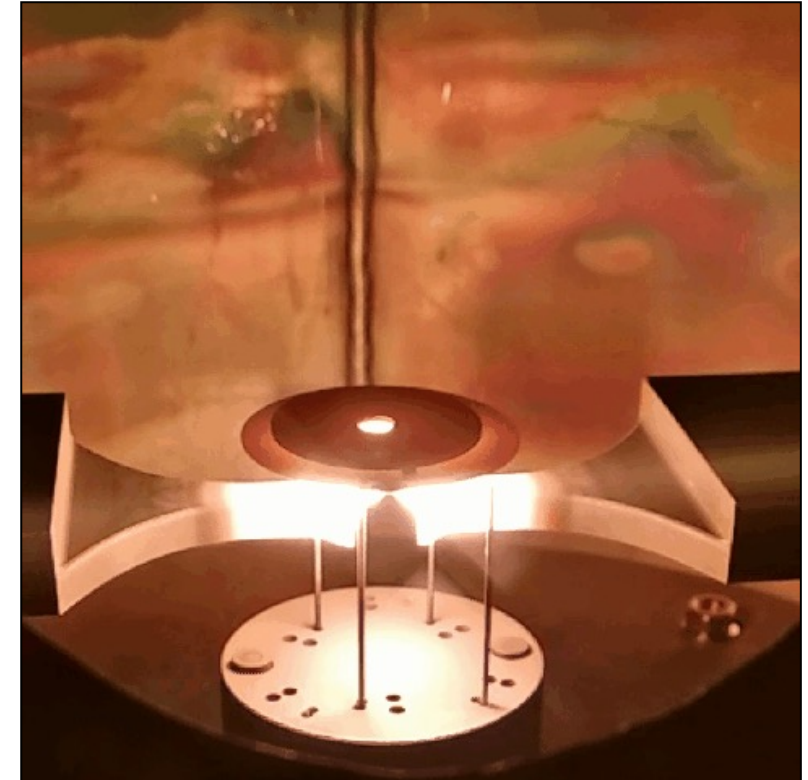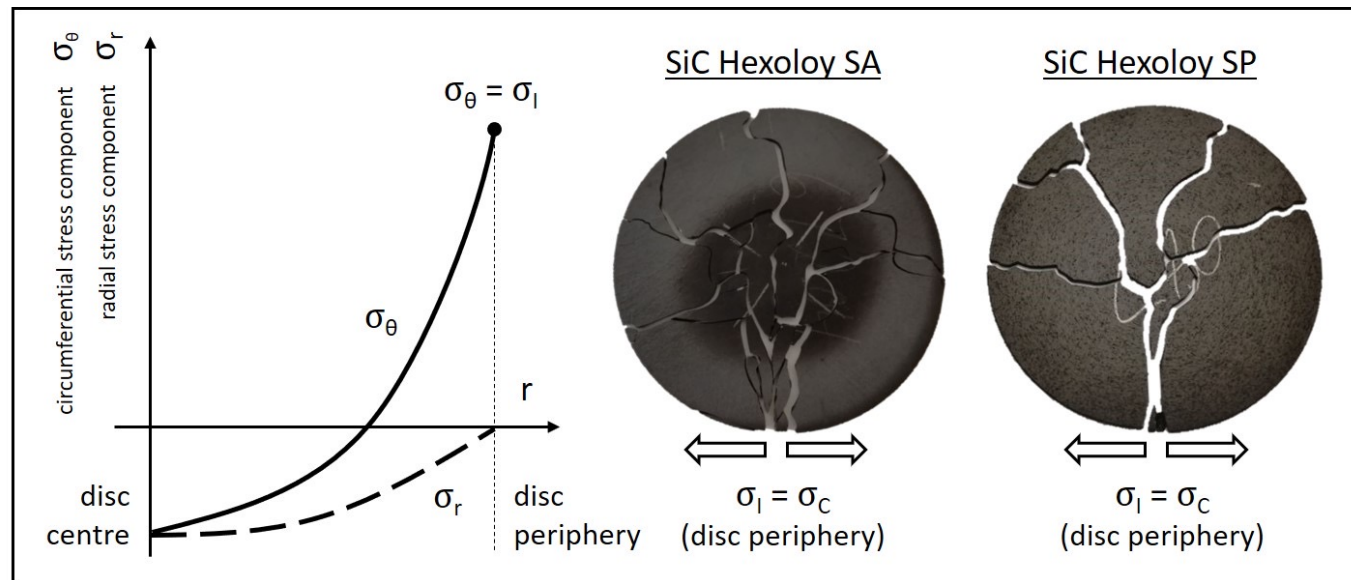
M. Manzolaro, S. Corradetti, M. Ballan et al., Materials 14 (2021) 1689.

Characterization: structural properties

Tensile, flexural or compression mechanical properties

Test type		Properties measured	Examples
Cantilever bend		Bending strength, elastic modulus	(Henry and Thomas, 2002; Caliaro et al., 2013)
Three-point bend		Bending strength, elastic modulus	(Skubisz, 2001, 2002; Petutschnigg and Katz, 2004; Green et al., 2006; Lim et al., 2011; Christoforo et al., 2012; Ampofo et al., 2013; Slater and Ennos, 2013; Lemloh et al., 2014)
Four-point bend		Bending strength, elastic modulus	(Goubet et al., 2009; Robertson et al., 2015)
Tension		Tensile strength, elastic modulus	(Spatz et al., 1998; Ryden et al., 2003; Cavalier et al., 2008; Abasolo et al., 2009)
Buckling		Critical buckling load	(Niklas, 1998; Spatz et al., 1998; Frese and Blass, 2014)
Compression		Compressive strength, elastic modulus	(Niklas, 1998; Wright et al., 2005; Frese and Blass, 2014)
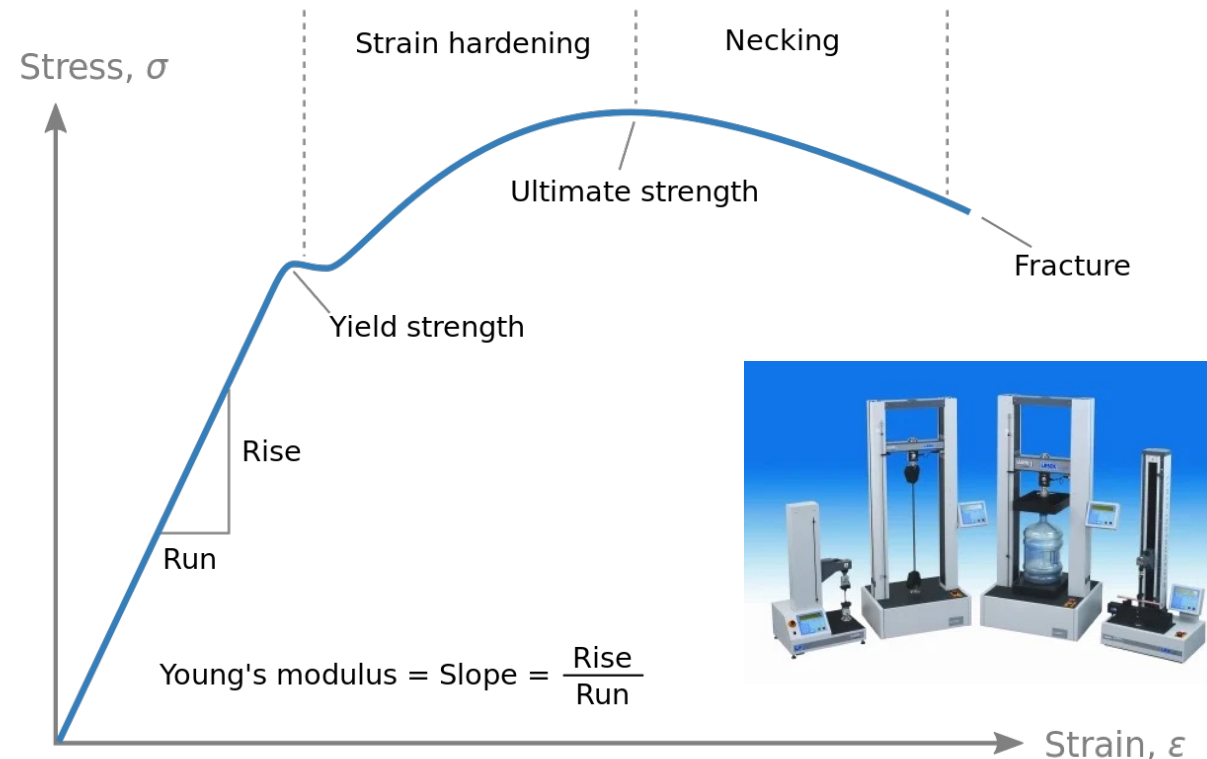
Stress, σ — Strain hardening — Necking — Ultimate strength — Yield strength — Fracture — Rise — Run — Strain, ε

$$\text{Young's modulus} = \text{Slope} = \frac{\text{Rise}}{\text{Run}}$$

Characterization: structural properties

Use of thermal gradients to measure mechanical properties
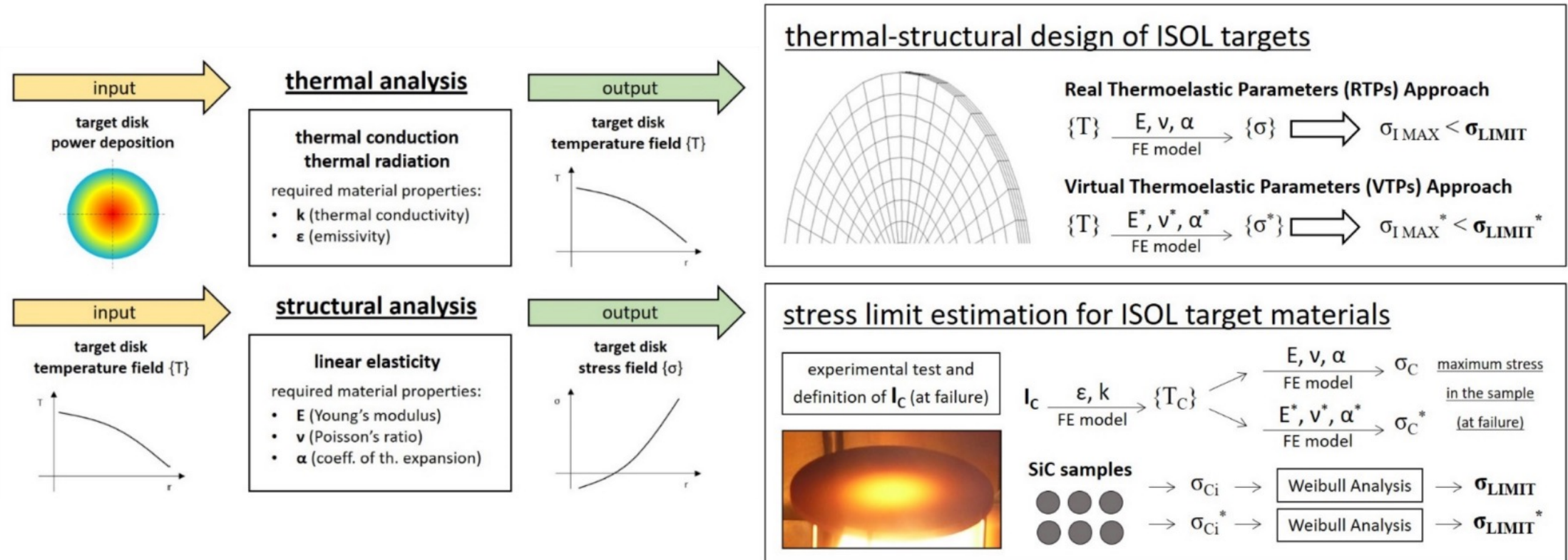
M. Manzolaro, S. Corradetti, M. Ballan et al., Materials 14 (2021) 1689.
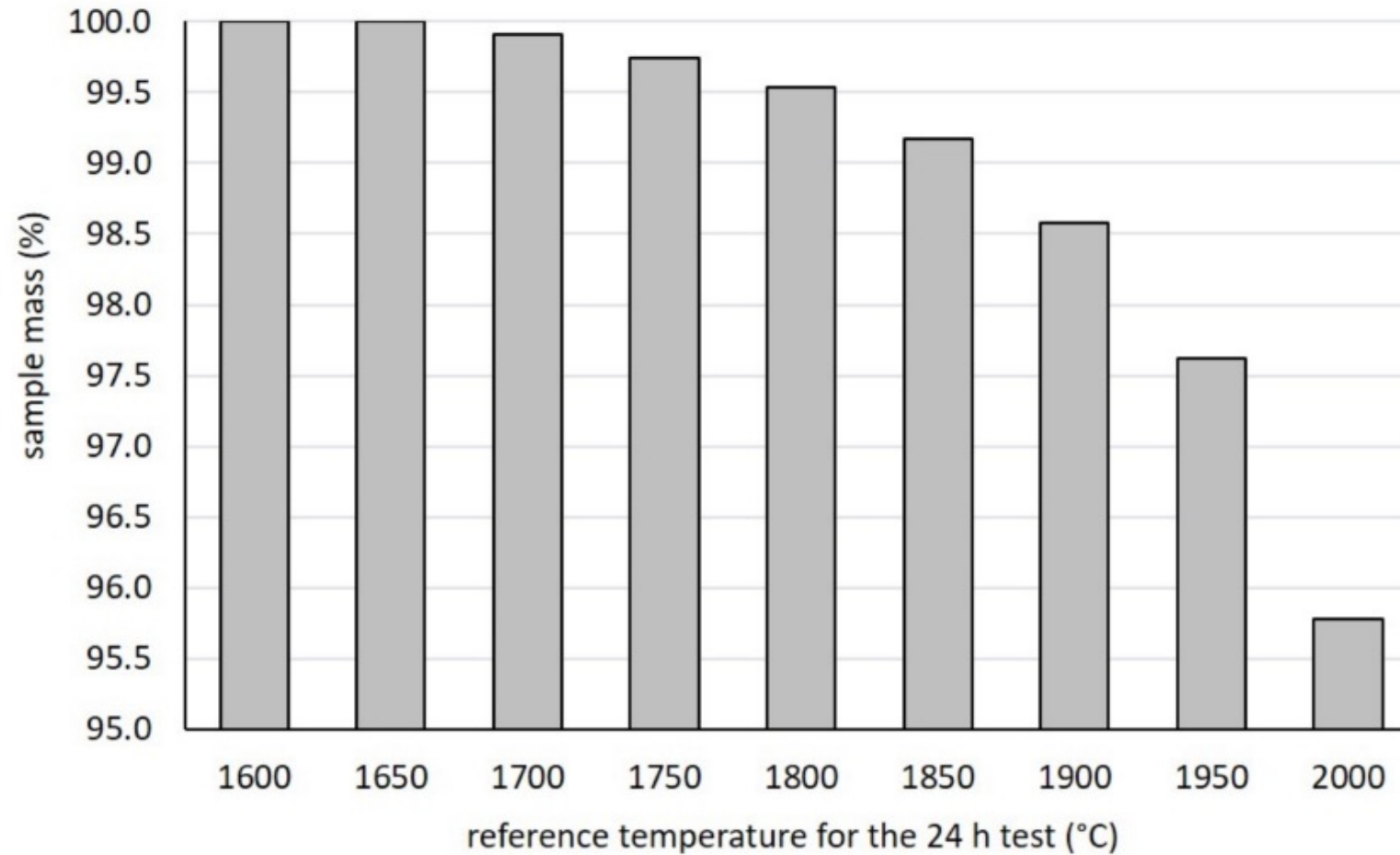
Characterization: structural properties

Use of thermal gradients to measure mechanical properties
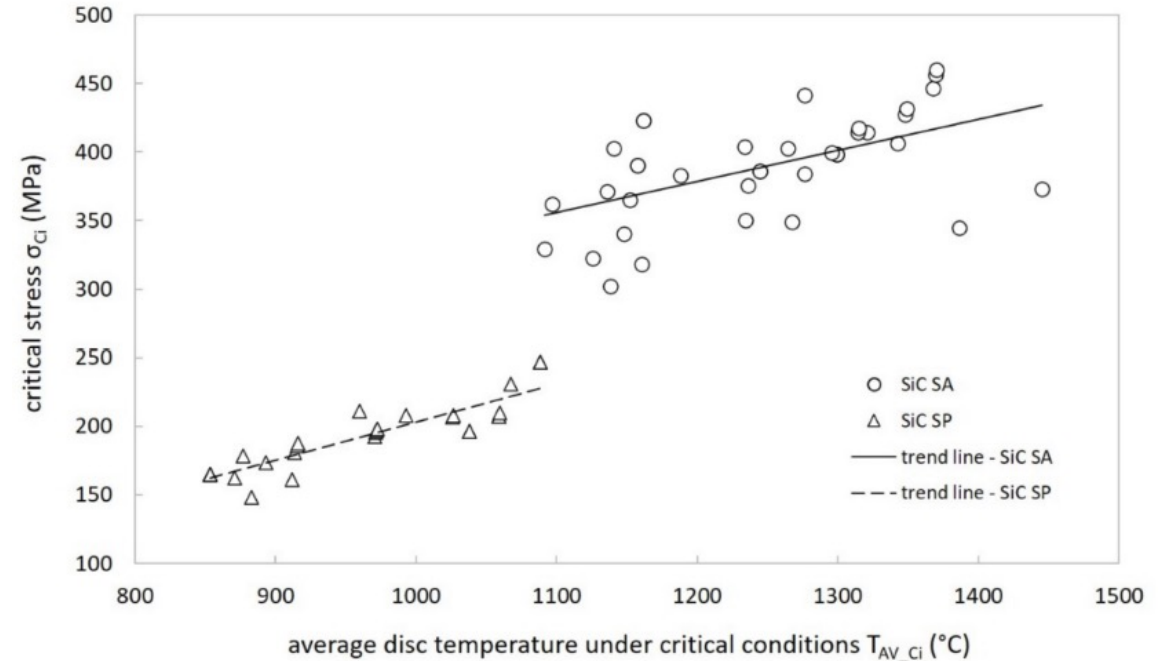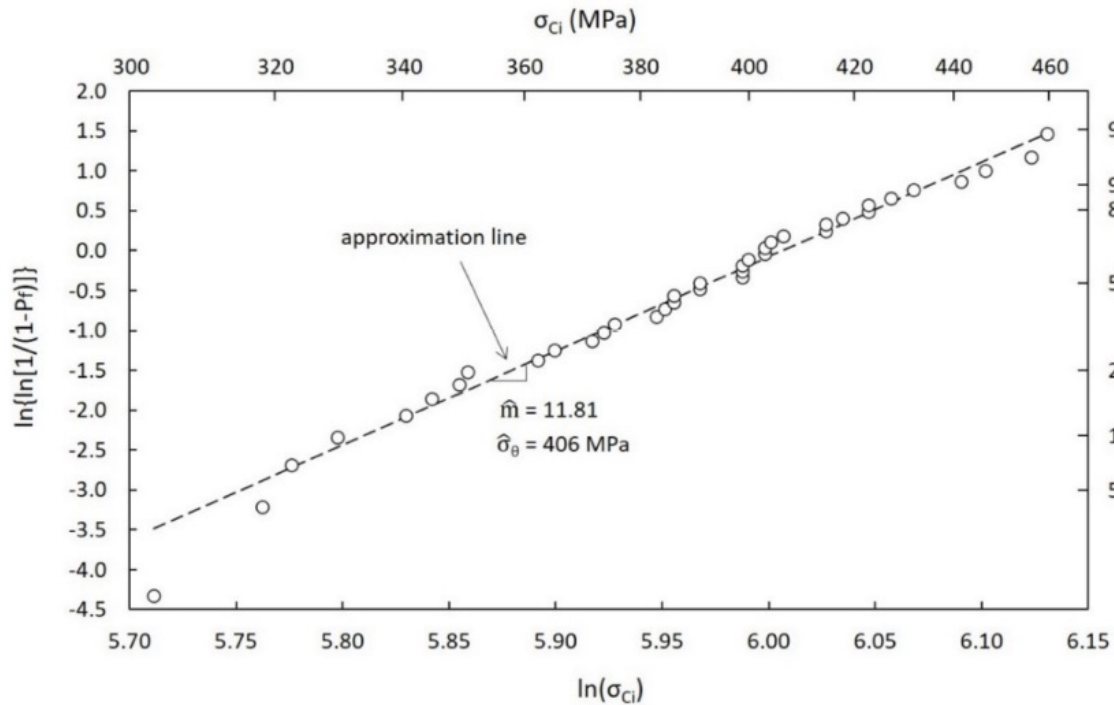
Two-parameter Weibull distribution $P_f = 1 - exp\left[-\left(\frac{\sigma}{\hat{\sigma}_0}\right)^{\hat{m}}\right]$

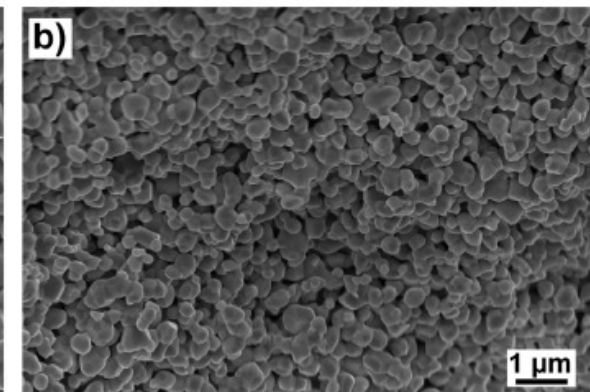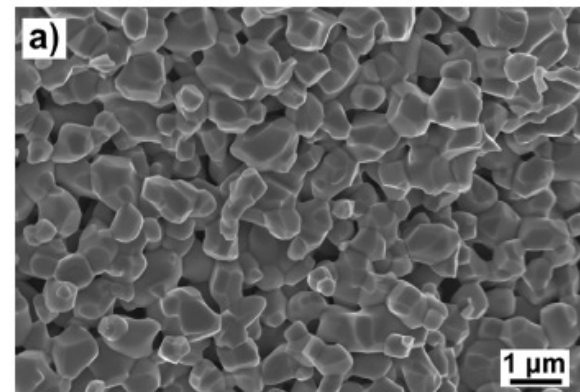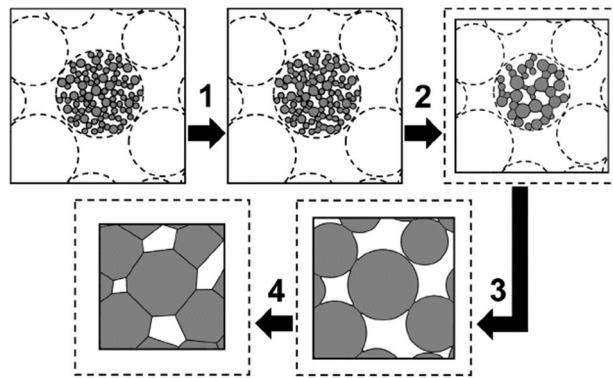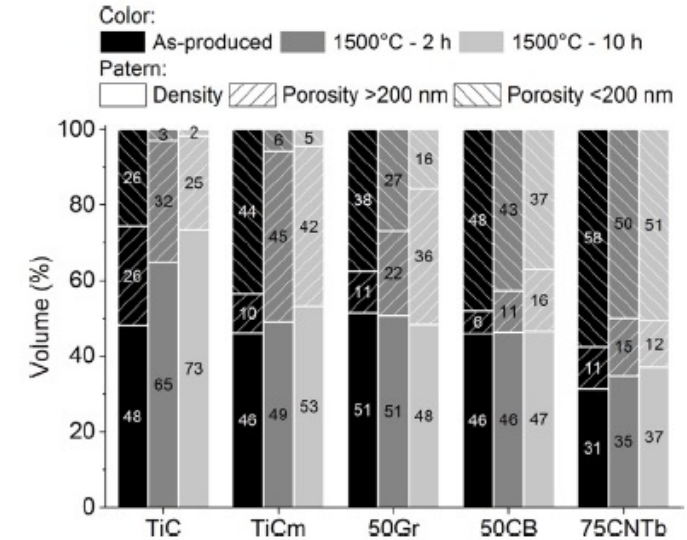*M. Manzolaro, S. Corradetti, M. Ballan et al., Materials 14 (2021) 1689.*

Characterization: limiting temperature

M. Manzolaro, S. Corradetti, M. Ballan et al., Materials 14 (2021) 1689.

Characterization: physico-chemical stability
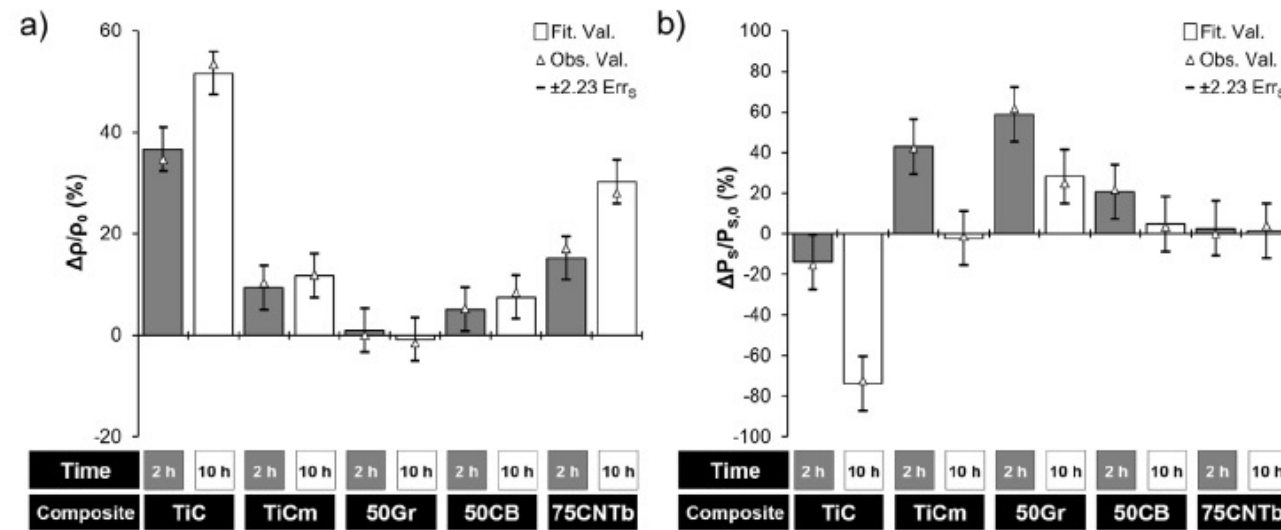
J.P. Ramos, A.M.R. Senos, T. Stora, et al., Journal of the European Ceramic Society 37 (2017) 3899-3908.
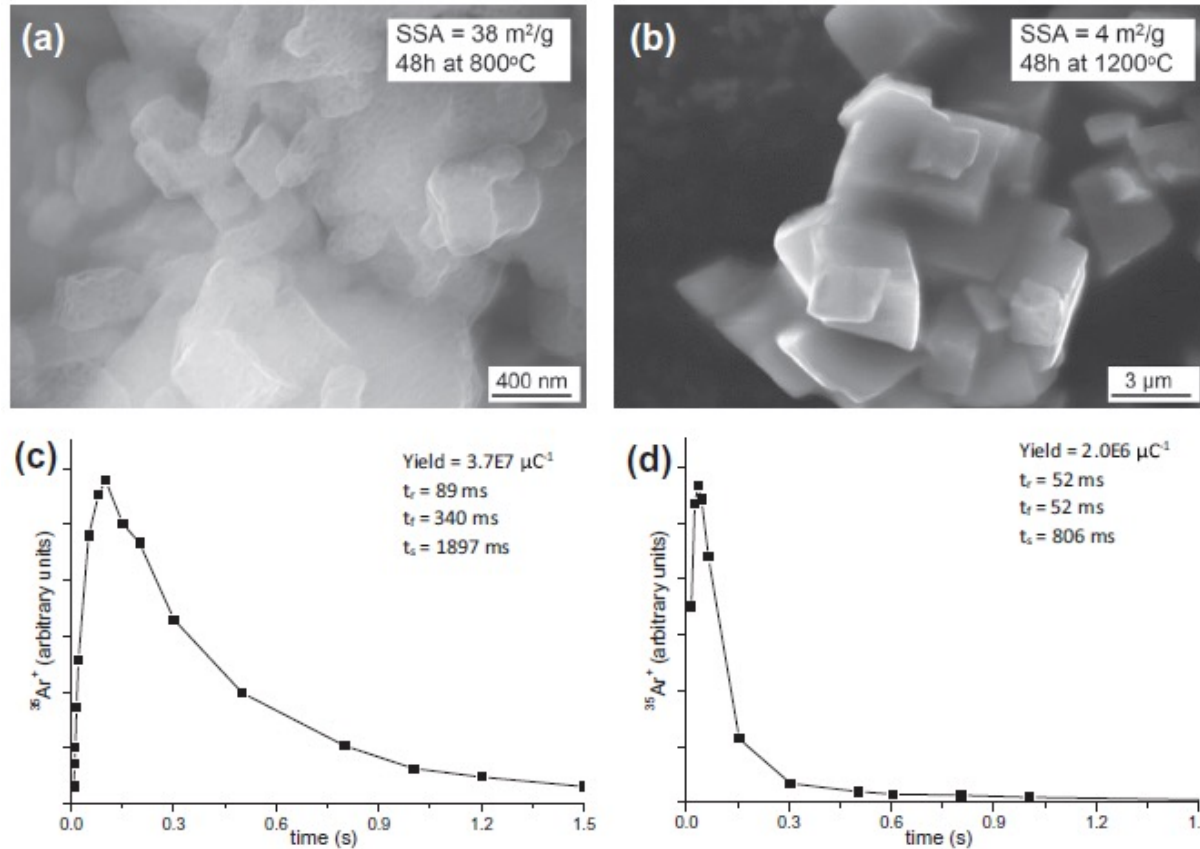
Characterization: physico-chemical stability
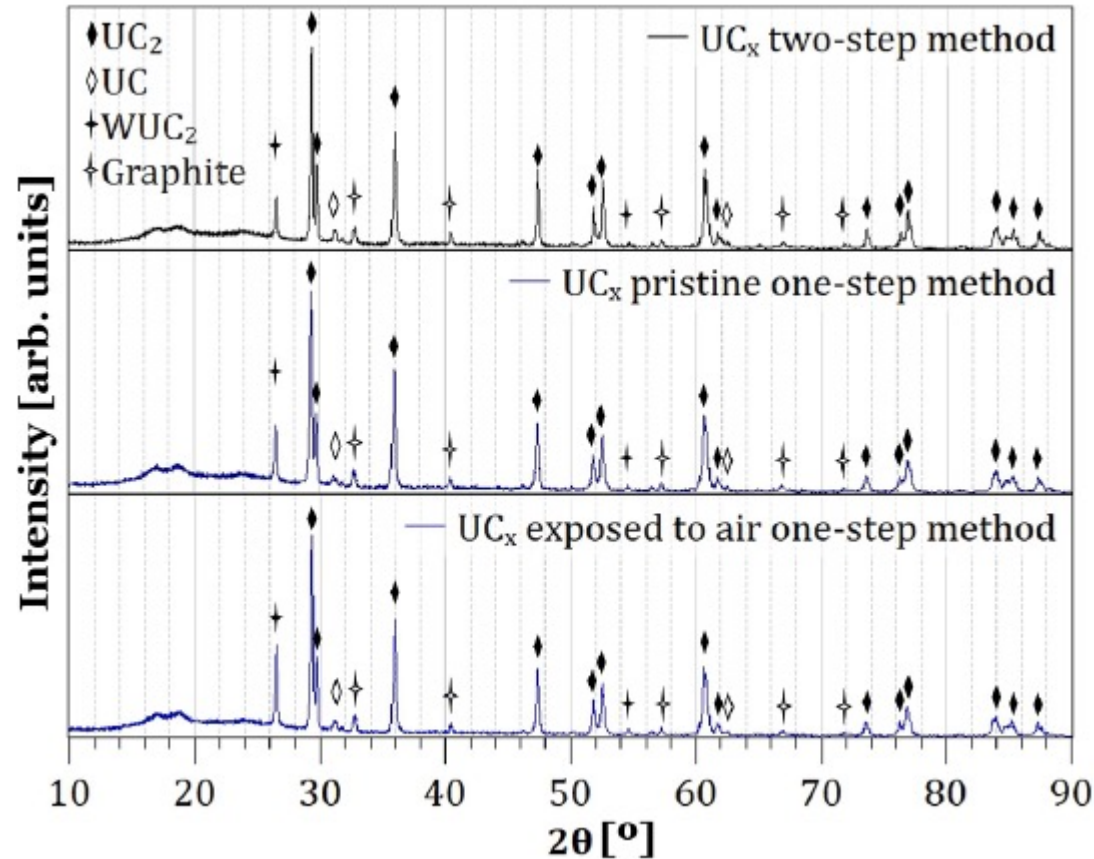
M. Cervantes, P. Fouquet-Métivier, P. Kunz, et al., Nuclear Instruments and Methods in Physics Research B 463 (2020) 367–370.
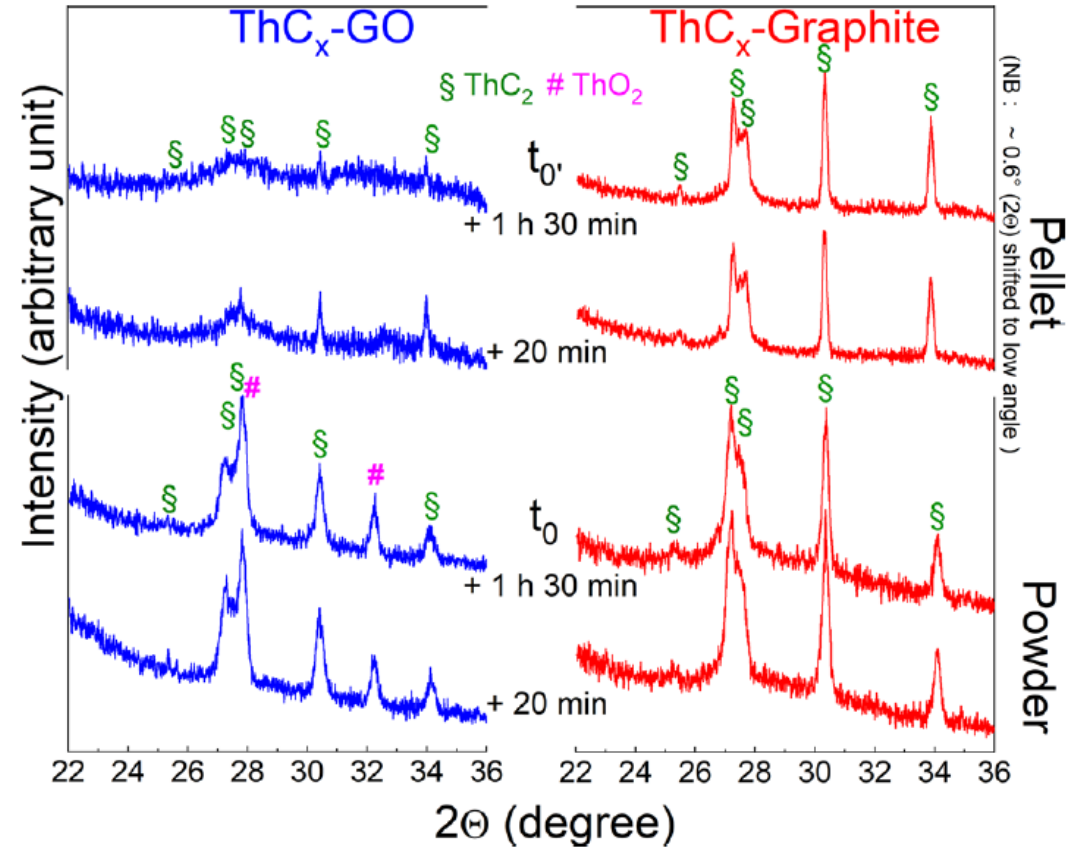
S. Corradetti, S.M. Carturan, M. Ballan, et al., Scientific Reports 11 (2021) 9058.
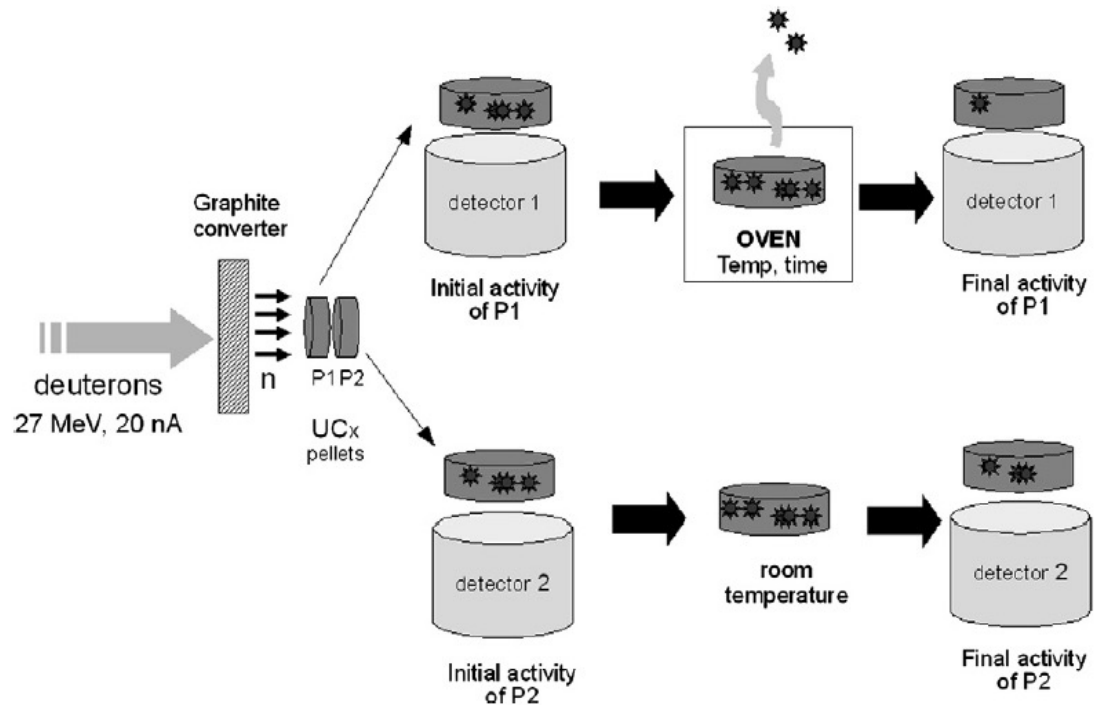
Characterization: release
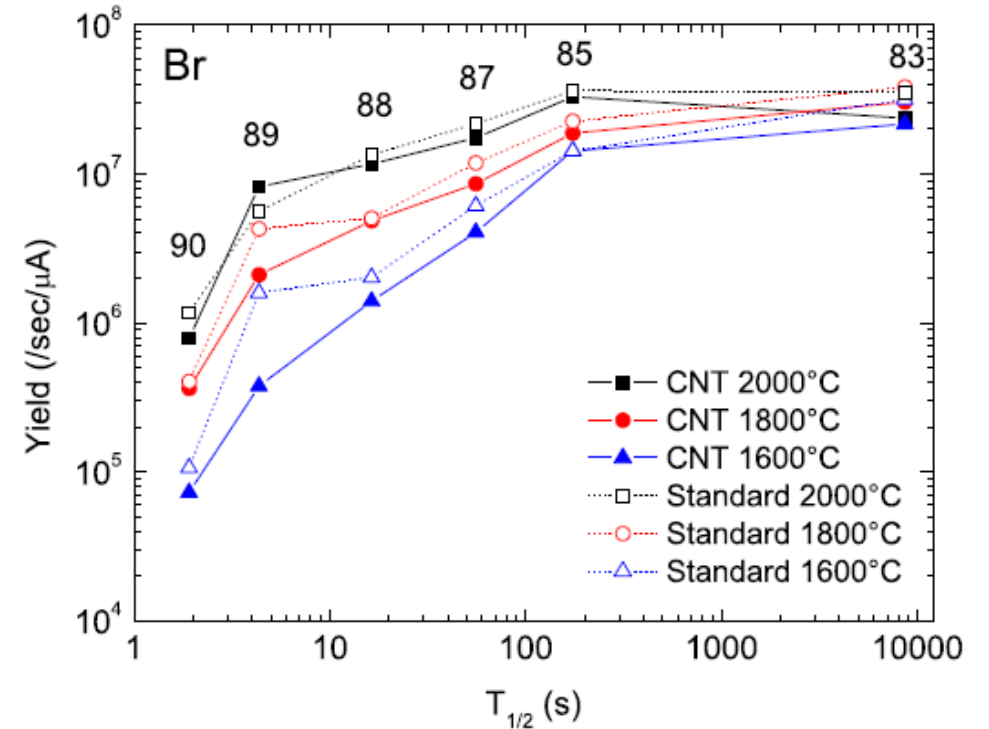
J.P. Ramos, A. Gottberg, R.S. Augusto, et al., Nuclear Inst. and Methods in Physics Research B 376 (2016) 81-85.
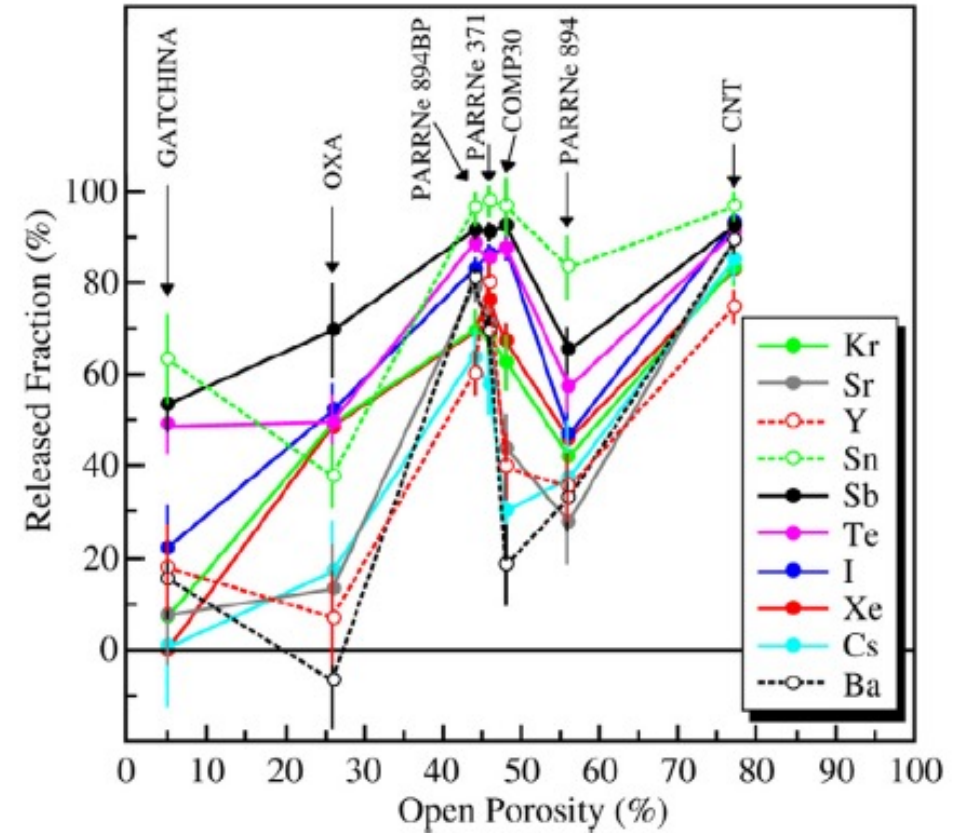
S. Corradetti, L. Biasetto, M. Manzolaro, et al., The European Physical Journal A 49 (2013) 56.

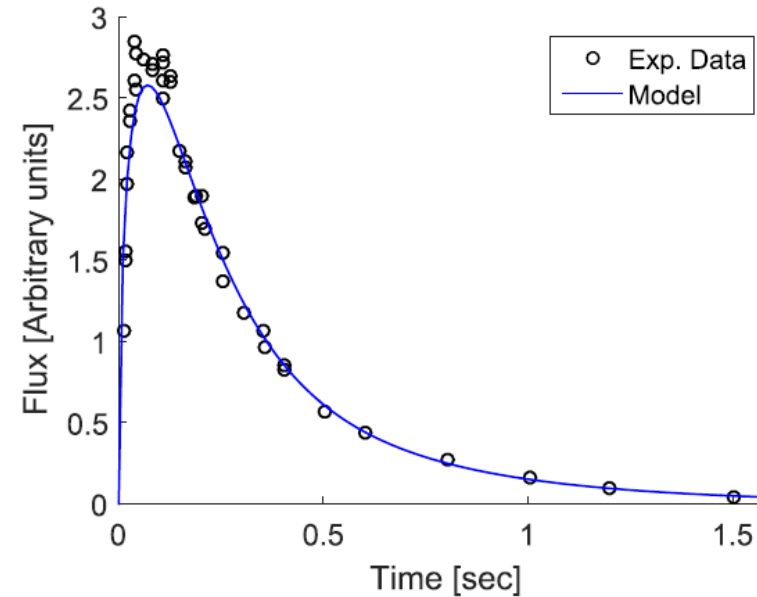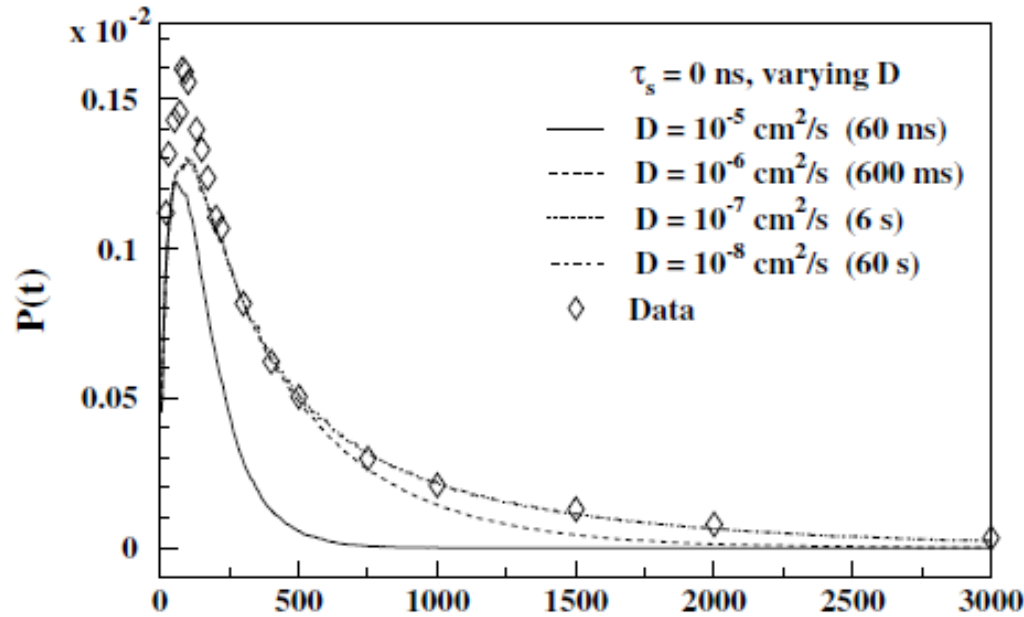# Characterization: release

B. Hy, N. Barré-Boscher, A. Özgümüs, et al., Nuclear Inst. and Methods in Physics Research B 288 (2012) 34-41.

S. Tusseau-Nenez, B. Roussière, N. Barré-Boscher, et al., Nuclear Inst. and Methods in Physics Research B 370 (2016) 19-31.

Simulations: diffusion

B. Mustapha, J.A. Nolen, Nuclear Inst. and Methods in Physics Research B 204 (2003) 286-292.

L. Egoriti, S. Boeckx, L. Ghys, et al., Nuclear Inst. and Methods in Physics Research A 832 (2016) 202-207.

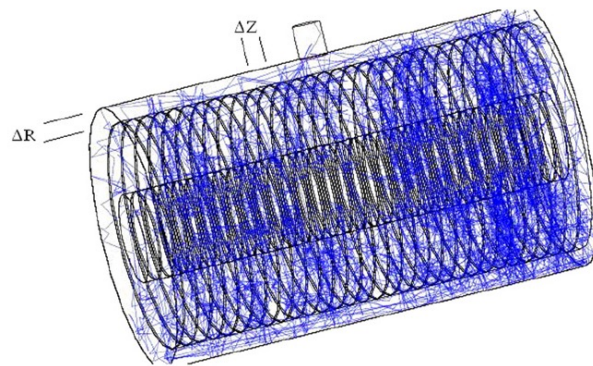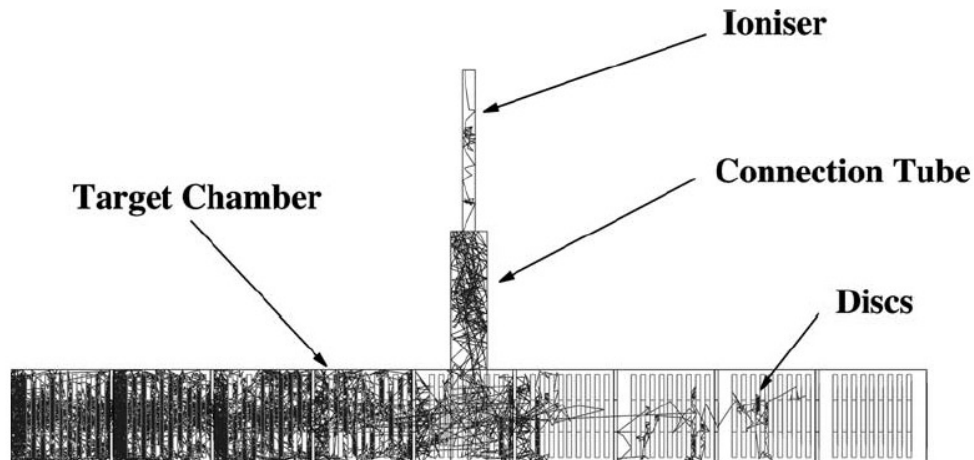Y. Zhang, I. Remec, G.D. Alton, et al., Nuclear Inst. and Methods in Physics Research A 620 (2010) 142-146.

$$\text{Sphere} : I(t) = \frac{\pi^2 SD}{a^2 \sum\limits_{k=1}^{\infty} \frac{1}{k^2}} \sum_{k=1}^{\infty} \left[\frac{1 - e^{-(\frac{Dk^2 \pi^2}{a^2} + \lambda)t}}{\frac{Dk^2 \pi^2}{a^2} + \lambda} \right]$$

$$\text{Thin film} : I(t) = \frac{2SD}{d^2} \sum_{k=0}^{\infty} \left\{ \frac{1 - e^{-\left[\frac{D(k+0.5)^2 \pi^2}{d^2} + \lambda\right]t}}{\frac{D(k+0.5)^2 \pi^2}{d^2} + \lambda} \right\}$$
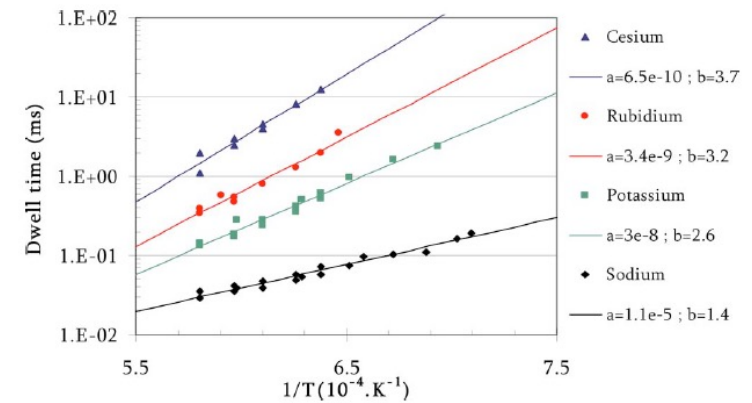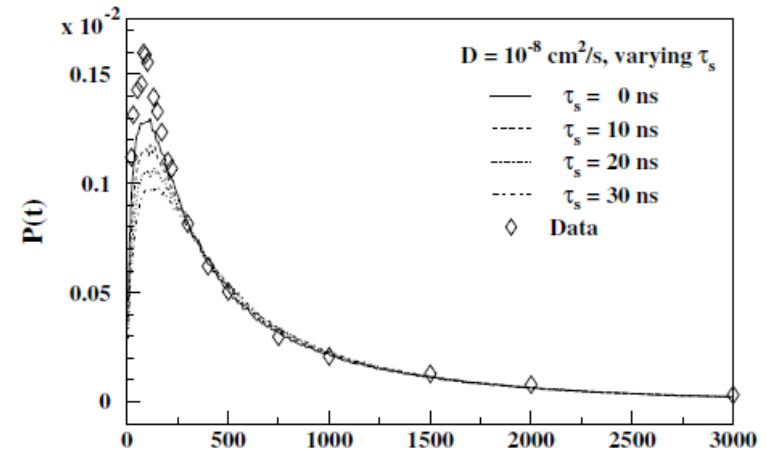
$$\text{Cylinder} : I(t) = \frac{SD}{a^2 \sum\limits_{k=1}^{\infty} \frac{1}{J_{0,k}^2}} \sum_{k=1}^{\infty} \left[\frac{1 - e^{-(\frac{D J_{0,k}^2}{a^2} + \lambda)t}}{\frac{D J_{0,k}^2}{a^2} + \lambda} \right]$$

$$\text{Thin slab} : I(t) = \frac{8SD}{d^2} \sum_{k=0}^{\infty} \left\{ \frac{1 - e^{-\left[\frac{D(2k+1)^2 \pi^2}{d^2} + \lambda\right]t}}{\frac{D(2k+1)^2 \pi^2}{d^2} + \lambda} \right\}$$
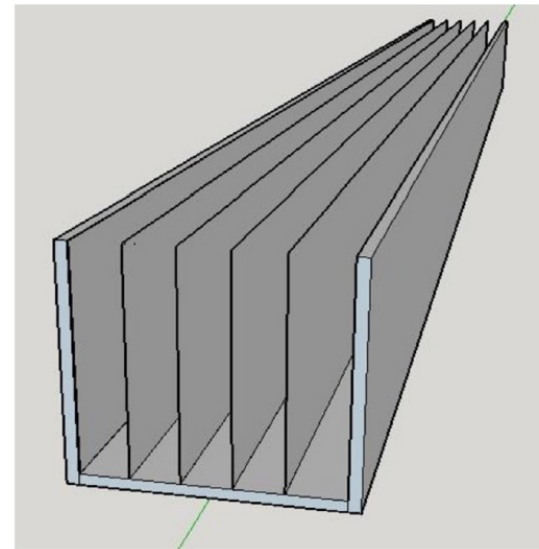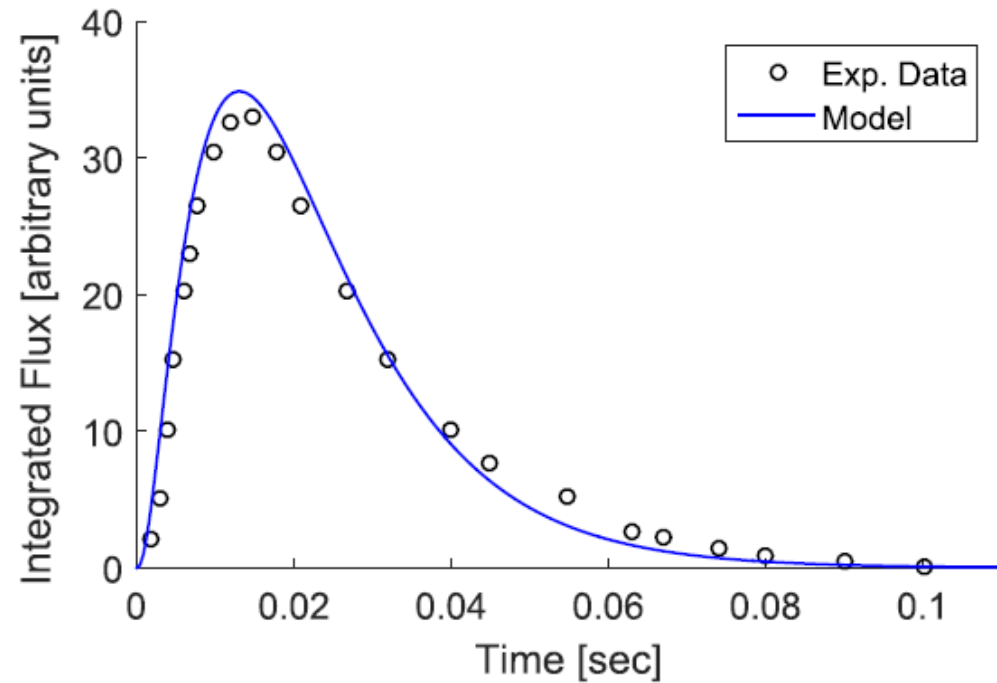
Simulations: effusion

B. Mustapha, J.A. Nolen, Nuclear Inst. and Methods in Physics Research B 204 (2003) 286-292.
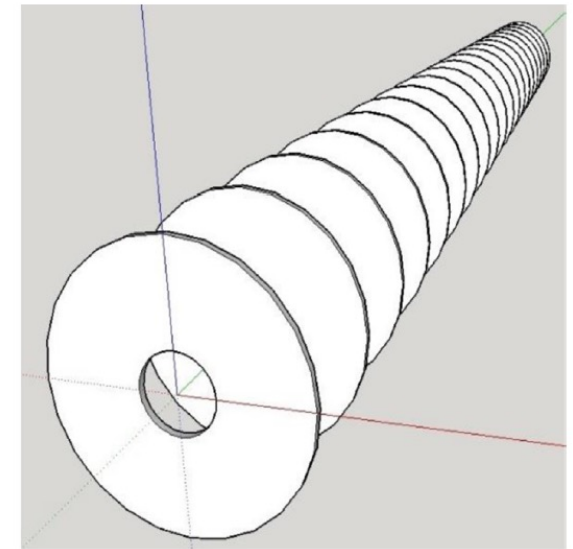
A. Pichard, P. Jardin, M.G. Saint-Laurent, et al., Review of Scientific Instruments 81 (2010) 02A908.

Simulations: overall release

(a) Ta129 target geometry.

(b) RIST-ISOLDE target geometry.

L. Egoriti, S. Boeckx, L. Ghys, et al., Nuclear Inst. and Methods in Physics Research A 832 (2016) 202-207.

Target examples: UC$_x$

Table 1

Typical target and driver parameters at different RIB facilities using the respective geometries. For all calculations UC$_x$ following the established composition (UC$_2$ + 2C) and density (3.5 g/cm^3) was used.

	Particle	Typical beam energy [MeV]	Typical beam current [μA]	Typical beam power [kW]	Instantaneous power if pulsed [GW]	Typical UC$_x$ target thickness [g/cm^2]	Typical UC$_x$ target diameter [cm]	Integrated[7] stopping power [MeV]	Absorbed power in target material[3] [kW]	Max. power density[3] [kW cm^{-3}]
ISOLDE-CERN	p	1400	2	2.8	pulsed, 1.2[8]	≈ 45	1.4	70	0.2	0.02
SPES-INFN [8]	p	40	200	8	c.w.	2.3	4.0	31	6.6	1.9
iThemba LABS [18]	p	70	115	8	c.w.	5.9	4.0	35	4.2	0.6
RISP-IBS [10]	p	70	140	10	c.w.	8.7	5.0	60	8.3	0.4
ISAC-TRIUMF	p	480	100[1]	48	c.w.	≈ 18	1.8	60	4.0	1.5
ARIEL-TRIUMF[2]	e → γ	35	2800	100	pseudo c.w.[9]	≈ 11	4.0[4]	35 → NaN	54 → 11	7.8 → 1.1
SPIRAL2-GANIL [19][5]	d → n	40	5000	200	pseudo c.w.[10]	≈ 8.9	8.0	40 → 0[6]	199 → 0.4	49 → 0.002

[1] Due to the current license the operation of actinide targets is restricted to 10 μA.

[2] ARIEL will have two target stations using 35–75 MeV electrons and 480 MeV protons (see ISAC-TRIUMF) respectively, values are based on the current electron target concept.

[3] Includes contribution from the fission process.

[4] Due to the limited interaction range of the photon the cylindrical target will likely be oriented perpendicular to the beam.

[5] For the calculations the design for a 50 kW neutron converter [20] was used.

[6] Not considering neutrons that induce fission reactions.

[7] Integrated over the full target thickness.

[8] The proton beam at ISOLDE-CERN is pulsed with ~3 · 10^{13} protons within a 2.4 μs bunch.

[9] The ARIEL linac is delivering ⩽8 pC electron bunches with bunch length of 35 ps and bunch repetition rates of 650 MHz.

[10] The GANIL driver linac is based on 88 MHz operation with a bunch length of 1.6 ns [21].

A. Gottberg, Nuclear Inst. and Methods in Physics Research B 376 (2016) 8-15.

# Target examples: "standard" UC$_X$ (or other MCx)

The uranium dioxide and graphite powders were mixed following eq. (1):

$$UO_2 + 6C \longrightarrow UC_2 + 2C + 2CO_g. \qquad (1)$$
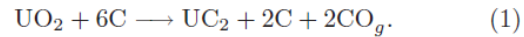
The UO$_2$ (powder mean grain size $< 300\,\mu m$) was purchased from CERAC Inc. (Milwaukee, WI, USA) and graphite (powder mean grain size $< 45\,\mu m$) from Sigma-Aldrich. These powders were used as received. Powders were manually ground and mixed in an agate mortar, inside a glove-box (O$_2$ and H$_2$O < 1 ppm), the weight percentages of the powders complying with the stochiometry of eq. (1) and 2 wt.% of phenolic resin was added as a binder. After mixing, the powders were placed in a 13 mm diameter mold and were uniaxially cold pressed at 750 MPa. The pressed samples possessed a nominal diameter of 13 mm, 1 mm thickness and a mass of approximately 500 mg. The thermal treatment was performed under high vacuum (10^{-4}–10^{-5} Pa) in a graphite crucible using the experimental setup described in [8]. The heating schedule was designed to
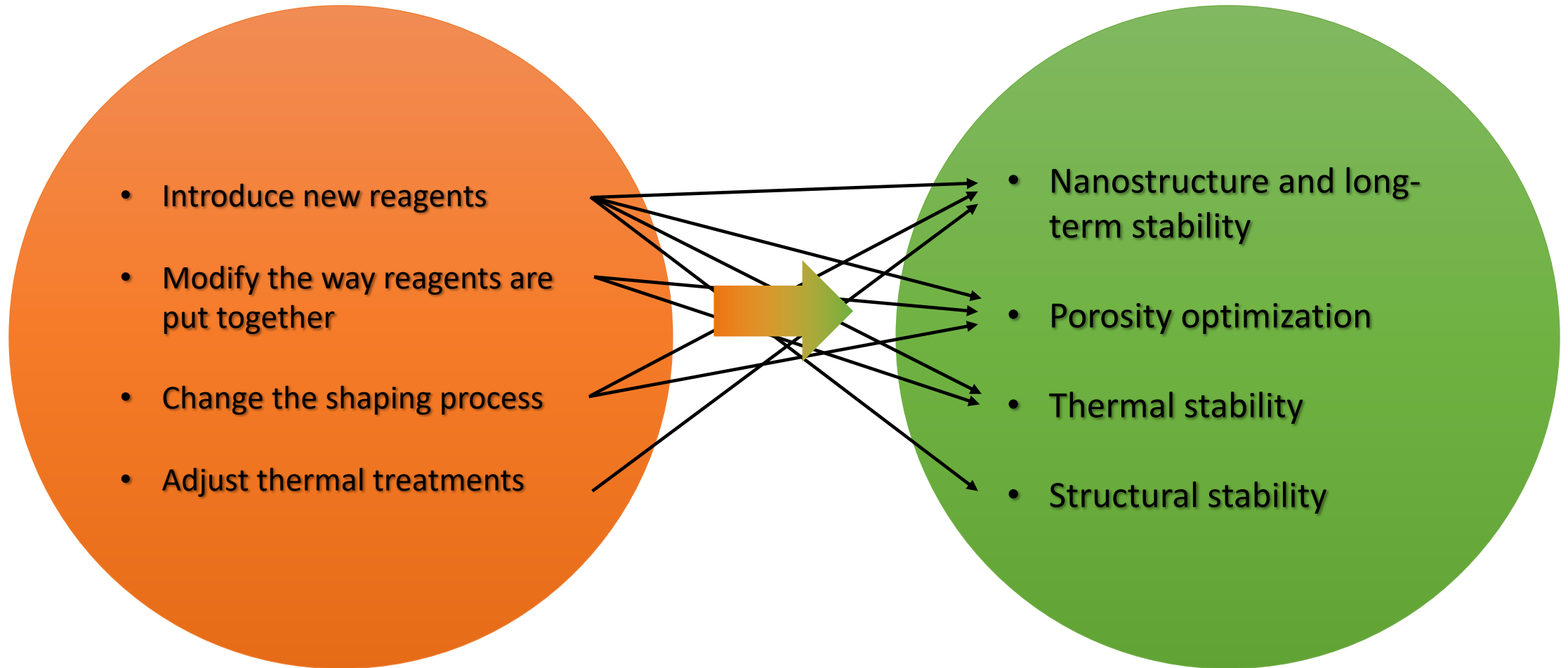
1. promote the carbothermal reaction (2 °C/min up to 1250 °C, 24 h at 1250 °C) and
2. sinter the carburized powders (2 °C/min up to 1600 °C, 4 h at 1600 °C).

Total porosity	30-60 %
Porosity type	Mainly open, macro
Specific Surface Area	Negligible

Oxide + Carbon (graphite) → Carbide + graphite + CO
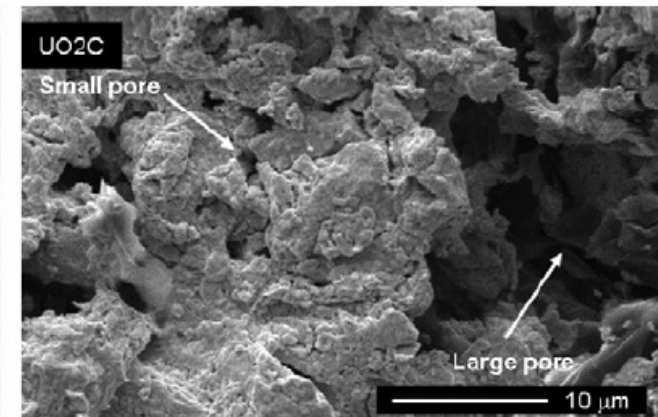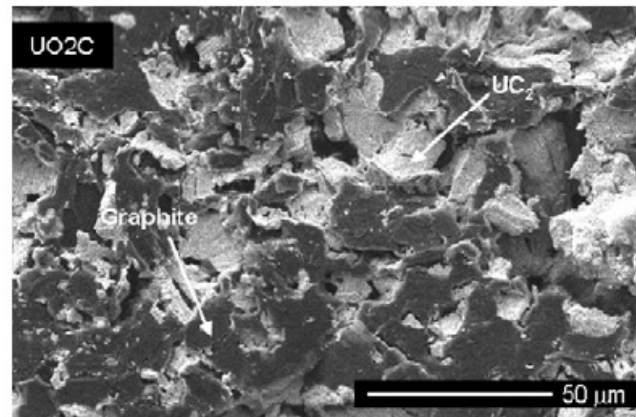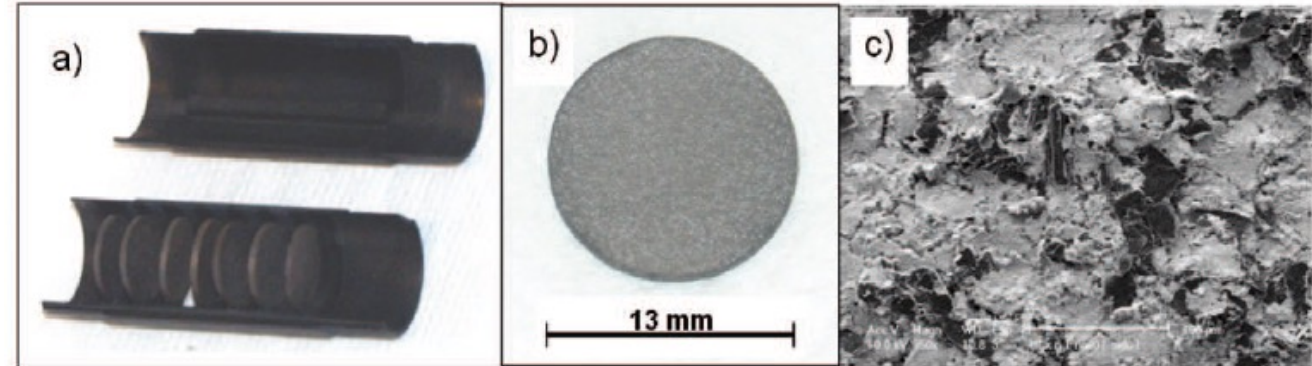
D. Scarpa, L. Biasetto, S. Corradetti, et al., The European Physical Journal A 47 (2011) 32.

Going beyond standard: how to

- Introduce new reagents
- Modify the way reagents are put together
- Change the shaping process
- Adjust thermal treatments

- Nanostructure and long-term stability
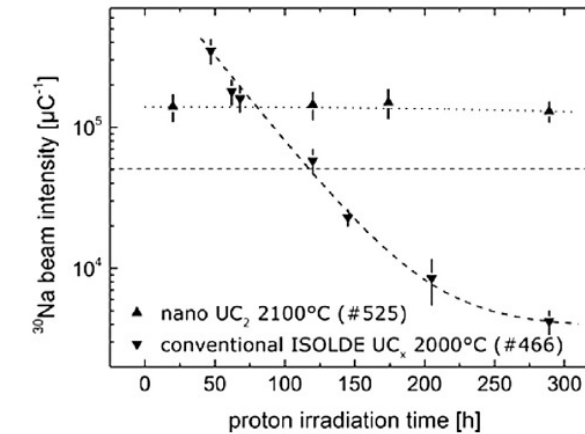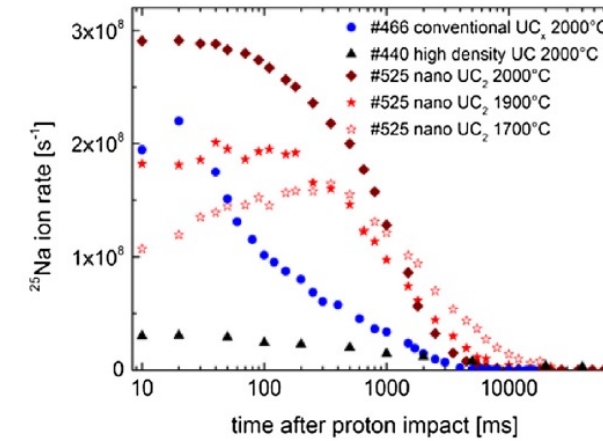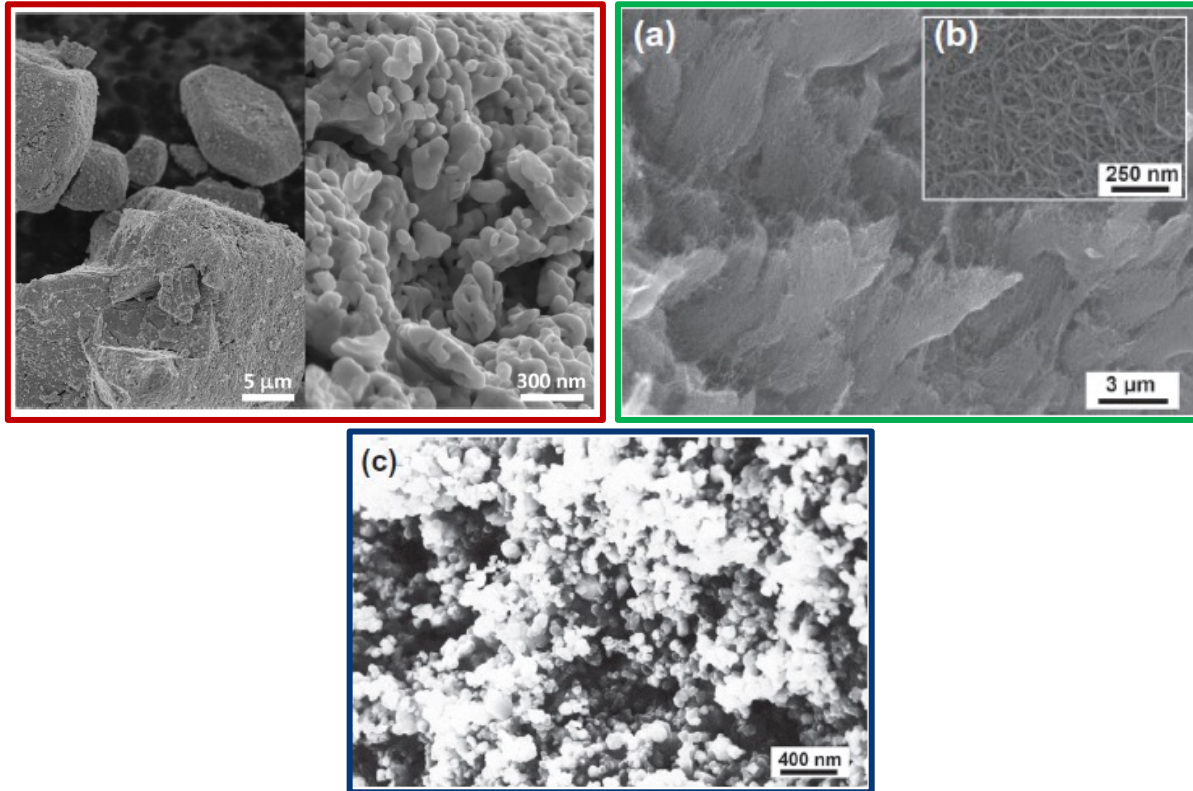- Porosity optimization
- Thermal stability
- Structural stability

Target examples: nano UCx-MWCNTs

Focus on (among others) nanostructure and long-term stability – Carbon source

Nano-Oxide + MWCNTs → Nano-carbide + Nano-carbon + CO

J.P. Ramos, A. Gottberg, R.S. Augusto, et al., Nuclear Inst. and Methods in Physics Research B 376 (2016) 81-85.

A. Gottberg, Nuclear Inst. and Methods in Physics Research B 376 (2016) 8-15.

Target examples: nano TiC

Focus on (among others) nanostructure and long-term stability – Carbon source

Nano-Oxide + MWCNTs (or carbon black) → Nano-carbide + Nano-carbon + CO
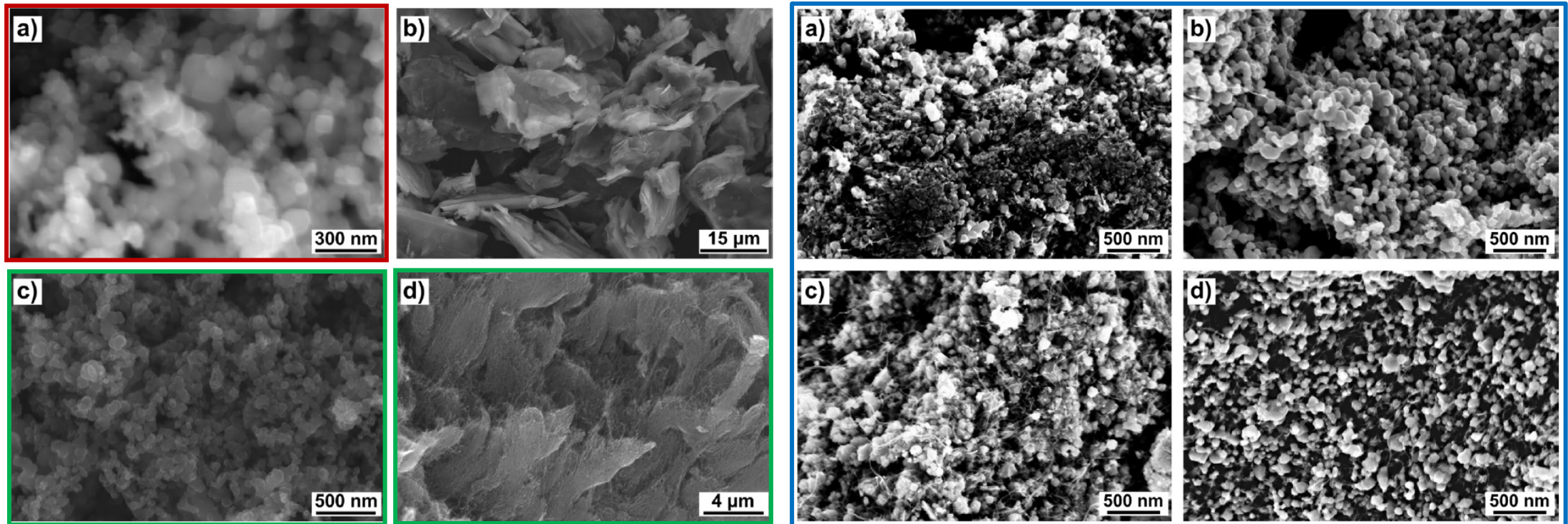
J.P. Ramos, A.M.R. Senos, T. Stora, et al., Journal of the European Ceramic Society 37 (2017) 3899-3908.
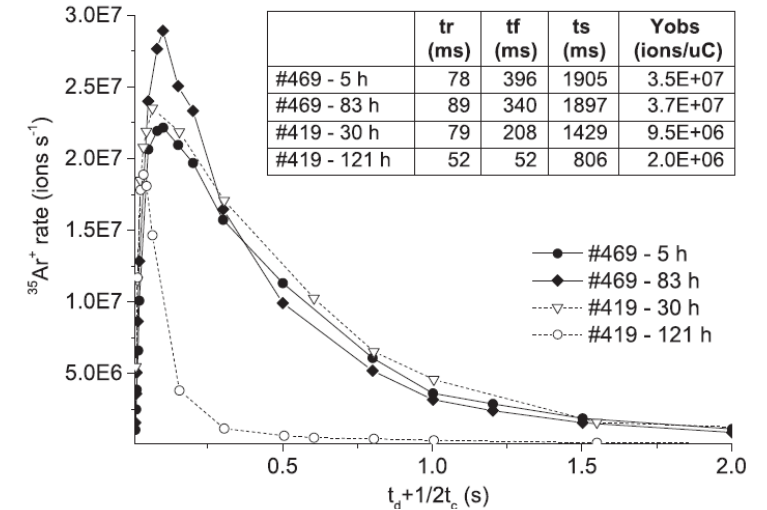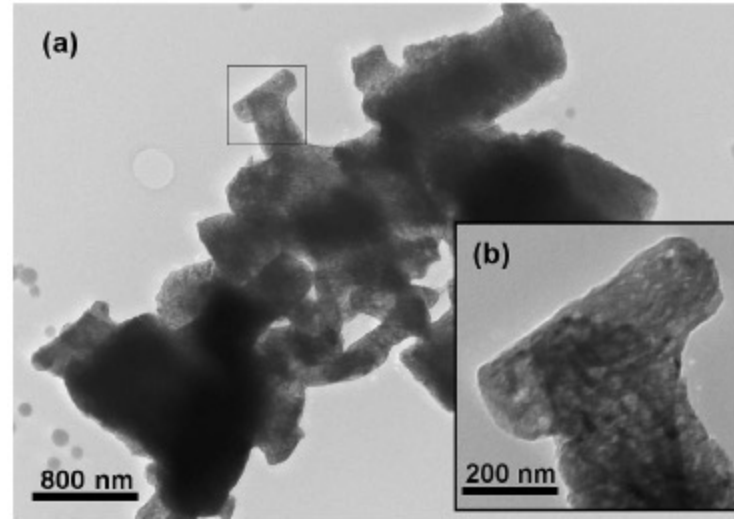J.P. Ramos, T. Stora, A.M.R. Senos, et al., Journal of the European Ceramic Society 38 (2018) 4882-4891.

Target examples: nano CaO

Focus on (among others) nanostructure and long-term stability – Thermal process

$$CaCO_3 \rightarrow CaO + CO_2$$

In order to obtain nanometric CaO powder, a CaCO$_3$ powder (Alfa Aesar, Germany) precursor with an average grain size $< 5 \mu m$, 99.5% pure (metal basis) was decomposed in vacuum ($\approx 10^{-1}$ Pa), at 800 °C, for 2 h, with heating and cooling rates of 10 °C min^{-1}. This decomposition temperature was chosen in a previous study [10] as the one that guarantees the complete conversion and high specific surface area powders. The decarbonation was done in a vertical alumina tube furnace (Termolab, Portugal), with a mullite support for the alumina crucible, connected to a rotary pump. At the end of


	tr (ms)	tf (ms)	ts (ms)	Yobs (ions/uC)
#469 - 5 h	78	396	1905	3.5E+07
#469 - 83 h	89	340	1897	3.7E+07
#419 - 30 h	79	208	1429	9.5E+06
#419 - 121 h	52	52	806	2.0E+06
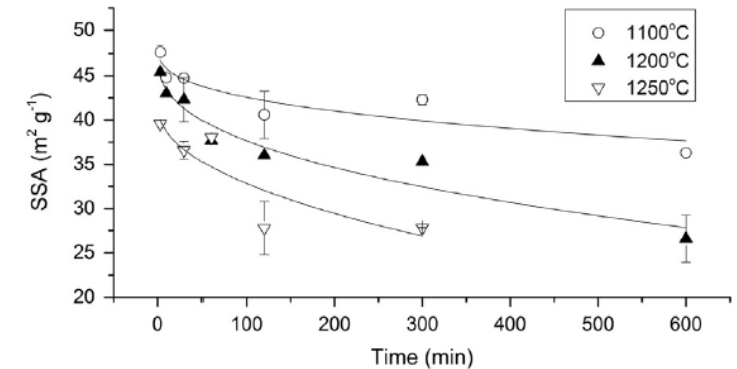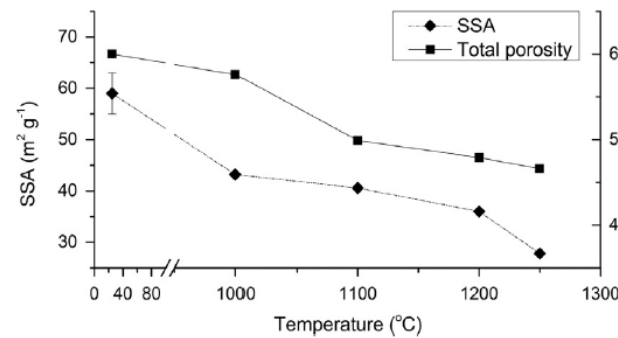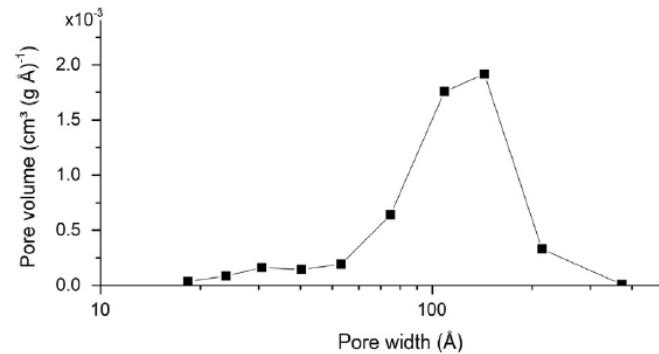
J.P. Ramos, A. Gottberg, T.M. Mendonça, et al., Nuclear Inst. and Methods in Physics Research B 320 (2014) 83-88.

J.P. Ramos, C.M. Fernandes, T.Stora, et al., Ceramics International 41 (2015) 8093-8099.

Target examples: UCx fibers

Focus on (among others) nanostructure and long-term stability – Production technique
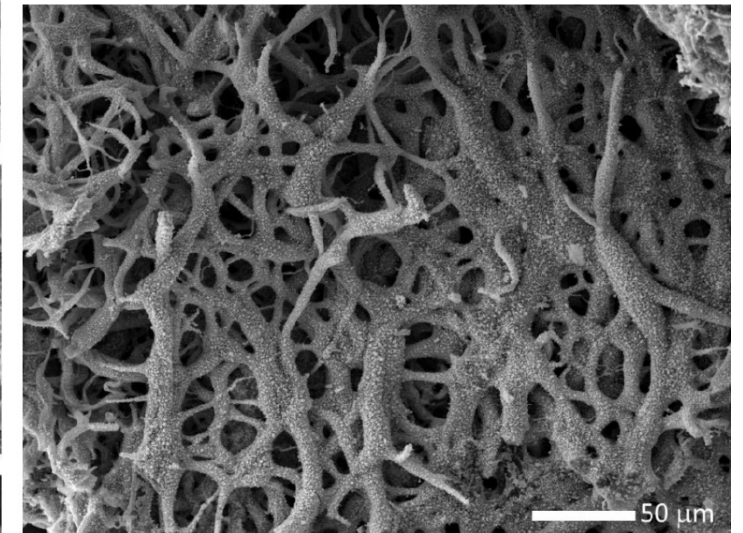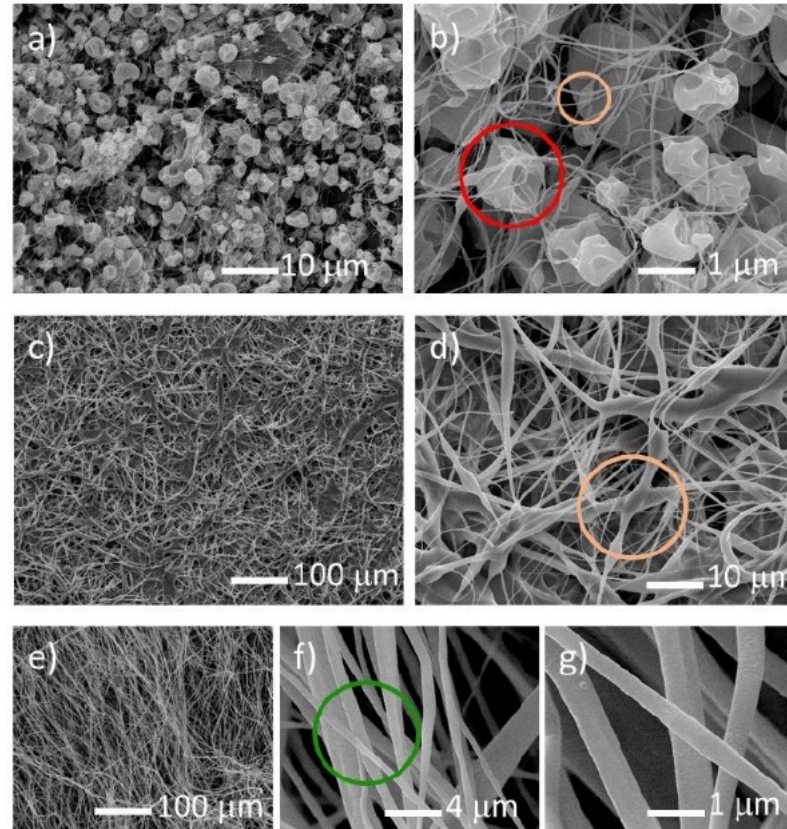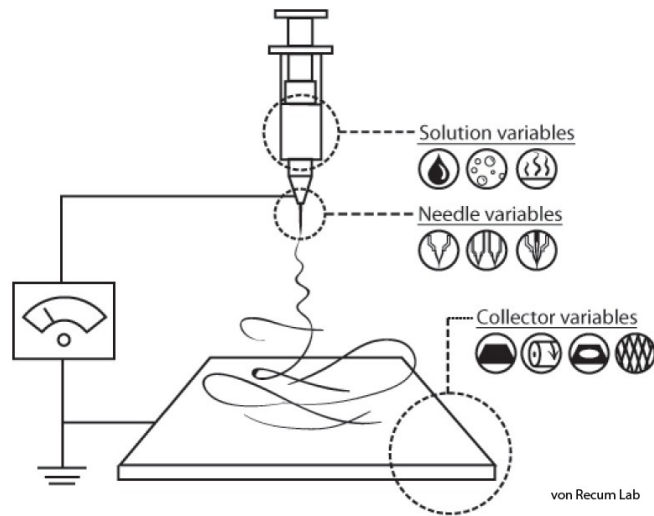
As produced (U salt containing O, C, H)

After thermal treatment (UCx)

Target examples: porous UCx

Focus on (among others) porosity optimization - grinding

Table 2

Summary of the carburized samples with the different quantitative variables used. P_{35}, P_{200}, P_{3000}, P_{10000} and P_{30000} represent the percentages of open porosity on the diameter pores 0.035 μm, 0.2 μm, 3 μm, 10 μm and 30 μm, respectively.

	XRD*					BET	SEM	He Pycnometry		Hg Porosimetry					
	Phase and proportion (%, ± 1%)			Crystallite size (nm, ± 5 nm)		UCx Grain size (nm)**	UCx Aggregate size (μm)	Porosity (%, ± 1%)		Open pore size distribution (%)					
	UC	UC₂	C	UC	UC₂			Open	Close	P₃₅	P₂₀₀	P₃₀₀₀	P₁₀₀₀₀	P₃₀₀₀₀
No.1 UO₂ ground + CNT CP	3	88	9	59	87	118	15	78	7	22	10	10	0	58
No.2 UO₂ ground + CNT DP	5	86	9	39	114	100	0.5	68	12	34	32	34	0	0
No.3 UO₂ ground + graphene GP	4	88	8	51	129	1200	18	49	7	3	22	56	0	19
No.4 OXA + graphite CP	4	87	9	55	160	820	23	55	5	2	12	86	0	0
No.5 OXA ground + CNT DP	13	78	9	40	127	94	0.6	70	15	24	29	47	0	0
No.6 OXA + CNT DP	7	84	9	65	149	82	3.2	74	14	17	17	66	0	0
No.7 PARRNe BP894	5	86	9	102	165	906	31	41	5	4	14	82	0	0
No.8 PARRNe BP897 CP	5	87	8	38	145	972	65	51	5	2	8	46	44	0
No.9 PARRNe BP897 CP 12d	5	87	8	46	144	914	56	49	8	2	5	49	44	0
No.10 UO₂ ground + CNT CP 12d	3	88	9	48	86	100	71	72	13	19	13	10	0	58
No.11 UO₂ ground + CNT DP 12d	5	86	9	42	110	96	0.5	64	17	30	33	37	0	0
No.12 UO₂ ground + graphene GP 12d	4	88	8	43	135	1412	14	48	4	3	17	65	0	15
No.13 UO₂ ground + CNT-5 mol DP	5	90	5	57	119	104	0.6	64	8	29	27	35	0	9
No.14 UO₂ ground + CNT-7 mol DP	4	84	12	40	102	92	0.2	69	15	33	37	30	0	0
Standard deviation	2	3	1	16	24	484	26	11	4	12	10	22	15	20

* For all the samples, the agreement factors were in the ranges: 11.6% < R_w < 14.8%, 5.8% < R_{exp} < 7.3%, 1.9 < χ^2 < 2.3.

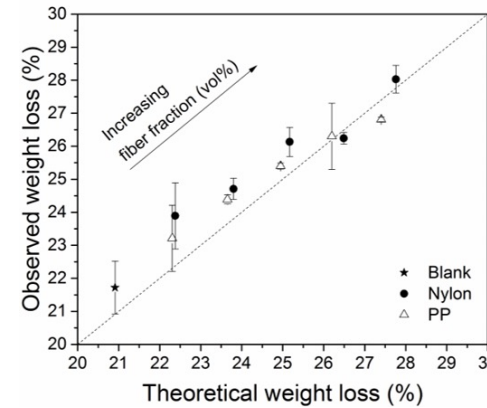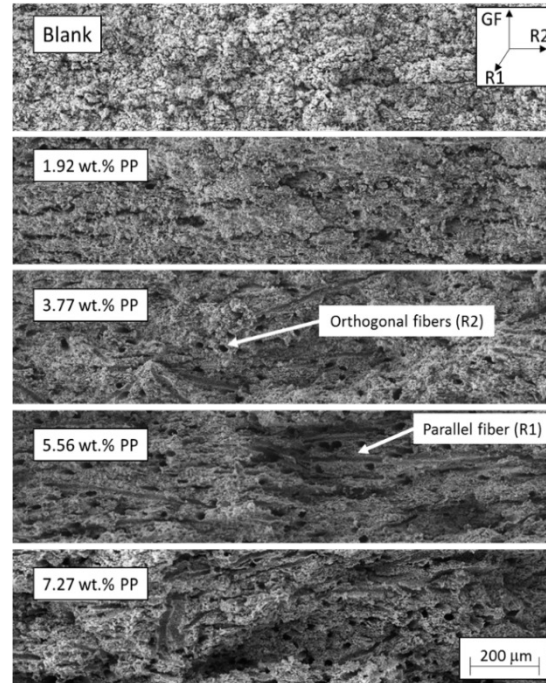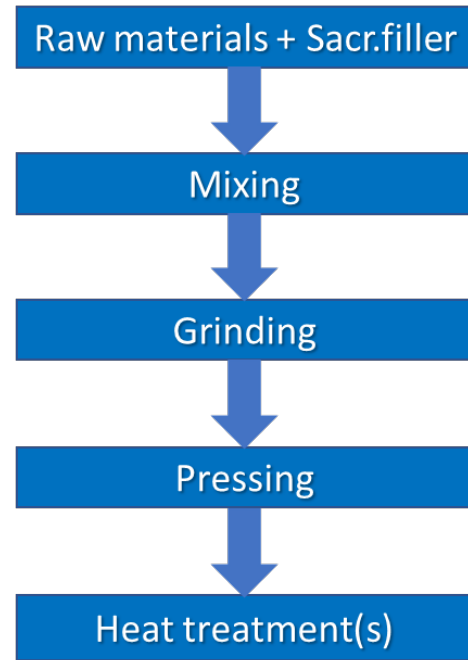** Error bar of SSA measurements is 5%.

J. Guillot, S. Tusseau-Nenez, B. Roussière, et al., Nuclear Inst. and Methods in Physics Research B 433 (2018) 60–68.

J. Guillot, B. Roussière, S. Tusseau-Nenez, et al., Nuclear Inst. and Methods in Physics Research B 440 (2019) 1–10.
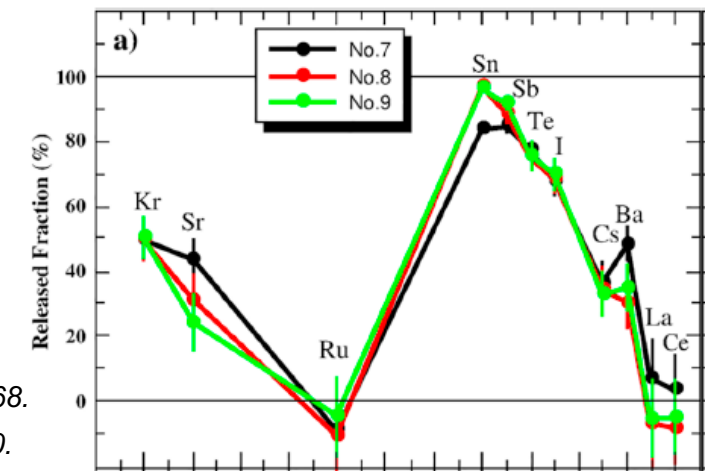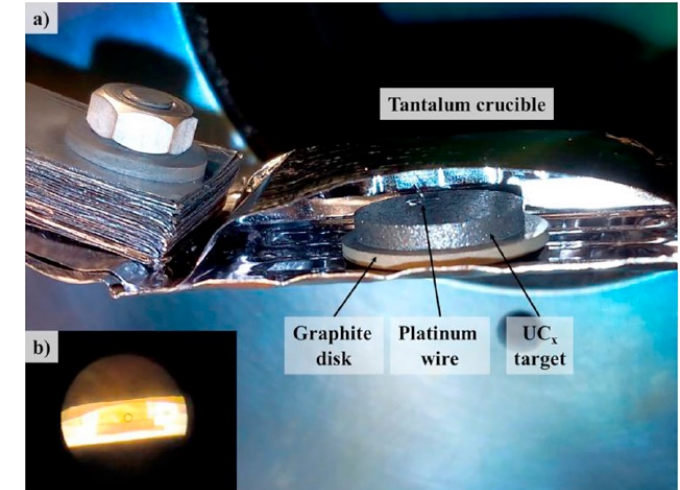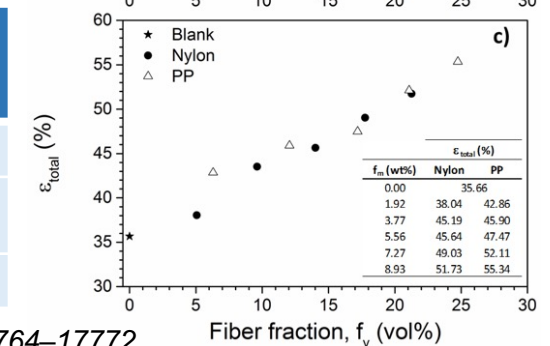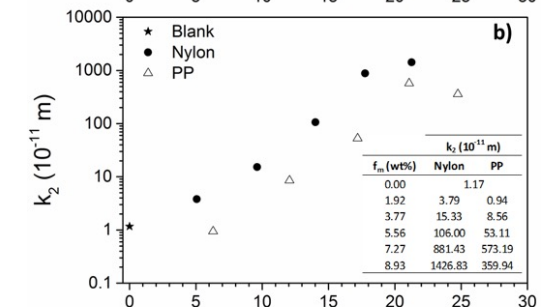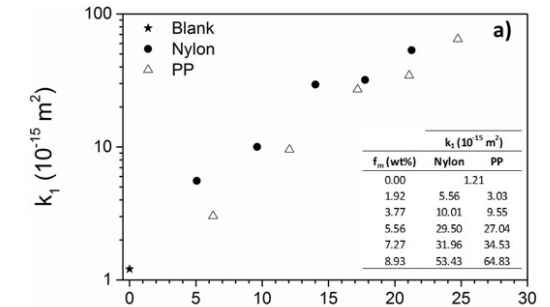
Target examples: macroporous LaCx

## Focus on (among others) porosity optimization – Sacrificial fillers

Optimization of properties by:

- Choice of carbon/metal precursors
- Quantity and type of sacrificial fillers
- Heat treatment parameters

Fibers allow to obtain similar permeability but with lower vol% of filler (lower total porosity) with respect to PMMA spheres

	K_1 ($*10^{-14} m^2$)	f_v (vol%)	Total porosity (%)
PP fibers	6.5	24.8	51.7
Nylon fibers	5.3	21.5	55.3
PMMA	9.4	60.6	**74.0**

S. Corradetti, L. Biasetto, M.D.M. Innocentini et al., Ceramics International 42 (2016) 17764–17772.

Target examples: micro-mesoporous TiC

Focus on (among others) porosity optimization – Sol-gel
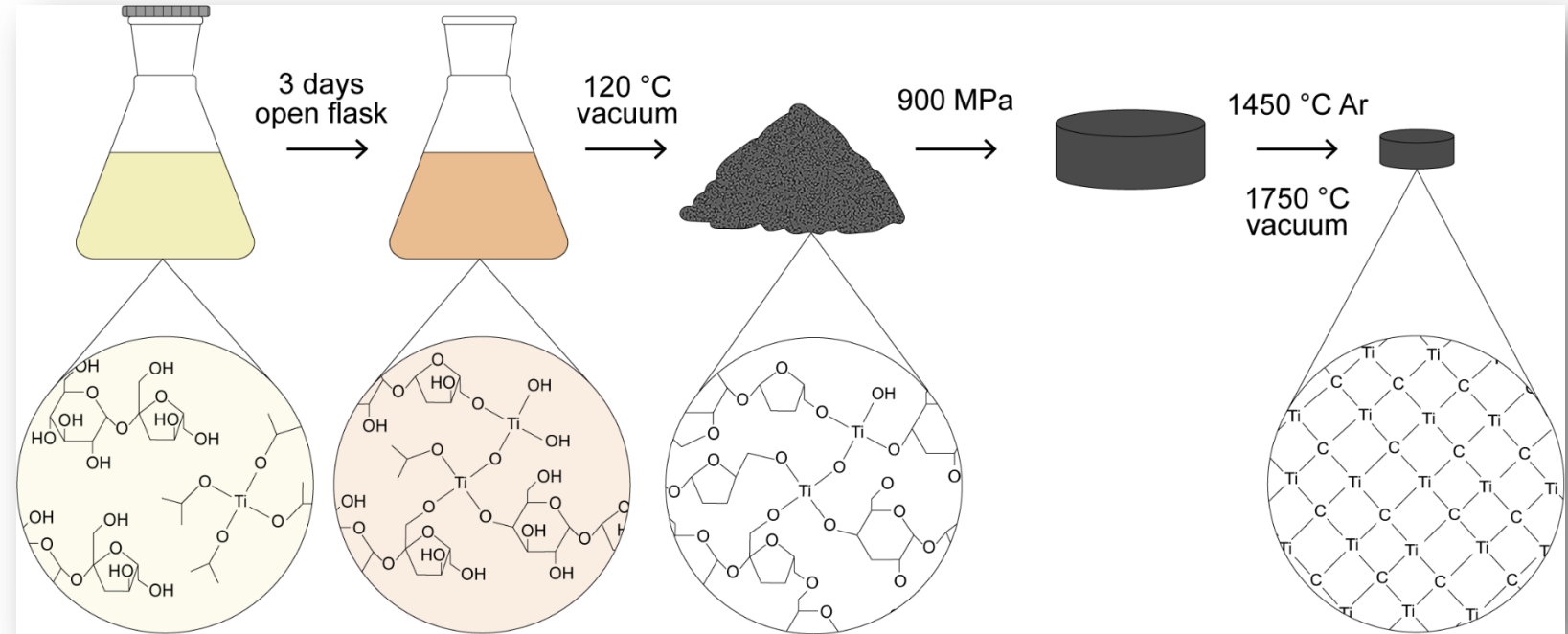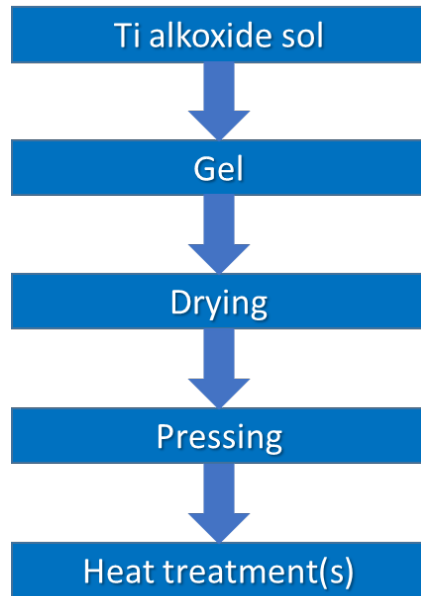
Optimization of properties by:

- Choice of initial reagents

- Temperature, pH of each production phase

- Heat treatments parameters

TiiP + ph. resin → TiC + 2C

Total porosity	65 %
Porosity type	Mostly open, meso (<50 nm)
Specific Surface Area	Very high (530 m²/g)

TiiP + sucrose → TiC + 2C

Total porosity	65 %
Porosity type	Totally open, micro (< 2 nm)
Specific Surface Area	Very high (650 m²/g)

A. Zanini, S. Corradetti, S.M. Carturan, et al., Microporous and Mesoporous Materials 337 (2022) 111917.

Target examples: additive manifactured TiC

Focus on (among others) porosity optimization – Production technology
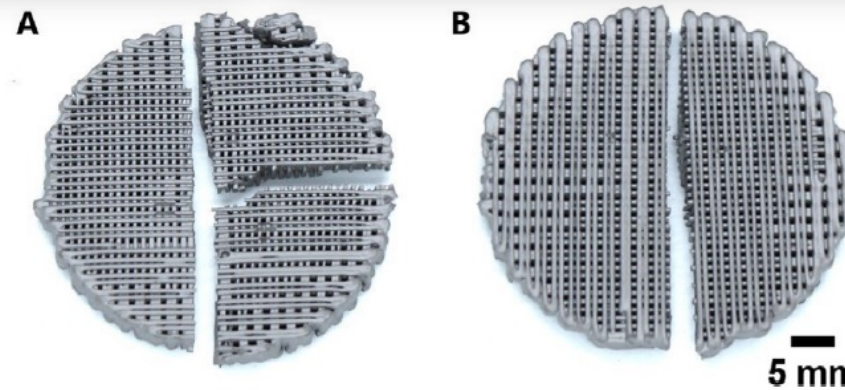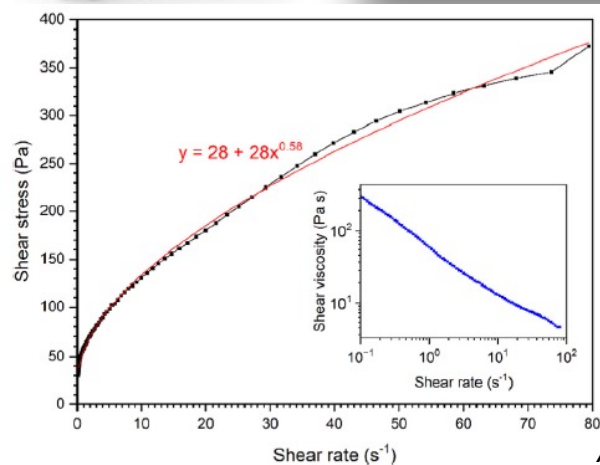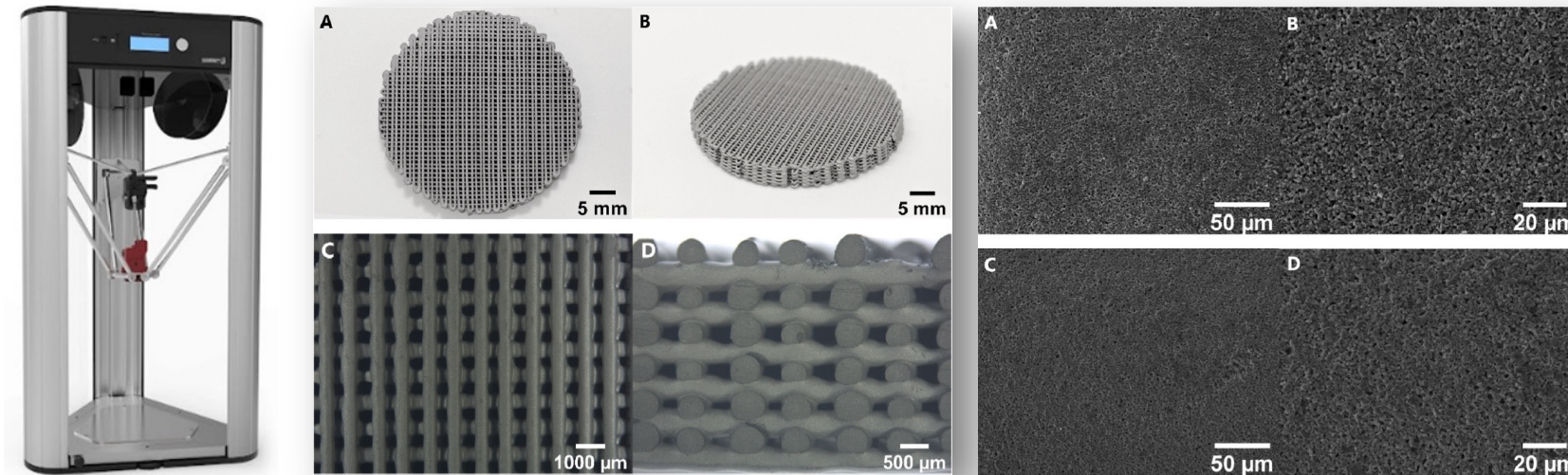
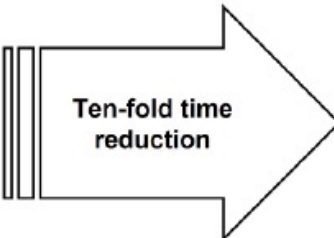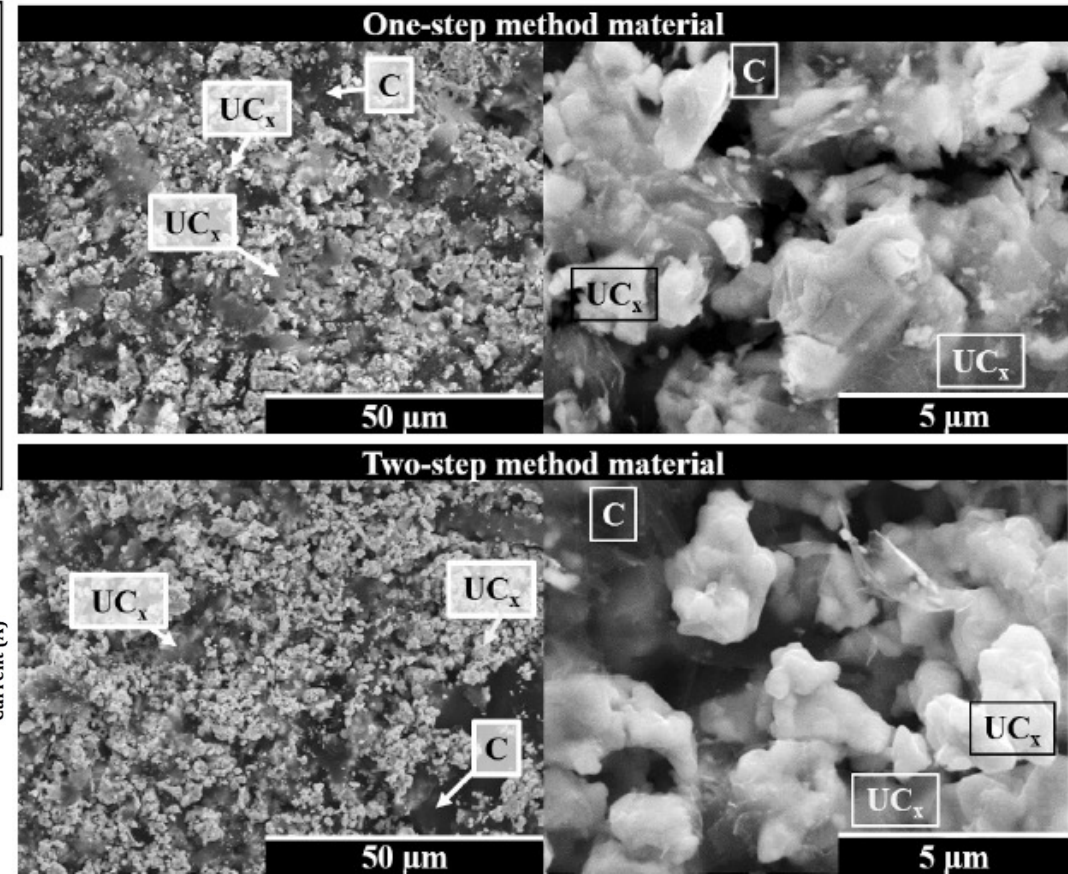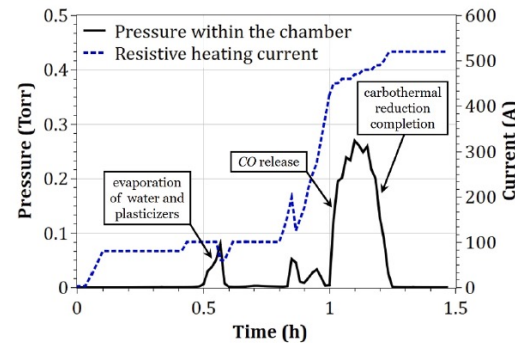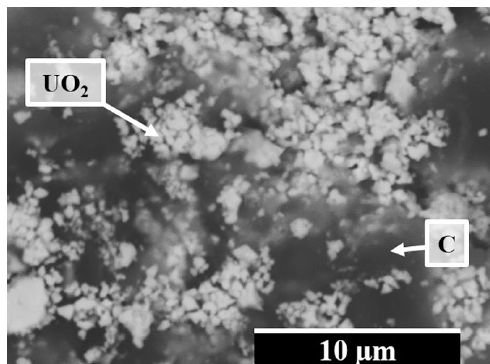*A. Breda, A. Zanini, A. Campagnolo, et al., Ceramics International 49 (2023) 31666–31678.*

Target examples: cast UCx

Focus on (among others) thermal stability – Production technology

M. Cervantes, P. Fouquet-Métivier, P. Kunz, et al., Nuclear Instruments and Methods in Physics Research B 463 (2020) 367–370.

Target examples: thermally improved UCx

Focus on (among others) thermal stability – Carbon sources

Use of graphene as a carbon source:

- Improvement of thermal properties

- No effect on reactivity and reaction completion

$$UO_2 + 6C \rightarrow UC_2 + 2C + 2CO$$

$$ThO_2 + 6C \rightarrow ThC_2 + 2C + 2CO$$

Will Any Crap We Put into Graphene Increase Its Electrocatalytic Effect?

Lu Wang, Zdenek Sofer, and Martin Pumera*

Thermal conductivity UCx — UCx-graphite Biasetto et al. 2018 S.R. / UCx-graphene Biasetto et al. 2018 S.R.
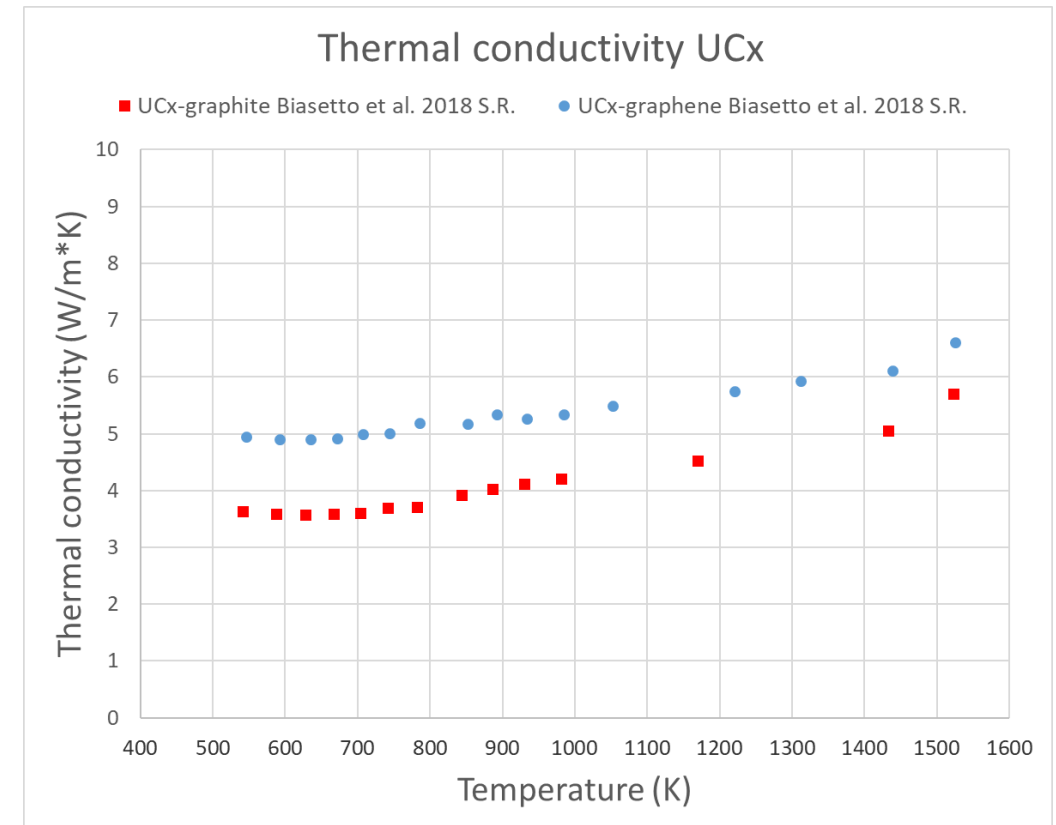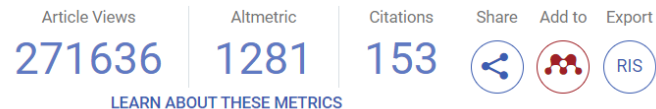
L. Biasetto, S. Corradetti, S.M. Carturan, et al., Scientific Reports 8 (2018) 8272.

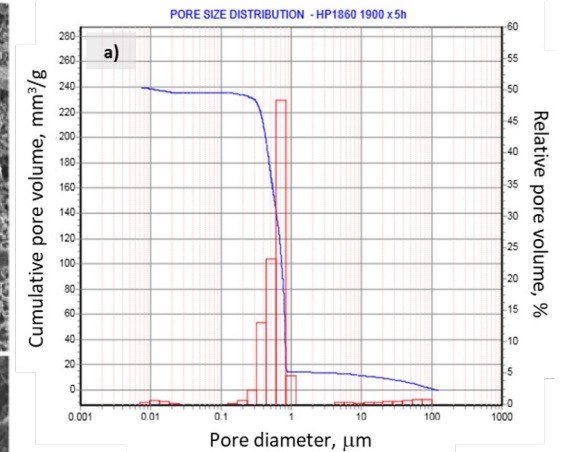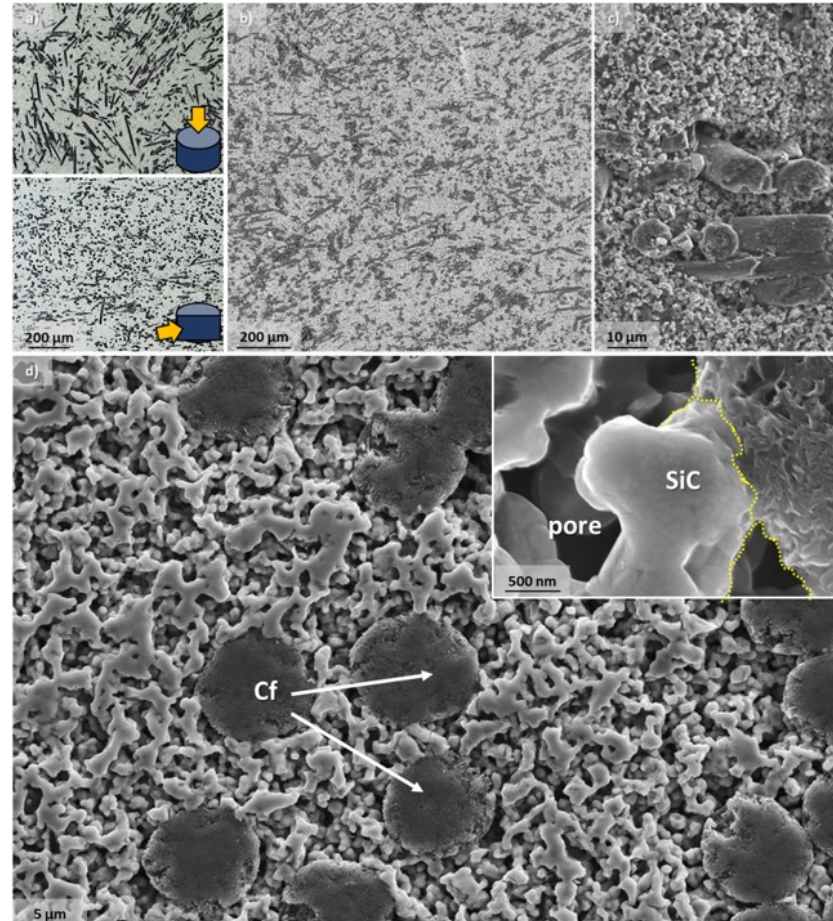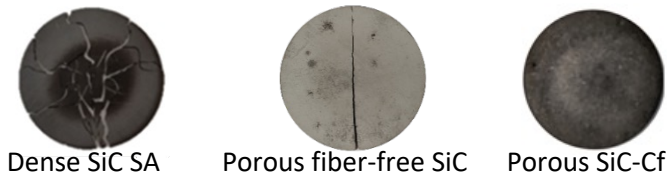*S. Corradetti, S.M. Carturan, M. Ballan, et al., Scientific Reports 11 (2021) 9058.*

Target examples: mechanically improved SiC

Focus on (among others) structural stability – Production technology

Use of dispersed carbon fibers:

- Porosity, but…

- Good thermal properties, and…

- Resistance to thermal induced stresses
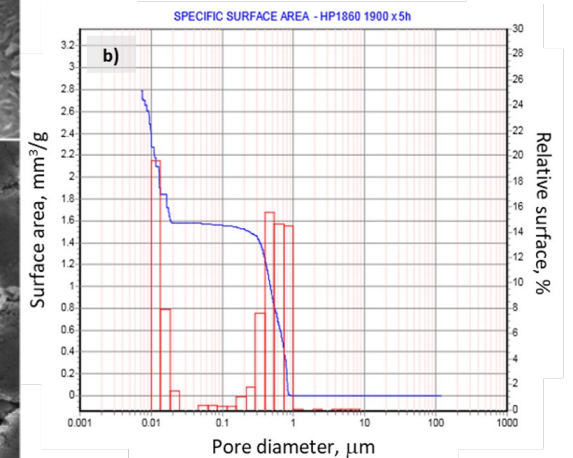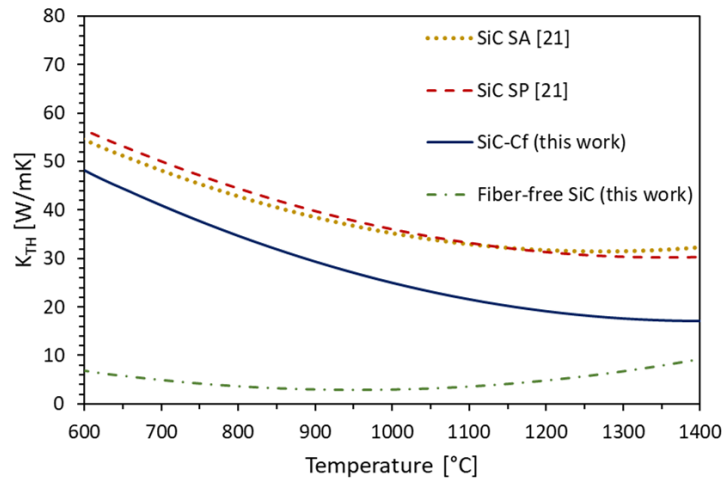
L. Silvestroni, S. Corradetti, M. Manzolaro, et al., Journal of the European Ceramic Society 42 (2022) 6750-6756.

…now, what about chemistry?

Table 2. Sc radionuclide release from target materials used at ISOLDE

Target Material	Operated Temperature, °C	Release Conditions
^{nat}Ti metallic foils	>1600	W surface ion source. Fluorination with CF_4. Only Sc^+ and ScF^+ observed and target molten after mass separation [36].
^{nat}TiC (1–50 μm)	1900	Slow release that did not increase by fluorination with CF_4 [28].
	2300	No Sc released [31].
^{nat}TiC-CNT (nanometric)	1500	No Sc released. [20].
^{nat}TiC-CB (nanometric)	1500–1740	Re surface source. No Sc was released. [20].
^{nat}V powder	1800	No Sc released [31].
^{nat}VC (1–50 μm)	1900	Slow release that did not increase by fluorination with CF_4 [28].
	2300	No Sc released. Higher other radionuclide release rates than from ^{nat}TiC [31].

Solutions are being developed (e.g. molecular beams), see next talks

E. Mamis, C. Duchemin, V. Berlin, et al., Pharmaceuticals 17 (2024) 390.

Istituto Nazionale di Fisica Nucleare
LABORATORI NAZIONALI DI LEGNARO

27 EU
P
Prismap

Thank you!